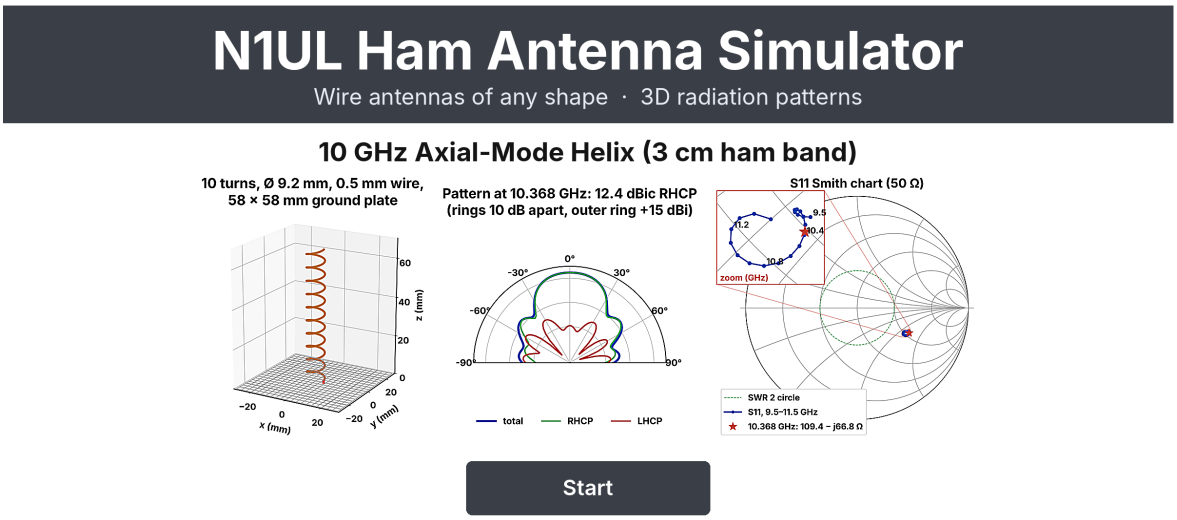
COMMUNICATIONS CONSULTING CORP.
990 Cape Marco Dr. PH2, Marco Island, FL 34145-6351
Dr. Ulrich L. Rohde
N1UL



COPYRIGHT © 2026 COMMUNICATIONS CONSULTING CORP.
The design and validation of the program was accompanied and supported by Trusha Kared (KD2YAP), Kai Siwiak (KE4PT), Martin Rothe (DF3MC), Klaus Buchenrieder (DL0UBW), my colleague Thomas Eibert, my friends and radio amateurs worldwide, and Claude AI.

Wire and Planar Antennas with Automatic Meshing and Three-Dimensional Radiation Patterns — User Manual and Verification

Prof. Dr.-Ing. habil. Ulrich L. Rohde

COPYRIGHT © 2026 COMMUNICATIONS CONSULTING CORP.

The design and validation of the program was accompanied and supported by Trusha Kared (KD2YAP), Kai Siwiak (KE4PT), Martin Rothe (DF3MC), Klaus Buchenrieder (DL0UBW), my colleague Thomas Eibert, my friends and radio amateurs worldwide, and Claude AI.

The N1UL Ham Antenna Simulator and this manual are freeware: they may be copied and distributed free of charge without limitation, provided they are not modified, not sold and this notice is retained. The software is provided “as is”, without warranty of any kind; the author accepts no liability for any damage resulting from its use.

Contents

About This Manual 4

1 Introduction 5

2 Installation and Start 6
2.1 Quick Start: the First Simulation in Six Steps . . . 8

3 The Program Window 9

4 Model Description 11

5 Mesh Generator 11

6 Numerical Method 12
6.1 Integral Equation . . . 12
6.2 Galerkin Solution . . . 12
6.3 Integration . . . 13
6.4 Ground . . . 13
6.5 Loads, Wire Loss and Networks . . . 15
6.6 Far Field, Gain and Average Gain Test . . . 15

7 Results Page 16
7.1 Current and Voltage on the Wires . . . 17

8 Variables, Optimizer and Matching Network 17
8.1 Named Variables . . . 17
8.2 Built-in Optimizer . . . 18
8.3 Automatic Matching Network . . . 18
8.4 Circular Polarization (RHCP and LHCP) . . . 22
8.5 Low Antennas: Sommerfeld Ground . . . 23
8.6 Printed Antennas on Circuit Boards . . . 25
8.7 Multi-Core Solution . . . 27

9 Parabolic Reflector Antennas 27
9.1 Model . . . 27
9.2 Method . . . 27
9.3 Example: the 46 m Dish of the Book Cover at 440 MHz . . . 28
9.4 Verification . . . 29

10 Example Antennas 30

11 Verification 40
11.1 Traceable Validation Suite . . . 40
11.2 Comparison with NEC-2 . . . 40
11.3 Closed Forms, Image Theory and Losses . . . 40
11.4 Mesh Convergence . . . 41

12 Limitations and Good Practice 48

© 2026 Communications Consulting Corp.

13 Command-line Use **49**

Appendix: Model Files of All Examples and Validation Cases **49**
Example antennas 49
NEC-2 decks (examples and NEC-2 validation cases) 64
Validation cases (analytic checks) 69

References **71**

© 2026 Communications Consulting Corp.

About This Manual

The N1UL Ham Antenna Simulator computes wire antennas of any shape: straight wires, polygons, loops, helices, smooth curves through given points and curves defined by formulas. The antenna can be in free space, over perfect ground or over real ground (with reflection coefficients, or with the exact Sommerfeld near field of the earth for low antennas), and printed antennas on circuit boards with or without a ground plane are included. You do not have to divide the wires into segments: the mesh generator does this from the wavelength, the curvature and the positions of feed points, loads and junctions, joins wires automatically and checks the geometry.

The program reports the feed-point impedance, SWR, gain, front-to-back ratio, beam widths, efficiency and the average gain test. It shows three-dimensional radiation patterns, elevation and azimuth cuts, impedance sweeps, a Smith chart and the current and voltage on the wires. NEC-2 input decks are read directly. Named variables, a built-in optimizer and automatic L matching networks help with the design, and all processor cores are used. Parabolic reflectors (dishes, also of wire mesh) are computed with the wire antenna as the feed. One hundred traceable validation checks against NEC-2, closed-form and published results are built into the program.

The program at a glance.

- Start window with an alphabetical list of all example antennas: open an example, start a new design or open another file.
- Results page with 3D pattern, elevation and azimuth cuts, SWR / return loss, Smith chart, matching networks with their harmonic attenuation, currents and voltages, and a *Back to the program* button.
- Near-field view (E and H fields compared with the FCC and ICNIRP limits, with compliance distances) and magnetic-loop view (loop current, capacitor voltage, efficiency, Q and bandwidth).
- Parabolic reflectors (`DISH`), printed antennas on circuit boards, Sommerfeld ground, NEC-2 import, named variables, optimizer and a help page with all commands.

© 2026 Communications Consulting Corp.

1 Introduction

Wire antennas are described well by the thin-wire integral equation: the current flows along the wire axis, and the tangential electric field on the wire surface must vanish except at the feed gap. The N1UL Ham Antenna Simulator solves this equation for any arrangement of wires and presents the results graphically. It was designed for three uses:

1. quick analysis of the common amateur and professional antennas (dipoles, verticals, Yagis, quads, Moxon rectangles, log-periodic arrays, loops, helices) with feed impedance, SWR and pattern;
2. antennas of arbitrary shape, such as the curved monopole of Figure 6, entered as a curve through a few points or as a formula;
3. checking of NEC-2 models, which are read unchanged.

The user does not have to divide the wires into segments: the mesh generator does this from the wavelength and refines automatically near feed points and junctions. A convergence check with twice the number of segments is part of every run.

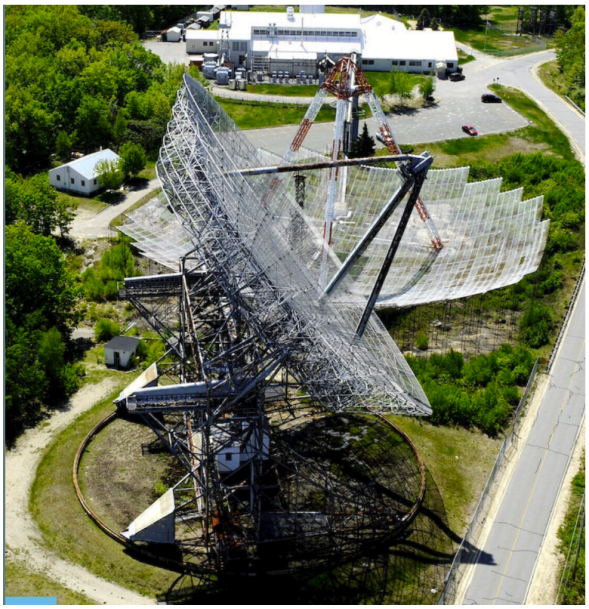


Figure 1. The 46 m diameter UHF antenna of MIT Haystack Observatory, Westford, Massachusetts; a dish of this kind is simulated in Section 9. Photo: MIT Haystack Observatory, with thanks to Phil Erickson, W1PJ, Director of MIT Haystack Observatory.

Companion textbook. The electromagnetic theory behind the program—Maxwell's equations, radiation, wire and aperture antennas, reflectors and the moment method—is treated in the textbook *Electromagnetic Waves: Theory and Applications, with a Special Focus on Circuit and Antenna Design* by R. K. Shevgaonkar and U. L. Rohde (Springer) [25], whose cover is shown in Figure 2. The reflector antennas on its cover are also a subject of this program (Section 9).

© 2026 Communications Consulting Corp.

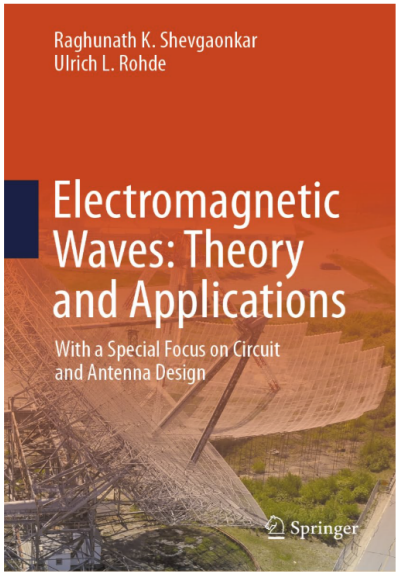


Figure 2. The companion textbook [25]. The cover shows the 46 m diameter (foreground) and 68 m diameter (background) UHF antennas used for large-aperture, high-power upper-atmospheric radar remote sensing at MIT Haystack Observatory, a multidisciplinary radio and radar remote-sensing observatory operated by the Massachusetts Institute of Technology in Westford, Massachusetts. Haystack's programs in radio astronomy, very long baseline interferometry and upper-atmospheric physics combine passive and active techniques to explore near-Earth space, the solar system and the universe, including frontier research on space weather, Earth orientation, rotation and universal time determination, and the dynamics of black-hole environments. The Observatory's scientific studies and technologies use a wide range of ultra-sensitive receivers and complex signal-processing chains at frequencies across the radio spectrum from HF to UHF, S band, X band and millimeter waves.

How to use this manual. Sections 2 and 3 get the program running and explain the window; Section 4 describes the model language and Section 5 the automatic mesh. Section 6 gives the numerical method for readers who want to know how the results are obtained, and Section 7 explains the results page. Section 8 introduces named variables, the built-in optimizer, the automatic matching network, circular polarization, the Sommerfeld ground for low antennas and printed antennas on circuit boards. Section 9 treats parabolic reflector antennas (dishes) fed by a wire antenna, with the 46 m dish of the book cover as the example. Section 10 presents the example antennas, Section 11 documents the traceable validation (100 checks with input file, reference and result) and how to repeat it with one click, and Sections 12 and 13 give limitations, good practice and command-line use. The appendix lists the model files of all examples and validation cases.

2 Installation and Start

Unpack the ZIP file `N1UL_Ham_Antenna_Simulator_1.1.zip` into any folder, for example `C:\Programs`. No installation is needed. Everything is in one folder, `N1UL_Ham_Antenna_Simulator_1.1`:

- `N1UL_Ham_Antenna_Simulator.exe`: the program;
- `N1UL_Ham_Antenna_Simulator_Manual.pdf` (and `.docx`): this manual;
- `VALIDATE N1UL Antenna Simulator.bat`: the one-click validation (Section 11);
- `bin\rsant.exe`: the simulator (also usable in a command window, Section 13);

© 2026 Communications Consulting Corp.

- `Examples`: example antennas (`.ant` models and NEC-2 decks);
- `results`: one folder per run with `results.html`, `results.json` and `log.txt`;
- `Validation`: the validation decks and reference results (Section 11);
- `viewer`: results-page template, help page and start picture.

Double-click `N1UL_Ham_Antenna_Simulator.exe`. The first start places an *N1UL Ham Antenna Simulator* icon on the desktop and in the Start menu. Windows may show a SmartScreen note for the unsigned program: click *More info*, then *Run anyway*.

Start window. The program opens with the start page (Figure 3), in the size of the program window. Click *Start* (or press Enter). The second page (Figure 4) lists all example antennas in alphabetical order of their titles, each with its file name. Select an example and click *Open selected example* (or double-click it), click *New design* for a new model (a half-wave dipole template), or *Open another file* ... for any `.ant` or NEC-2 file. *Back* returns to the start page; closing the start window ends the program. When a model file is opened directly (double-click on an `.ant` file or command line), the start window is skipped.

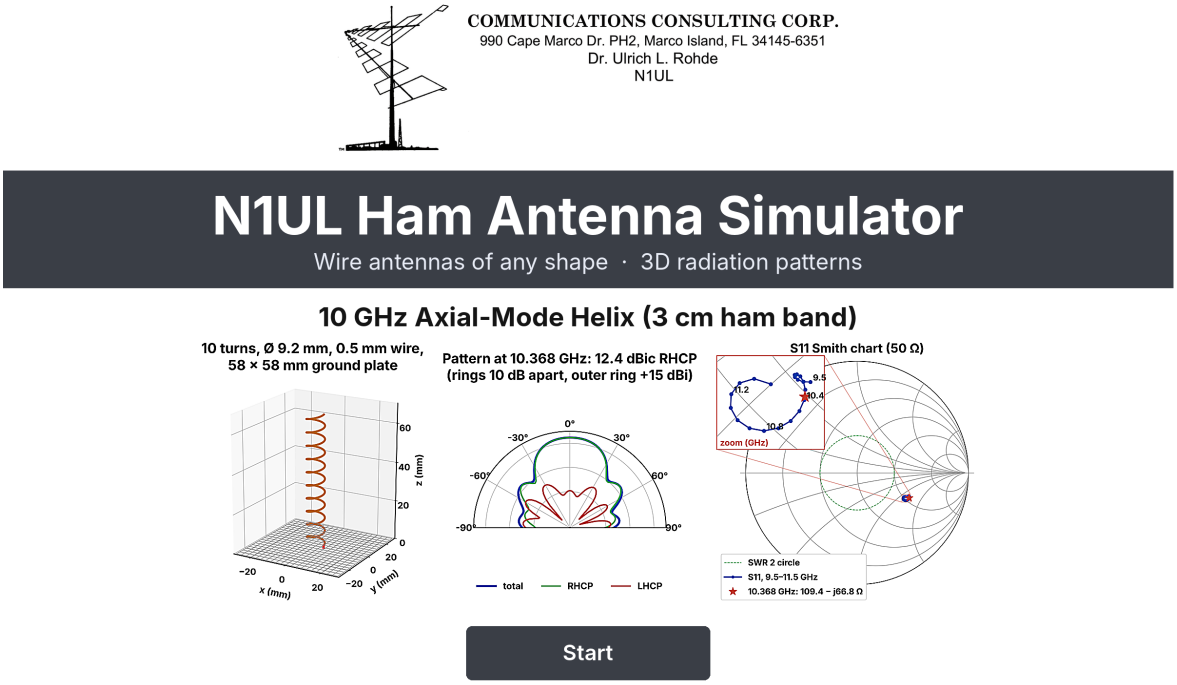


Figure 3. Start page of the program. The pictures show the example `helix_axial_10GHz.ant` (Section 10).

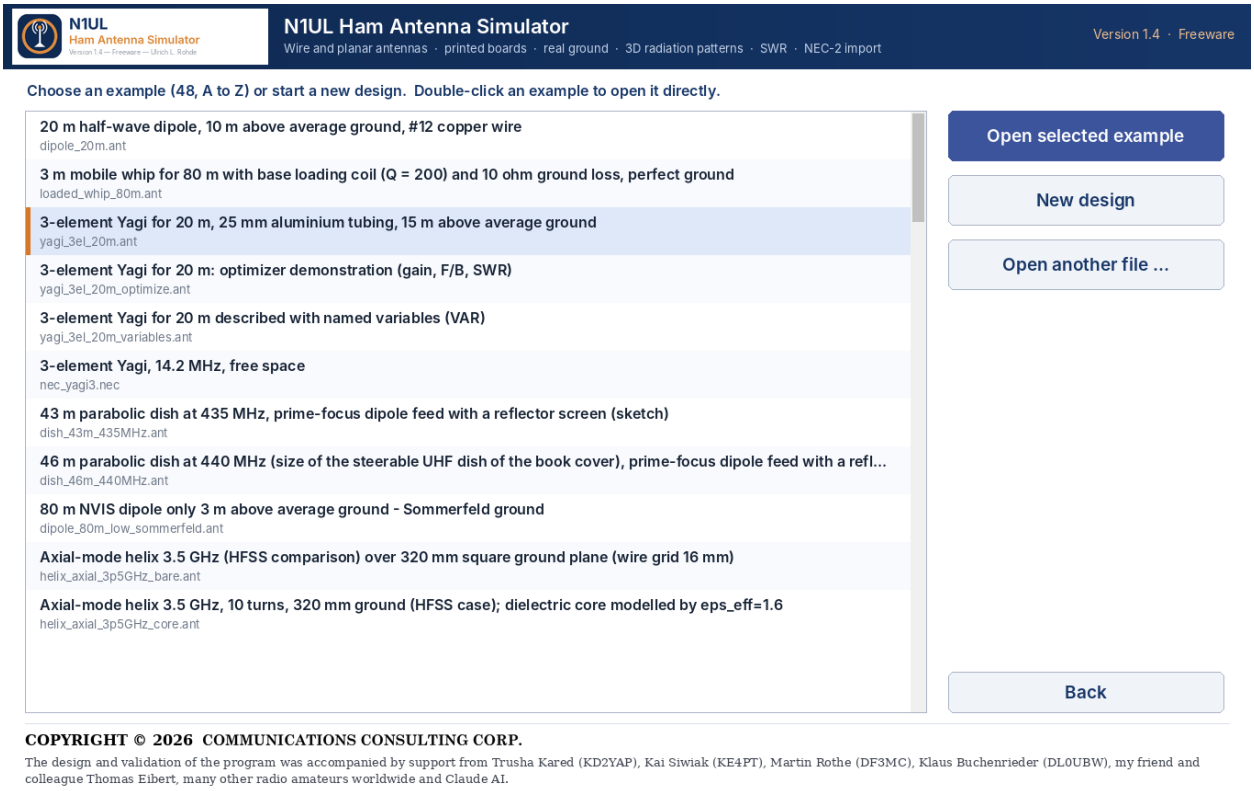


Figure 4. Second page of the start window: example antennas from A to Z, new design or another file.

2.1 Quick Start: the First Simulation in Six Steps

1. Start the program (desktop icon).
2. Click *3-element Yagi for 20 m* in the example list on the left. The model text appears in the centre and the antenna in the 3D view.
3. Check the settings on the right: frequency 14.15 MHz, real ground, aluminium.
4. Press *Run simulation*. After about one second the summary appears on the right and the results page opens in the browser.
5. On the results page read the cards at the top: feed impedance, SWR, gain, front-to-back ratio and the matching network. Click the views on the left: 3D pattern, elevation and azimuth patterns, SWR, Smith chart, matching network, currents.
6. Change a number in the model text (for example the director length), press *Run* again and compare. *Save as* keeps your version.

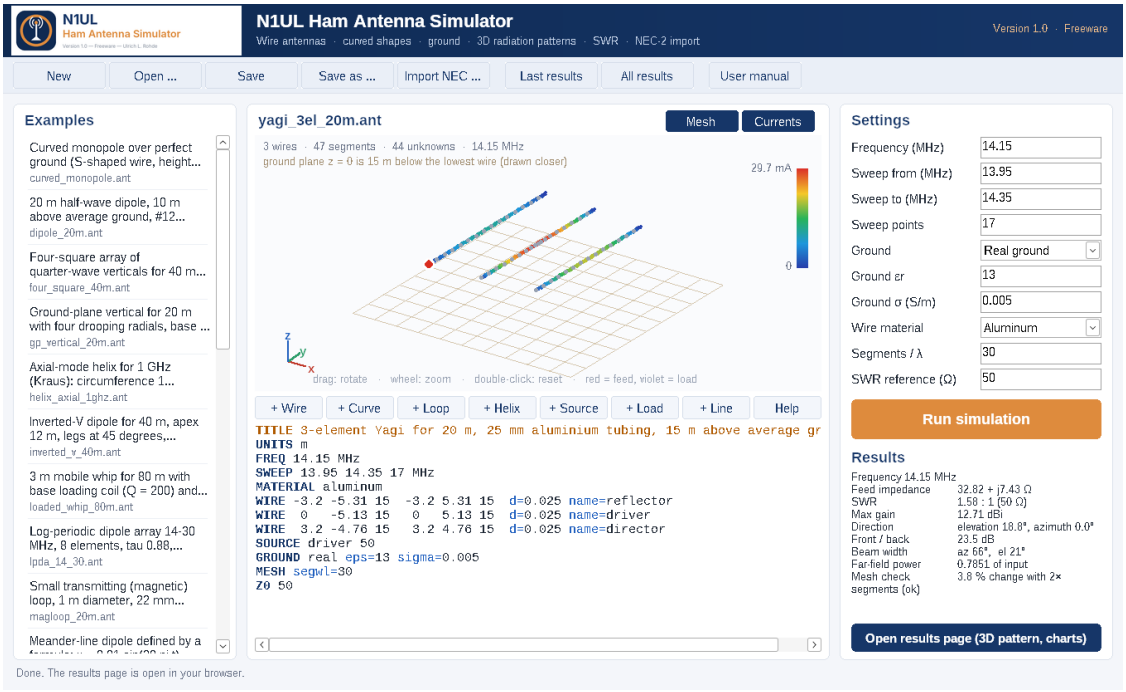


Figure 5. Program window after a run of the 3-element Yagi. Left: example antennas. Center: three-dimensional view of the geometry and mesh, colored by the current magnitude after the run (drag to rotate, wheel to zoom), command buttons and the model text with syntax coloring. Right: settings, Run button and summary of the results.

3 The Program Window

The window (Figure 5) has three columns.

Examples (left). One click loads an example. *New*, *Open*, *Save*, *Save as* and *Import NEC* are in the toolbar.

Model (center). The upper part shows the antenna in three dimensions as the mesh generator has divided it: segment ends as gray dots, the feed point in red, loads in violet, the ground as a grid. The view follows the text: about one second after an edit, the mesh is rebuilt and redrawn, and the first mesh warning, if any, is shown above the drawing. After a run the wires are colored by the current magnitude (button *Currents*). Below the view are buttons that insert a template line for a wire, curve, loop, helix, source, load or transmission line, and a *Help* button with the command summary. The model text below uses colors: commands in bold blue, unknown commands in red, `key=value` parameters in blue, comments in green.

Settings (right). Frequency, sweep range and number of points, ground (free space, perfect, real with ε_r and σ), wire material, segments per wavelength and the SWR reference impedance. Changes are written into the model text at once, so the text and the form always agree. *Run simulation* starts the calculation in the background; the summary appears below the button, and the results page (Section 7) opens in the browser.

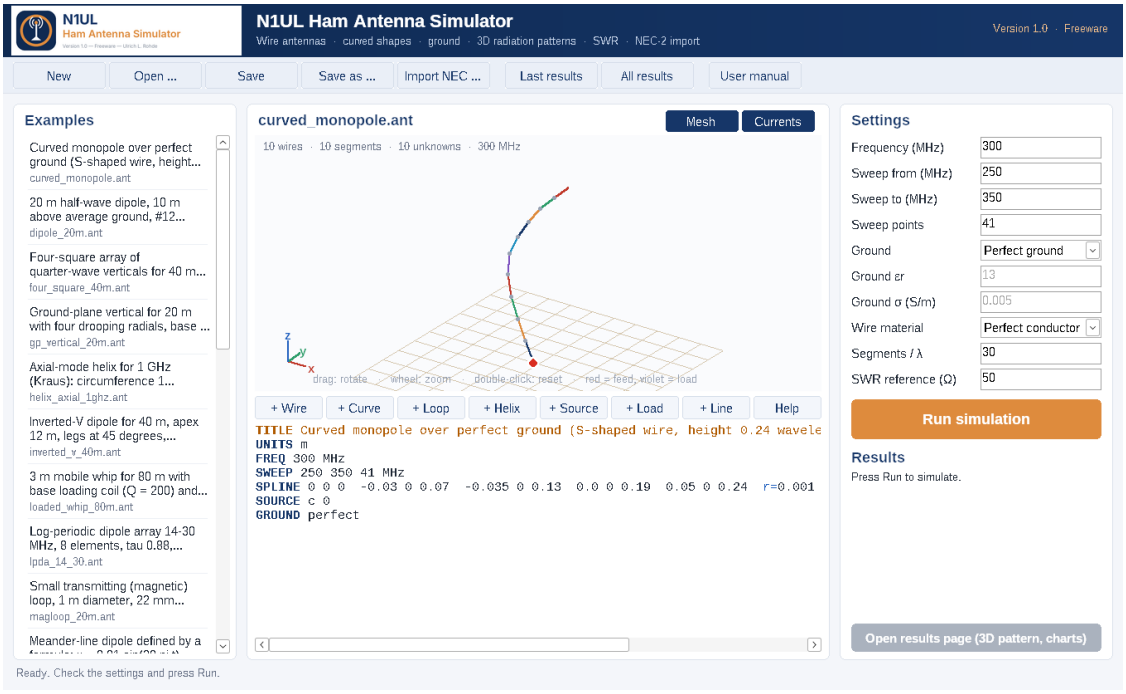


Figure 6. The curved monopole of the example `curved_monopole.ant`, entered with a single `SPLINE` command through five points. The mesh generator divides the smooth curve into ten segments (gray dots).

Table 1: Model Commands (One per Line, # Starts a Comment)

Command	**Meaning**
TITLE text	name of the model (first line of the results page)
UNITS m cm mm ft in	length unit of all coordinates (default m)
FREQ f MHz	design frequency: pattern, currents, summary
SWEEP f1 f2 n MHz	frequency sweep: impedance, SWR, gain, F/B
WIRE x1 y1 z1 x2 y2 z2 d= r= awg= [seg=] [name=] [mat=]	straight wire; diameter, radius or AWG size
SPLINE x1 y1 z1 x2 y2 z2 … d= name=	smooth curve through the points (Catmull–Rom)
POLYLINE x1 y1 z1 … d= name=	straight pieces through the points
CURVE “x(t)” “y(t)” “z(t)” [t0= t1=] d= name=	parametric wire; +, —, *, /, ^, sin, cos, tan, exp, log, sqrt, abs, pi, t
LOOP cx cy cz R n [axis=] [rot=] d= name=	regular polygon loop, n sides, radius R
HELIX x y z R p N [sides=] [left] d= name=	helix along $+z$: radius, pitch, turns
SOURCE wire pos [V=] [phase=]	voltage source; wire name or number, position 0–100 % from the first end
LOAD wire pos R= L= C= [par] X=	series (or parallel) RLC load, or $R + jX$
TL w1 p1 w2 p2 Z0= [len=] [vf=] [loss=] [rev]	transmission line between two points; loss in dB/100 m; rev = crossed
GROUND pcb eps= tand= h= [groundplane]	printed circuit board, top surface at $z = 0$, thickness h (unit suffix mm, mil, in allowed), with or without ground plane at $z = -h$ (Section 8.6)
GROUND free perfect real eps= sigma= [sommerfeld]	ground model (real: Fresnel reflection coefficients; with `sommerfeld`: exact near field of the earth, Section 8.5)
MATERIAL perfect copper aluminum brass steel stainless silver	conductivity of all wires (skin effect)
MESH segwl=30 [taper=onoff]	segments per wavelength; tapering at feeds and junctions
Z0 50	reference impedance for the SWR
PATTERN dth=2 dph=5	pattern grid in degrees

© 2026 Communications Consulting Corp.

4 Model Description

A model is a text file (extension `.ant`) with one command per line (Table 1). Wires can be referred to by name or by number in the order of definition; curves (`SPLINE`, `CURVE`, `HELIX`) are referred to by their name, and the position is measured along the curve. The 3-element Yagi of Figure 5 is completely described by

```
TITLE 3-element Yagi for 20 m
FREQ 14.15 MHz
SWEEP 13.95 14.35 17 MHz
MATERIAL aluminum
WIRE -3.2 -5.31 15 -3.2 5.31 15 d=0.025 name=refl
WIRE  0   -5.13 15  0   5.13 15 d=0.025 name=driver
WIRE  3.2 -4.76 15  3.2 4.76 15 d=0.025 name=dir
SOURCE driver 50
GROUND real eps=13 sigma=0.005
```

and the curved monopole of Figure 6 by

```
FREQ 300 MHz
SPLINE 0 0 0  -0.03 0 0.07  -0.035 0 0.13
       0 0 0.19  0.05 0 0.24  r=0.001 name=c
SOURCE c 0
GROUND perfect
```

(one line in the file). A meander dipole defined by a formula is

```
CURVE "0.008*sin(20*pi*t)" "0"
      "-0.052+0.104*t" r=0.0004 name=m
SOURCE m 50
```

NEC-2 decks (`.nec`, or a file beginning with `CM`, `CE` or `GW`) are read with the cards GW (also tapered wires with GC), GA, GH, GM, GR, GX, GS, GE, GN, EX (voltage sources), LD (types 0–5), TL, NT and FR. The segmentation of the deck is kept; a segment that carries a source, a lumped load or a network port is divided in two so that the source or load sits exactly at the segment center, as in NEC-2. Radiation-pattern and output cards are not needed, since the pattern is always computed.

5 Mesh Generator

The current is represented on segments; their size controls accuracy and run time. The mesh generator applies the following rules for native models.

1. *Length.* The target segment length is $\lambda_{\min}/s$, where $\lambda_{\min}$ is the wavelength at the highest frequency of the sweep and s is `segwl` (default 30). A wire longer than 0.02λ gets at least five segments.
2. *Tapering.* Near feed points, loads, transmission-line ends and true junctions (three or more wires, a change of radius, or a bend sharper than 60°) the segments start at max $(\Delta_0/2.5, 4a)$ and grow by a factor of at most 1.3 to the target length Δ_0. Plain bends of a bent wire need no tapering.
3. *Exact points.* Feed points, loads and line ends are always segment ends, so the source or load sits exactly where it is specified.
4. *Curves.* A smooth curve is sampled finely and resampled by arc length; the number of segments

© 2026 Communications Consulting Corp.

follows both the target length and the curvature, with at most 12° change of direction per segment.

5. *Automatic junctions.* A wire end that lies on another wire (a T-junction) splits that wire there, and the two are connected. Ends that coincide within 10^{-3} of the segment length are joined.
6. *Checks.* The mesh report lists segment length relative to the wavelength and to the wire radius (thin-wire validity: length $> 4a$ recommended), the largest length ratio at a junction, wires that cross without a junction, wires closer than the sum of their radii, wires below the ground and wires touching a real ground.

Every run computes the feed impedance a second time with twice the segment density and reports the change (*mesh check*). A change below 3–5 % indicates a converged mesh.

6 Numerical Method

6.1 Integral Equation

On the surface of a perfectly conducting wire the tangential total field vanishes except across the feed gap:

$$\hat{\mathbf{s}} \cdot (\mathbf{E}^{\text{inc}} + \mathbf{E}^{\text{s}}) = 0. \qquad (1)$$

The scattered field follows from the vector and scalar potentials of the axial current $I(l)$ and its line charge $q = -\frac{1}{j\omega}\, dI/dl$:

$$\mathbf{E}^{\text{s}} = -j\omega \mathbf{A} - \nabla\phi, \qquad (2)$$

$$\mathbf{A} = \mu \int I(l')\, \hat{\mathbf{s}}'\, G\, dl', \qquad \phi = -\frac{1}{j\omega\varepsilon} \int \frac{dI}{dl'}\, G\, dl', \qquad (3)$$

with the thin-wire (reduced) kernel

$$G = \frac{e^{-jkR}}{4\pi R}, \qquad R = \sqrt{|\mathbf{r} - \mathbf{r}'|^2 + a^2}, \qquad (4)$$

where a is the wire radius and $\mathbf{r}$, $\mathbf{r}'$ lie on the wire axes.

6.2 Galerkin Solution

The current is expanded in triangle functions f_n that span the two segments meeting at node n and are 1 at the node:

$$I(l) = \sum_{n=1}^{N} I_n f_n(l). \qquad (5)$$

At a junction of m wires, $m - 1$ functions pair the first wire with each of the others, which enforces Kirchhoff's current law. Free wire ends carry no function (zero current); a wire end on a ground plane

© 2026 Communications Consulting Corp.

carries a half function completed by its image. Testing (1) with the same functions and integrating the scalar-potential term by parts gives

$$\sum_n Z_{mn} I_n = V_m, \qquad (6)$$

$$Z_{mn} = j\omega\mu \iint f_m f_n \, \hat{\mathbf{s}}_m \cdot \hat{\mathbf{s}}_n \, G \, dl \, dl' + \frac{1}{j\omega\varepsilon} \iint f_m{}' f_n{}' \, G \, dl \, dl', \qquad (7)$$

where $f' = df/dl$ is constant on each segment. A delta-gap source of voltage V at node m gives $V_m = V$, and the feed impedance is $Z_{\text{in}} = V/I_m$.

6.3 Integration

For distant segment pairs (7) is integrated by Gauss–Legendre quadrature with 3 to 8 points per segment. For the self term, neighbors and other close pairs the singular part of the kernel is integrated analytically along the source segment. With l_0 the projection of the observation point on the source axis and $c^2 = \rho^2 + a^2$,

$$\int_0^{\Delta} \frac{dl'}{\sqrt{(l' - l_0)^2 + c^2}} = asinh\frac{\Delta - l_0}{c} + asinh\frac{l_0}{c}, \qquad (8)$$

and similarly for the linear weight; the smooth remainder $\left(e^{-jkR} - 1\right)/(4\pi R)$ is integrated numerically, and the outer integral uses 16 Gauss points. This keeps the matrix accurate for bent wires and junctions, where segments meet at an angle.

6.4 Ground

Over a perfect ground the image of every segment is included: the image current has the horizontal components reversed and the vertical component unchanged, and the image charge is reversed. Over real ground the image terms are multiplied by the Fresnel reflection coefficients at the specular angle ψ (reflection-coefficient approximation),

$$\begin{aligned} \Gamma_v &= \frac{\varepsilon_c \sin\psi - \sqrt{\varepsilon_c - \cos^2\psi}}{\varepsilon_c \sin\psi + \sqrt{\varepsilon_c - \cos^2\psi}}, \\ \Gamma_h &= \frac{\sin\psi - \sqrt{\varepsilon_c - \cos^2\psi}}{\sin\psi + \sqrt{\varepsilon_c - \cos^2\psi}}, \end{aligned} \qquad (9)$$

with $\varepsilon_c = \varepsilon_r - j\sigma/(\omega\varepsilon_0)$; Γ_h scales the horizontal, Γ_v the vertical current components and (with reversed sign) the charge. The same coefficients form the space wave of the far field. The reflection coefficients are exact for plane waves; they describe the coupling of a wire to its own image well only when the wire is higher than about 0.1λ.

Sommerfeld ground. With the keyword `sommerfeld` (or the NEC-2 card `GN 2`) the near field reflected by the earth is computed exactly [15], [16]. For a current element $I\,d\mathbf{l}$ at height z' the reflected Hertz potential is, with $C = I\,dl/(4\pi j\omega\varepsilon_0)$, $\zeta = z + z'$ and the horizontal distance ρ,

$$\begin{aligned}\Pi_z^r &= C\int_0^\infty R_V\, e^{-u_0\zeta} J_0(\lambda\rho)\tfrac{\lambda}{u_0}\, d\lambda \quad \text{(vertical)},\\ \Pi_x^r &= C\int_0^\infty R_H\, e^{-u_0\zeta} J_0(\lambda\rho)\tfrac{\lambda}{u_0}\, d\lambda \quad \text{(horizontal, } x\text{)},\\ \Pi_z^r &= C\,\tfrac{\partial}{\partial x}\int_0^\infty W\, e^{-u_0\zeta} J_0(\lambda\rho)\,\lambda\, d\lambda,\end{aligned} \qquad (10)$$

$$\begin{aligned}R_V &= \tfrac{\varepsilon_c u_0 - u_1}{\varepsilon_c u_0 + u_1}, \qquad R_H = \tfrac{u_0 - u_1}{u_0 + u_1},\\ W &= \tfrac{2(u_0-u_1)}{k_1^2 u_0 + k_0^2 u_1}, \qquad u_i = \sqrt{\lambda^2 - k_i^2}, \quad k_1^2 = \varepsilon_c k_0^2,\end{aligned} \qquad (11)$$

and $\mathbf{E}^r = \nabla\nabla\cdot\Pi^r + k_0^2\Pi^r$. All field components follow from seven scalar integrals of (ρ, ζ). The reflected field enters the matrix as $Z_{mn} += -\iint f_m f_n\, \hat{\mathbf{s}}_m \cdot \mathbf{E}^r\, dl\, dl'$. It is split into a quasi-static image with the factor $K = (\varepsilon_c - 1)/(\varepsilon_c + 1)$ (image charge $-K$, image of vertical currents $+K$), which carries the near singularity and is integrated with the same singularity extraction as the free-space term, and a smooth remainder [17]. The remainder is tabulated for each frequency on a grid of ρ and ζ (geometric near the source, $\lambda/40$ beyond), with the phase $e^{-jk_0 R}$ removed, and interpolated with 4×4 Lagrange polynomials. The integrals are evaluated along a path above the real axis that passes the branch points k_0 and k_1 and the surface-wave pole; the oscillating tail is integrated over half periods π/ρ and summed with Wynn's ε algorithm (partition-extrapolation [18], [19]); the large-λ asymptote is subtracted and added back in closed form. Two different integration paths agree to 10^{-7}, and the table reproduces the direct integration to 10^{-4} of the reflected field. With $\varepsilon_r = 1$ the result is exactly free space, and for $\varepsilon_c \to \infty$ it tends to the perfect ground (Table 8). The far field uses the space wave with the Fresnel coefficients, as in NEC-2; the surface wave, which decays along the ground, is not included in the pattern.

Printed boards. The same formulation holds for any layered medium below $z = 0$: only the spectral reflection coefficients change. With the Hertz potentials above, R_V is the reflection coefficient of the TM waves (E_z), R_H that of the TE waves (H_z), and requiring the reflected E_z of a horizontal element to be a TM reflection gives the general identity

$$-R_H + \lambda^2 W = R_V, \qquad (12)$$

which reproduces the half-space W exactly. For a board of thickness d and permittivity $\varepsilon_c = \varepsilon_r(1 - j\tan\delta)$ with $t = \tanh(u_1 d)$ the transmission-line transformation of the wave admittances (TE $\propto u$, TM $\propto \varepsilon/u$) gives [20], [21]

$$\begin{aligned}R_V^{(g)} &= \tfrac{\varepsilon_c u_0 - u_1 t}{\varepsilon_c u_0 + u_1 t}, \qquad R_H^{(g)} = \tfrac{u_0 t - u_1}{u_0 t + u_1},\\ R_V^{(a)} &= \tfrac{\varepsilon_c u_0 n - u_1 m}{\varepsilon_c u_0 n + u_1 m},\\ R_H^{(a)} &= \tfrac{(u_0^2 - u_1^2)\,t}{2u_0 u_1 + (u_0^2 + u_1^2)\,t},\end{aligned} \qquad (13)$$

for a board with ground plane at $z = -d$ (g) and a board in air (a), with $n = u_1 + \varepsilon_c u_0 t$ and $m = \varepsilon_c u_0 + u_1 t$. These functions are even in u_1 (no branch point at k_1); the surface-wave poles lie between k_0 and $Re k_1$ and are passed by the integration path. For large λ both reduce to the half-space values, so the same quasi-static image applies; it contains the image charge $-K$ and the vertical current $+K$, but no image of the vector potential of horizontal currents, because $R_H \to 0$ for a non-magnetic medium. This matters for traces lying on the board ($\zeta \to 0$), where an image of the horizontal current would leave a singular remainder. The remainder is linear in ζ near the surface and is extrapolated from the table to $\zeta = 0$. In the far field the upper half space uses the plane-wave reflection coefficients R_V, R_H at $\lambda = k_0 \sin\theta$,

© 2026 Communications Consulting Corp.

$u_0 = jk_0\,|\cos\theta|$; below a board without ground plane the field is the free-space field multiplied by the slab transmission coefficient

$$T = \frac{e^{u_0 d}}{\cosh u_1 d + \frac{1}{2}\left(r + r^{-1}\right)\sinh u_1 d}, \qquad (14)$$

with $r = u_0/u_1$ (TE, E_ϕ) and $r = u_1/\left(\varepsilon_c u_0\right)$ (TM, E_θ). The board is laterally infinite. Power carried by the surface waves of the board and the dielectric loss are not part of the far-field power. Checks: two integration paths agree to 10^{-9}, a grounded board with $\varepsilon_r = 1$ equals a perfect ground at depth d to 10^{-8}, a thick board equals the half-space, and the general formulas agree with a numerical transmission-line transformation to 10^{-13}.

6.5 Loads, Wire Loss and Networks

A lumped load Z_L at node m adds Z_L to Z_{mm}. Wire loss is a distributed series impedance per unit length,

$$Z_i = \frac{1+j}{2\pi a\,\sigma\,\delta}, \qquad \delta = \sqrt{\frac{2}{\omega\mu_0\sigma}}, \qquad (15)$$

blended into the dc resistance and internal inductance when the wire is thin compared with the skin depth; it adds $Z_i \int f_m f_n\, dl$ to Z_{mn}. Transmission lines and general two-ports (NEC TL and NT cards) are connected in parallel across the gap of their nodes, as in NEC-2. Their admittance matrix

$$\mathbf{Y}_{\mathrm{TL}} = \frac{1}{Z_0}\begin{bmatrix} \coth\gamma\ell & \mp csch\gamma\ell \\ \mp csch\gamma\ell & \coth\gamma\ell \end{bmatrix}, \qquad (16)$$

(lower sign for a crossed line) couples the gap voltages $\mathbf{v}$ of the network nodes, which become additional unknowns:

$$\begin{bmatrix} \mathbf{Z} & -\mathbf{E} \\ \mathbf{E}^T & \mathbf{Y} \end{bmatrix}\begin{bmatrix} \mathbf{I} \\ \mathbf{v} \end{bmatrix} = \begin{bmatrix} \mathbf{V} \\ -\mathbf{Y}_s\mathbf{V}_s \end{bmatrix}, \qquad (17)$$

where $\mathbf{E}$ selects the network nodes and $\mathbf{V}_s$ are source voltages at network ports. The source current then includes the current drawn by the networks at its gap. The system is solved by LU decomposition with partial pivoting.

6.6 Far Field, Gain and Average Gain Test

With the current known, the far field in direction $\hat{\mathbf{r}}$ is

$$\mathbf{E} = -\frac{j\omega\mu}{4\pi r}e^{-jkr}\left[\mathbf{N} - (\mathbf{N}\cdot\hat{\mathbf{r}})\,\hat{\mathbf{r}}\right], \quad \mathbf{N} = \int I(l')\hat{\mathbf{s}}' e^{jk\hat{\mathbf{r}}\cdot\mathbf{r}'}dl', \qquad (18)$$

where $\mathbf{N}$ is integrated analytically for the linear current on each segment. The gain is

© 2026 Communications Consulting Corp.

$$G(\theta,\phi) = \frac{4\pi r^2 \,|\mathbf{E}|^2/(2\eta)}{P_{\text{in}}}, \qquad P_{\text{in}} = \sum \frac{1}{2} Re\{VI^*\}, \qquad (19)$$

split into vertical (E_θ) and horizontal (E_ϕ) parts. The radiated power P_{rad} is integrated over the sphere (or the upper half space) with Gauss quadrature in $\cos\theta$. For a lossless antenna in free space or over perfect ground the *average gain test* AGT $= P_{\text{rad}}/P_{\text{in}}$ must equal 1; it checks that the impedance and the pattern are consistent. With losses the same ratio is the efficiency; over real ground it is the fraction of the input power that reaches the far field.

7 Results Page

After each run the browser shows the results page (Figs. 4–5). The cards at the top give frequency, feed impedance, SWR, maximum gain with its direction, front-to-back ratio, -3 dB beam widths and the average gain test (or the far-field power over real ground). The views on the left are:

- *3D radiation pattern*: gain surface, colored and scaled over 20, 30 or 40 dB below the maximum; total, vertical, horizontal, right-hand or left-hand circular polarization; antenna drawn in the centre; drag to rotate, wheel to zoom, preset views from the top and the sides;
- *Elevation pattern*: vertical cut at any azimuth (default: direction of maximum), total, vertical and horizontal;
- *Azimuth pattern*: horizontal cut at any elevation (default: elevation of maximum);
- *SWR*, *Feed impedance* (with sweep table), *Smith chart* with SWR = 3 circle, *Gain vs frequency* with front-to-back ratio;
- *Currents*: current and voltage distribution on the wires (Section 7.1), and magnitude along the wires;
- *Geometry and mesh*: wires, segment ends, sources, loads, lines, mesh-quality table, warnings and the convergence check;
- *Input file* and *Simulator output*.

Every chart shows its values when the mouse is moved over it.

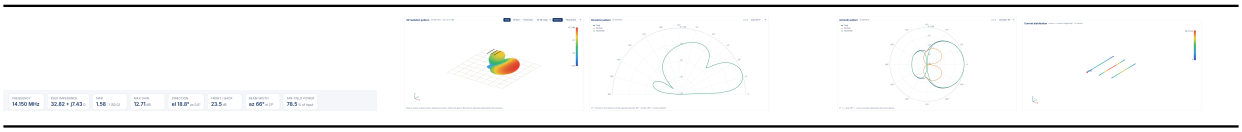


Figure 7. Results page of the 3-element Yagi (14.15 MHz, 15 m over average ground): summary cards, 3D radiation pattern, elevation pattern at azimuth 0°, azimuth pattern at the elevation of maximum gain (19°), current distribution.

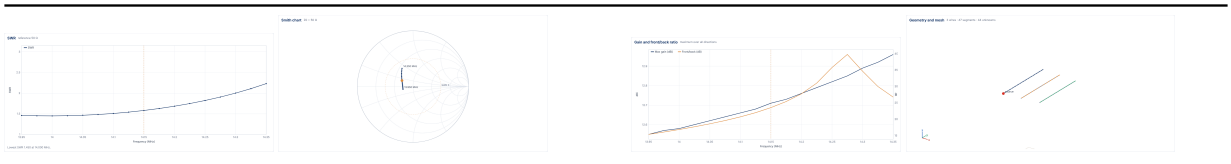


Figure 8. Results page of the 3-element Yagi, continued: SWR, Smith chart, gain and front-to-back ratio versus frequency, geometry and mesh.

© 2026 Communications Consulting Corp.

7.1 Current and Voltage on the Wires

The view *Currents* shows either the current or the voltage along every wire. In the *Envelope* style, as in NEC programs, the magnitude is drawn as a curve beside each wire, at a distance proportional to the value, and colored by it; the wire itself is drawn in light gray and joined to the curve by thin lines (Figure 9). The *Color* style colors the wire itself. The feed point is marked in red.

The current is the solution of the moment method, linear along each segment. The voltage is the potential of the wire against infinity (scalar potential in the Lorenz gauge). It follows from the line charge, which the continuity equation gives from the change of the current along the segment,

$$q_j = \frac{j}{\omega}\frac{dI}{ds}\Big|_j, \qquad V_i = \frac{1}{4\pi\varepsilon_0}\sum_j q_j \int_{\text{seg } j} \frac{e^{-jkR}}{R}\, ds, \qquad (20)$$

with $R = \sqrt{|\mathbf{r}_i - \mathbf{r}'|^2 + a_j^2}$,

evaluated at the segment centers $\mathbf{r}_i$ with eight-point Gauss quadrature and the thin-wire kernel (a_j wire radius); over ground the image charges $-q_j$ are included. The voltage is the quantity that sets the stress on insulators and the field strength at the element ends.

Both quantities are given for a source of 1 V. They scale with the source voltage: for a transmitter power P into the feed impedance $Z = R + jX$ the peak source voltage is $|Z|\sqrt{2P/R}$, and every displayed value is multiplied by it. Example: the half-wave dipole for 20 m (`dipole_20m.ant`, $Z = 71.3 - j12.7\,\Omega$) has 3.66 V at each end for 1 V at the feed, opposite in phase. At 100 W this is about 310 V peak at each end, or 620 V between the ends, in agreement with the usual estimate $\sqrt{2PR_{\text{end}}}$ for an end impedance of a few kΩ. On a Yagi the voltage is largest at the tips of the driven element and the reflector, while the current is largest at the center of the driven element.

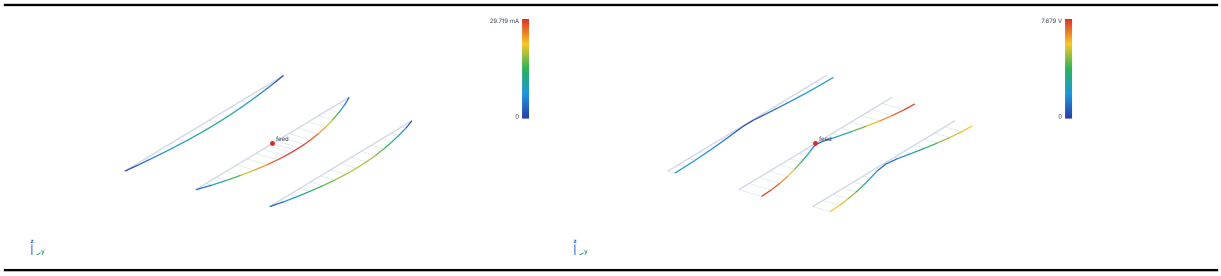


Figure 9. Current (left, maximum 29.7 mA) and voltage (right, maximum 7.7 V) on the 3-element Yagi for 1 V at the feed point, envelope style.

8 Variables, Optimizer and Matching Network

8.1 Named Variables

Any number in a model can be replaced by a name or an expression. Variables are defined with `VAR` and may depend on variables defined before:

```
VAR h=15 d=0.025
VAR Lr=5.31 Ld=5.13 Lx=4.76   # half lengths
```

```
VAR Sr=3.2 Sd=3.2                # spacings
WIRE -Sr -Lr h  -Sr Lr h  d=d name=reflector
WIRE 0 -Ld h  0 Ld h  d=d name=driver
WIRE Sd -Lx h  Sd Lx h  d=d name=director
```

Expressions use `+ - * / ^`, parentheses, `pi` and the functions `sin cos tan sqrt exp log abs` and others; they are written without spaces (`-Lr/2+0.1`). The example `yagi_3el_20m_variables.ant` gives exactly the same result as `yagi_3el_20m.ant`.

8.2 Built-in Optimizer

Variables become design parameters with `OPTVAR name min max`; `GOAL` lines state what is wanted:

- `GOAL gmax` – maximum gain; `GOAL gain elev=20 az=0` – gain in a given direction;
- `GOAL fb target=25` – front-to-back ratio (counted up to the target);
- `GOAL swr target=1.5` – SWR at the design frequency not above the target;
- `GOAL r target=50`, `GOAL x target=0` – feed resistance and reactance;
- `weight=w` on any goal sets its importance; `OPTSET pop=30 gen=40 seed=1` sets population, generations and random seed.

The goals are combined into one cost (differential evolution [9], simplex refinement [10]), $C = -\sum w\,G - \sum w \min\left(F/B, F/B_t\right) + \sum 10\,w \max\left(0, SWR - SWR_t\right) + \sum w\,|R - R_t|\,/10 + \ldots$, which is minimized by differential evolution: each trial design is a full moment-method solution at the design frequency. When the model contains `OPTVAR` lines, the *Run* button optimizes instead of simulating; the optimized model (with the new `VAR` values) appears in the editor and the results page shows the optimized antenna. From the command line: `rsant -opt model.ant -o outdir`.

Figure 10 shows the optimization of the 3-element 20 m Yagi of `yagi_3el_20m_optimize.ant` for maximum gain, a front-to-back ratio of 25 dB and SWR below 1.3, with the five element lengths and spacings free (24 designs, 25 generations, 7 s). Starting from the published dimensions (12.71 dBi, F/B 23.5 dB, SWR 1.58) the optimizer finds 12.66 dBi, F/B 26.3 dB and SWR 1.29: it trades 0.05 dB of gain for the match and the rear rejection, the classical Yagi compromise.

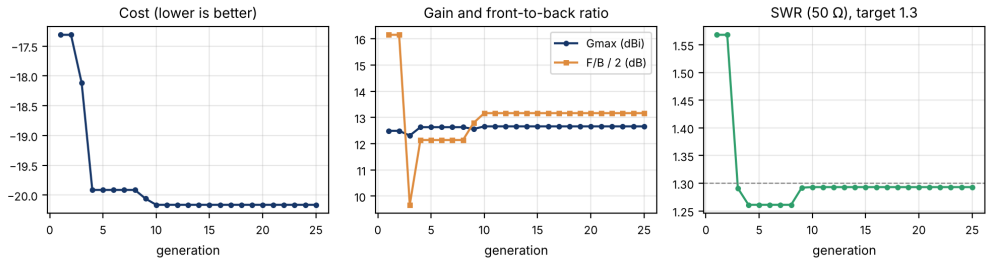


Figure 10. Built-in optimizer: 3-element Yagi for 20 m, five variables, goals maximum gain, F/B 25 dB and SWR ≤1.3. Best design of each generation.

8.3 Automatic Matching Network

Every run calculates how the antenna is matched to the line. For the feed impedance $Z_A = R_A + jX_A$ at the design frequency the program computes the two lossless L networks [8] to the reference impedance

R_0 (`Z0`, default 50 Ω). Two circuits are possible (Figure 11): for $R_A < R_0$ the series element is at the antenna and the shunt element across the line,

$$X_s = \pm\sqrt{R_A\,(R_0 - R_A)} - X_A, \qquad B = \pm\frac{1}{R_0}\sqrt{\frac{R_0 - R_A}{R_A}}, \qquad (21)$$

for $R_A > R_0$ the shunt element is at the antenna,

$$\begin{aligned} B &= \frac{X_A \pm \sqrt{R_A/R_0}\,\sqrt{R_A^2 + X_A^2 - R_0 R_A}}{R_A^2 + X_A^2}, \qquad (22)\\ X_s &= \frac{1}{B} + \frac{X_A R_0}{R_A} - \frac{R_0}{B R_A}. \end{aligned}$$

A positive X_s is a coil $L = X_s/\omega$, a negative one a capacitor $C = -1/(\omega X_s)$; a positive B is a capacitor $C = B/\omega$, a negative one a coil $L = -1/(\omega B)$. Solution 1 is the low-pass network (series coil, shunt capacitor) when it exists; it also suppresses harmonics.

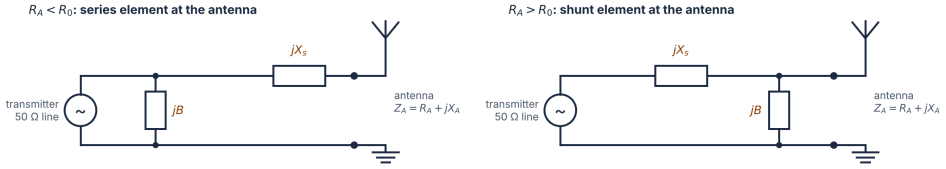


Figure 11. The two L-network circuits computed by the program. The element next to the antenna depends on whether the antenna resistance is below or above the line impedance.

How to use it.

1. Run the antenna. The card *Matching to 50 Ω* at the top of the results page shows the recommended network.
2. Open the view *Matching network*: it draws the circuit of both solutions with their component values (Figure 13).
3. The chart below the circuits shows the SWR over the sweep for the antenna alone and with each network; the view *SWR* shows the antenna alone and with solution 1.
4. Build the network with the listed values. Real coils and capacitors have losses and the values change slightly with frequency; trim the coil on the real antenna.

Example 1: short vertical for 40 m (`short_vertical_40m.ant`). A 5 m aluminum tube over perfect ground is only 0.12λ high at 7.1 MHz. Its feed impedance is $5.6 - j301\ \Omega$ (SWR 335). The program proposes a series coil of 7.108 µH at the base of the antenna—the classical loading coil, which cancels the capacitive reactance—and a shunt capacitor of 1266 pF across the line, which transforms the remaining 5.6 Ω up to 50 Ω (Figure 12a, Figure 13). The SWR is 1.0 at 7.1 MHz and below 2 over only about 20 kHz: a short antenna has a high Q (Chu limit [12], [13]).

Example 2: curvilinear 7 MHz monopole (`paper_curvilinear_7MHz.ant`). The optimized $3\lambda/4$ curved wire has $60.8 - j162.5\ \Omega$ (SWR 10.6). Here $R_A > R_0$, so the shunt element is at the antenna: 14.25 pF across the feed point and a series coil of 3.393 µH toward the line (Figure 12b). With this network the SWR stays below 2 from 6.90 to 7.09 MHz (Figure 14).

© 2026 Communications Consulting Corp.

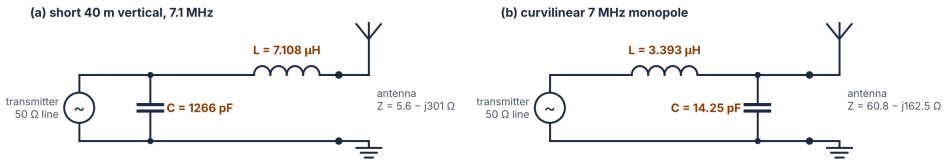


Figure 12. Matching networks computed by the program: (a) short 40 m vertical, series coil at the antenna and shunt capacitor across the line; (b) curvilinear 7 MHz monopole, shunt capacitor at the antenna and series coil toward the line.

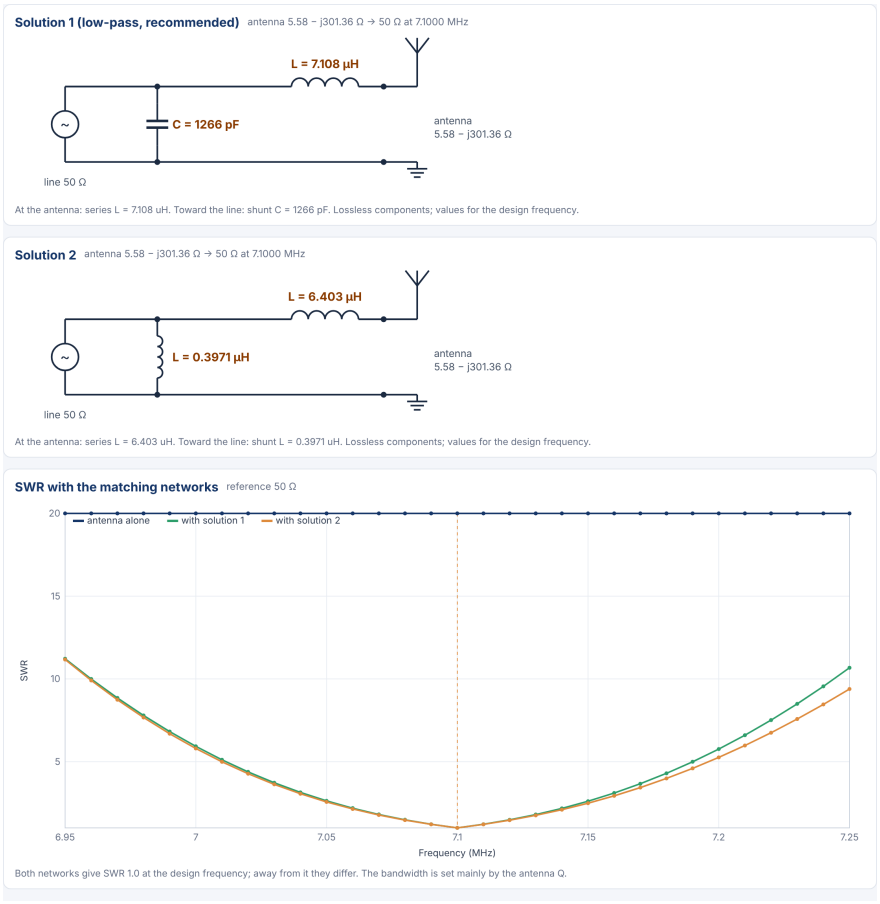


Figure 13. Results page, view Matching network, *for the short 40 m vertical: circuits of both solutions with component values, and the SWR of the antenna alone (top line, SWR far above 20) and with each network.*

© 2026 Communications Consulting Corp.

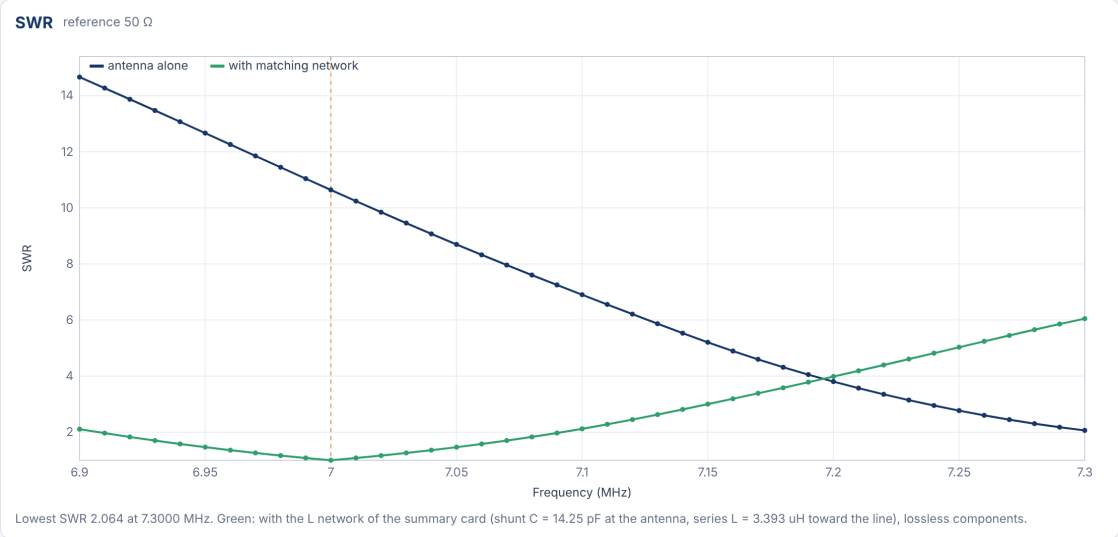


Figure 14. View SWR *for the curvilinear 7 MHz monopole: antenna alone (blue) and with the L network of solution 1 (green).*

Table 2 and Figure 15 give the networks, with circuit and values, that the program finds for further examples. Antennas close to 50 Ω need only small components; the loaded mobile whip ($18.5\,\Omega$) needs a large shunt capacitor; the quad ($75 + j29\,\Omega$) is matched with the shunt capacitor at the antenna.

Table 2: Matching Networks Computed for Example Antennas (Solution 1, to 50 \Omega)

Example	f (MHz)	Z_A (Ω)	SWR	at the antenna	toward the line
`short_vertical_40m`	7.1	$5.6 - j301.4$	334.86	series L = 7.108 μH	shunt C = 1266 pF
`loaded_whip_80m`	3.75	$18.5 + j0.5$	2.70	series L = 1.004 μH	shunt C = 1106 pF
`inverted_v_40m`	7.1	$47.6 - j23.2$	1.60	series L = 0.7576 μH	shunt C = 100 pF
`dipole_20m`	14.18	$71.3 - j12.7$	1.51	shunt C = 77.45 pF	series L = 0.3852 μH
`quad_2el_20m`	14.15	$75.1 + j29.1$	1.85	shunt C = 161.4 pF	series L = 0.4796 μH
`moxon_20m`	14.15	$41.2 + j8.2$	1.30	series L = 0.1219 μH	shunt C = 103.7 pF
`paper_curvilinear_7MHz`	7	$60.8 - j162.5$	10.64	shunt C = 14.25 pF	series L = 3.393 μH

© 2026 Communications Consulting Corp.

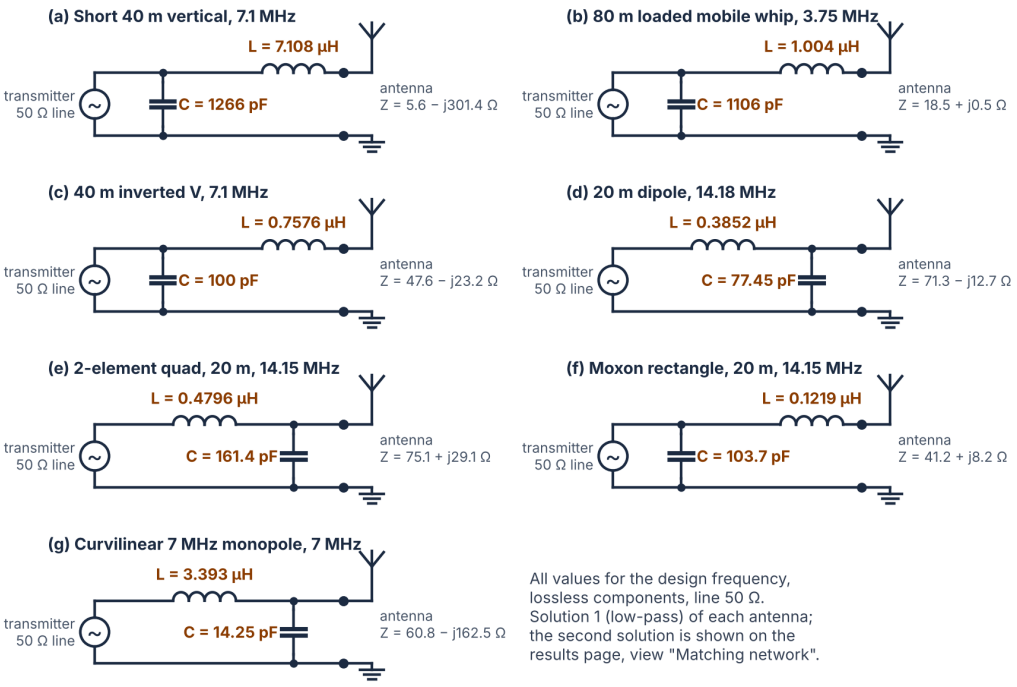


Figure 15. Circuits and component values of the matching networks of Table II, as computed by the program.

8.4 Circular Polarization (RHCP and LHCP)

A circularly polarized wave rotates its electric field once per period. Seen in the direction of propagation, a clockwise rotation is right-hand (RHCP), a counter-clockwise one left-hand (LHCP), following the IEEE definition [11]. The program splits the far field into the two components,

$$E_R = \frac{E_\vartheta + jE_\varphi}{\sqrt{2}}, \qquad E_L = \frac{E_\vartheta - jE_\varphi}{\sqrt{2}}, \qquad (23)$$

and gives the RHCP and LHCP gain in every direction; their sum is the total gain. A good circularly polarized antenna has a large difference between the wanted and the unwanted component (the cross-polar discrimination); the axial ratio follows from it.

How to use it. On the results page, view *3D radiation pattern*, press *RHCP* or *LHCP*; in the views *Elevation pattern* and *Azimuth pattern* press *RHCP / LHCP*: the vertical and horizontal curves are replaced by the RHCP (violet) and LHCP (red) curves.

Example 3: axial-mode helix, right- and left-hand (`helix_axial_1ghz.ant`, `helix_axial_1ghz_left.ant`). The 6-turn helix for 1 GHz with the normal (right-hand) winding radiates RHCP along its axis: 9.6 dBi RHCP and -12.5 dBi LHCP at the zenith, a discrimination of 22 dB (Figure 16, left). The same helix with `left` in the `HELIX` command radiates the mirror image: LHCP 9.6 dBi, RHCP -12.5 dBi (right). Transmit and receive antennas must have the same sense of rotation; the wrong one costs about 20 dB.

Example 4: turnstile for 2 m (`turnstile_2m.ant`). Two crossed half-wave dipoles fed with equal amplitude and 90° phase difference (`SOURCE dx 50 V=1 phase=0`, `SOURCE dy 50 V=1 phase=-90`) produce circular polarization along the axis, used for satellite reception. Upward the wave is RHCP (2.1 dBi;

LHCP -28 dBi), downward it is LHCP, because the direction of propagation is reversed (Figure 17). Changing the phase to $+90^\circ$ reverses both.

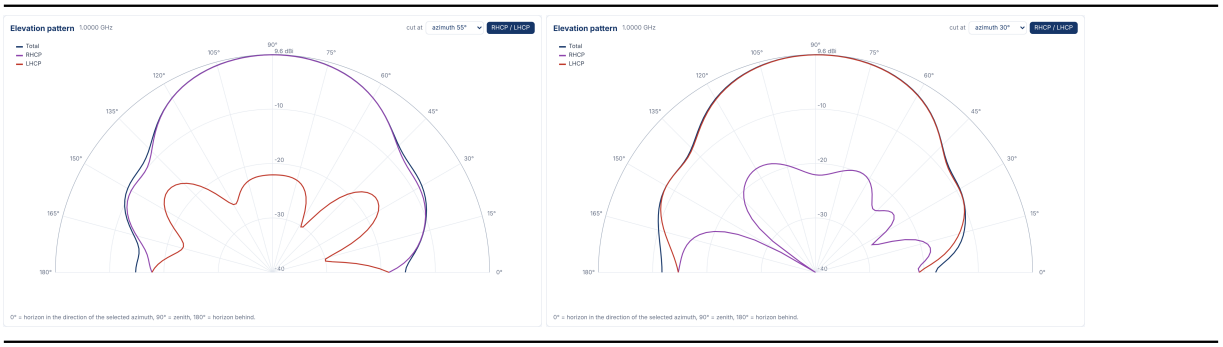


Figure 16. Elevation patterns with the button RHCP / LHCP*: axial-mode helix for 1 GHz with right-hand winding (left: RHCP dominant, 9.6 dBi) and with left-hand winding (right: LHCP dominant).*

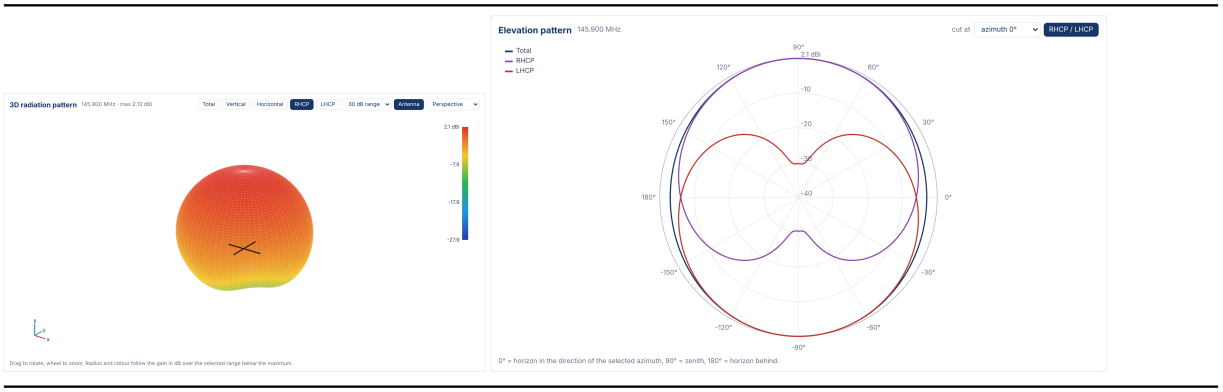


Figure 17. Turnstile for 2 m: 3D pattern of the RHCP component (left) and elevation pattern with RHCP and LHCP (right). Upward (elevation 90°) the radiation is RHCP, downward LHCP.

8.5 Low Antennas: Sommerfeld Ground

Below about 0.1λ a wire couples strongly to the lossy earth. The reflection-coefficient ground then fails: Figure 18 shows the feed impedance of a 20 m dipole over average ground against height. At 0.02λ the reflection coefficients give $22-j78\,\Omega$, the Sommerfeld ground $85+j11\,\Omega$, and NEC-2 with its Sommerfeld ground (`GN 2`) $86+j12\,\Omega$. Above 0.15λ both ground models agree. Add the keyword to the ground line, or choose *Real*, *Sommerfeld* as ground in the settings:

```
GROUND real eps=13 sigma=0.005 sommerfeld
```

NEC-2 decks with `GN 2` use it automatically. The example `dipole_80m_low_sommerfeld.ant` is an 80 m NVIS dipole only 3 m (0.036λ) high: $50.3-j38.3\,\Omega$ and -1.07 dBi at the zenith, against $25.8-j74.9\,\Omega$ and $+1.71$ dBi with the reflection coefficients; the Sommerfeld ground shows the real loss in the earth (efficiency 13 % instead of 25 %). Table 3 compares seven decks with NEC-2. The Sommerfeld ground needs a table per frequency and takes about 0.5–5 s more per frequency.

A wire that touches a lossy earth (a vertical fed against a ground rod) is idealised in every thin-wire program: the feed resistance depends on the real earth connection (rods, radials). The program warns; model such antennas with elevated radials or over perfect ground with a loss resistance.

© 2026 Communications Consulting Corp.

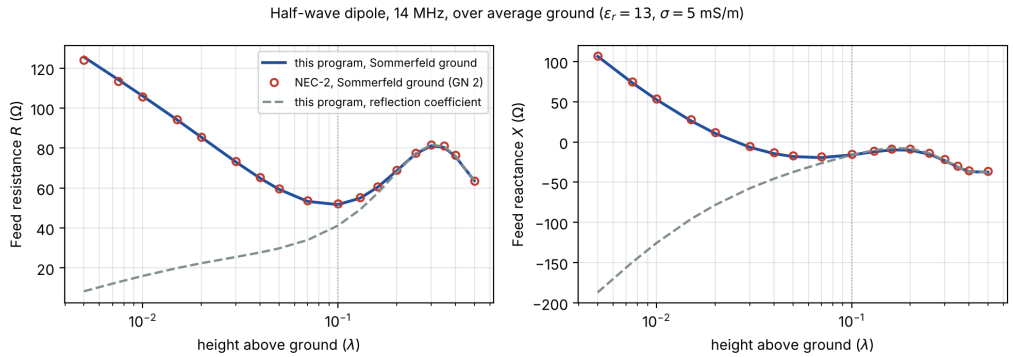


Figure 18. Feed impedance of a half-wave dipole for 14 MHz against its height over average ground: Sommerfeld ground of this program (line), NEC-2 with Sommerfeld ground (circles) and reflection-coefficient ground (dashed). Below 0.1λ (dotted) only the Sommerfeld ground is correct.

Table 3: Sommerfeld Ground: Comparison with NEC-2 (GN 2) on the Same Decks

Deck	Antenna	Height	NEC-2 Z_{in} (Ω)	Z_{in} (Ω)	NEC-2 / this G (dBi)	Refl. coeff. Z_{in} (Ω)
`som_hd_low`	dipole 14 MHz, average ground	0.012λ	$101.4 + j43.3$	$101.5 + j42.1$	-6.26 / -6.25	$17.6 - j113.6$
`som_hd_h1p07`	dipole 14 MHz, average ground	0.05λ	$59.7 - j17.0$	$59.3 - j18.1$	-0.43 / -0.43	$29.8 - j37.5$
`som_hd_poor`	dipole 14 MHz, poor ground	0.05λ	$73.2 - j15.2$	$72.8 - j16.4$	-0.50 / -0.50	$39.1 - j38.9$
`som_hd_sea`	dipole 14 MHz, sea water	0.05λ	$8.25 - j28.1$	$8.18 - j28.9$	7.22 / 7.22	$7.28 - j30.7$
`som_vd_low`	vertical dipole, average ground	0.023λ	$85.9 - j27.8$	$85.1 - j29.3$	0.24 / 0.26	$81.2 - j27.9$
`som_gp`	ground plane, 4 radials	0.047λ	$30.9 - j7.9$	$30.2 - j8.4$	0.08 / 0.16	$25.8 - j6.8$
`som_nvis80`	NVIS dipole 3.6 MHz	0.036λ	$49.2 - j37.9$	$48.9 - j38.4$	-0.93 / -0.94	$24.3 - j75.1$

Average ground $\varepsilon_r = 13$, $\sigma = 5$ mS/m; poor ground 5, 1 mS/m; sea water 81, 5 S/m. The small reactance offset of about 1 Ω is the same in free space (different feed-gap models); the change of impedance caused by the ground agrees within 1–2 %.

© 2026 Communications Consulting Corp.

8.6 Printed Antennas on Circuit Boards

Printed antennas are traces on a circuit board. The board is described in the ground line; its top surface is the plane $z = 0$, and the traces are wires lying on it:

```
GROUND pcb eps=4.4 tand=0.02 h=1.6mm
GROUND pcb eps=4.4 tand=0.02 h=1.6mm groundplane
WIRE -21.7 0 0  21.7 0 0  w=1 name=dipole
```

The first line is a board in air, the second a board with a ground plane underneath, the third a 1 mm trace on the board. `eps` is the relative permittivity, `tand` the loss tangent, `h` the thickness (units mm, mil or in may be appended), and `groundplane` adds a perfect ground plane at $z = -h$. The trace option `w=` gives the width of a flat trace, which is represented by a round wire of radius $w/4$. In the program window choose *Printed board* or *Board + ground* as ground. The near field of the board is computed exactly with the layered-medium formulation of Section 6.4; the radiation pattern covers the full sphere for a board in air and the upper half space with a ground plane.

Example: printed dipole (`printed_dipole_2p45GHz.ant`, Figure 20). A dipole of two 1 mm traces on FR-4 (1.6 mm, tan $\delta = 0.02$) resonates at 2.456 GHz with a total length of 43.4 mm instead of about 58 mm in free space: $53.3 - j1.2\,\Omega$, 0.96 dBi. The far-field power is 67.6 % of the input (72.5 % without dielectric loss); the rest is dielectric loss and the surface wave guided by the board, which on a real, finite board largely radiates from its edges.

Example: microstrip resonator (`microstrip_resonator_fr4.ant`). A center-fed 0.5 mm trace over a ground plane is a half-wave microstrip resonator. Its series resonance agrees with the closed-form microstrip model of Hammerstad and Jensen [23] within 0.4 % on FR-4, RT/duroid 5880 and RO3010 (Table 4).

Example: patch antenna (`patch_2p45GHz_fr4.ant`). A rectangular patch 37.3×28.8 mm on FR-4 with ground plane (dimensions from the transmission-line model for 2.45 GHz [4]) is modeled as a grid of wires (radius = cell/2π). In the validation decks (`patch_air`, `patch_fr4`) it is fed by a gap at the center of a radiating edge; the frequency ratio between the patch on air and on FR-4 agrees with the cavity model within 0.9 % (Table 4), so the board is represented correctly. A wire grid, however, resonates lower than the solid patch it represents. For the patch on a board with $\varepsilon_r = 1$ (gap feed) the resonance is 4.380, 4.455 and 4.504 GHz with 2.1, 1.4 and 1.0 mm cells against 4.82 GHz from the transmission-line model (NEC-2 gives 4.48 GHz for the 2.1 mm grid); for the dual-resonance patch below a finer grid gives no change. Expect the resonance of a wire-grid patch 7–10 % below that of the solid patch, and scale the dimensions accordingly. With the 2 mm grid of the example the FR-4 patch, fed by a 6 mm microstrip line, resonates at 2.23 GHz with 2.0 dBi and 36 % far-field power (dielectric loss with tan $\delta = 0.02$ and surface waves; Figure 20).

Test case: patch with two resonances (`patch_dual_resonance_rt5880.ant`, Figure 19). A rectangular patch with unequal sides (40×30 mm on RT/duroid 5880, 1.575 mm, ground plane) has two fundamental cavity modes, one along each side. A microstrip feed 10 mm off the center line excites both. The cavity (transmission-line) model [4] gives 2.501 and 3.272 GHz; the program finds 2.327 and 2.994 GHz with 2 mm cells and 2.330 and 2.987 GHz with 1.33 mm cells. Both modes are found; the ratio of the two frequencies, 1.287, agrees with the cavity model (1.308) within 1.6 %, while the absolute frequencies show the wire-grid offset of 7–8.5 %.

© 2026 Communications Consulting Corp.

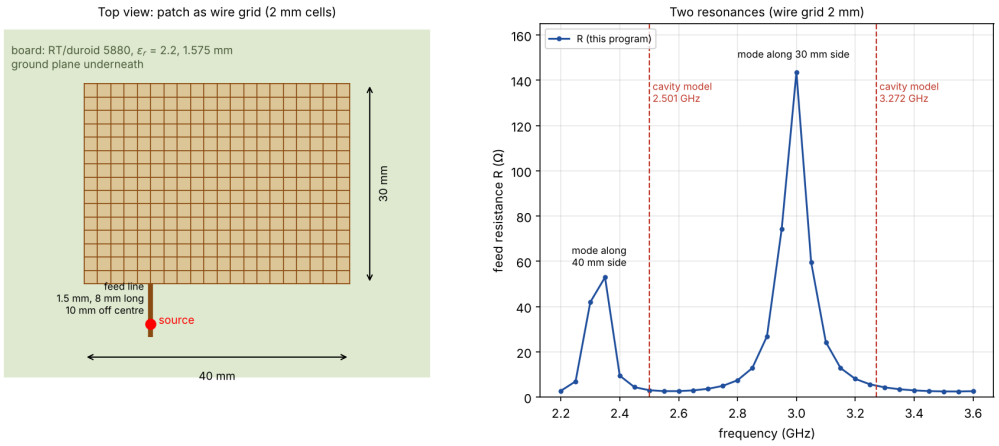


Figure 19. Test case with two resonances: patch 40×30 mm on RT/duroid 5880 with off-center microstrip feed, modeled as a 2 mm wire grid (left), and its feed resistance with the two resonances compared with the cavity model (right).

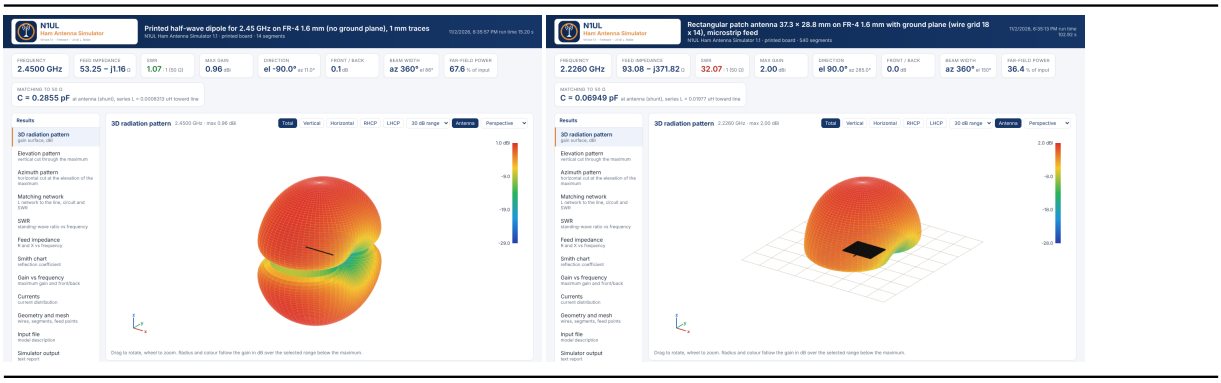


Figure 20. Printed antennas: dipole on FR-4 without ground plane (left; the pattern covers the full sphere, with a null along the board) and wire-grid patch on FR-4 with ground plane (right).

Table 4: Printed Boards: Validation of the Board Model

Deck	Structure	Reference	This program	Deviation
`v_pcb_free`	dipole on board with $\varepsilon_r = 1$, no ground plane	free space $85.898 + j46.257\,\Omega$	$85.898 + j46.257\,\Omega$	exact
`v_pcb_image`	dipole on board with $\varepsilon_r = 1$, ground plane at depth 0.2λ	perfect ground $86.012 + j92.591\,\Omega$	$86.012 + j92.592\,\Omega$	exact
`ms_fr4`	microstrip resonator, FR-4 1.6 mm, $w = 0.5$ mm	MHz (Hammerstad–Jensen)	2440.4 MHz	$-0.39\,\%$
`ms_rt5880`	microstrip resonator, RT/duroid 5880 0.787 mm	MHz	2446.0 MHz	$-0.16\,\%$
`ms_ro3010`	microstrip resonator, RO3010 0.635 mm, $w = 0.3$ mm	MHz	2443.2 MHz	$-0.28\,\%$

© 2026 Communications Consulting Corp.

Deck	Structure	Reference	This program	Deviation
`cps_fr4`	coplanar strips on FR-4, no ground plane	MHz ($\varepsilon_{\text{eff}} = 2.590$, 2D)	3025.1 MHz	$+0.04\,\%$
`cps_ro3010`	coplanar strips on RO3010, no ground plane	MHz ($\varepsilon_{\text{eff}} = 4.042$, 2D)	2366.7 MHz	$-0.14\,\%$
`patch_fr4`	wire-grid patch, air/FR-4 frequency ratio	ratio 1.9694 (cavity model [4])	1.9516 (4379.5/2244.1 MHz)	$-0.9\,\%$
`patch_dual_b`	patch 40×30 mm, RT/duroid 5880: ratio of the two resonances	ratio 1.3080 (cavity model [4])	1.2866 (2994.2/2327.3 MHz)	$-1.6\,\%$
`patch_dual_a`	the same patch, first resonance (absolute)	MHz (cavity model)	2327.3 MHz	$-7.0\,\%$ (wire grid)

Coplanar strips: resonance of a shorted 30 mm line, referred to the same line in air; ε_{eff} from an independent two-dimensional quasi-static moment-method calculation of the flat strips on the board (the conformal-mapping formula [24] gives 2.595 and 4.380; for the thin RO3010 board it is 8 % too high).

8.7 Multi-Core Solution

The filling of the impedance matrix, the LU decomposition and the pattern grid run in parallel on all processor cores (native threads, no additional libraries); the results are bit-identical to the single-core solution. On two cores a model with 2400 unknowns runs 1.5 times faster; the gain grows with the number of cores.

9 Parabolic Reflector Antennas

A dish of many wavelengths cannot be modeled as a wire grid: the 46 m dish of the book cover (Figure 2) is 67 wavelengths wide at 440 MHz and would need millions of segments. The program therefore combines the moment method for the feed with physical optics (PO) for the reflector [4], [26]. The feed is any wire antenna of the model: a dipole with a reflector screen, a crossed dipole for circular polarization, a short backfire, a helix; or, for studies, an ideal $\cos^q$ feed.

9.1 Model

One line adds the reflector:

```
DISH D=46 FD=0.4 [F=18.4] [mesh=5cm wire=2mm]
     [block=1] [q=1]
```

`D` is the aperture diameter and `F` the focal length (or `FD` the ratio F/D). The focus is at the origin, the vertex at $z = -F$, and the main beam points toward $+z$: the wires of the feed are placed around the origin and radiate toward $-z$. `mesh` and `wire` describe a wire-mesh surface (square cells and wire diameter), `block` the diameter of the central blockage by the feed housing, and `q` replaces the wire feed by the ideal feed $E \propto \cos^q \psi$ (ψ = angle from the feed axis), a Huygens source without cross-polarization.

9.2 Method

The feed currents I from the moment method give the far field $\mathbf{F}(\theta', \phi')$ of the feed, $\mathbf{E} = \mathbf{F}\, e^{-jkr}/r$. The reflector ($\rho \le D/2$, $z = \rho^2/4F - F$) is far from the feed ($F \gg \lambda$), so its incident field is

$$\mathbf{H}_i = \frac{1}{\eta_0}\,\hat{\mathbf{r}} \times \mathbf{F}(\theta', \phi')\,\frac{e^{-jkr}}{r}, \qquad (24)$$

and the PO current on the illuminated side is $\mathbf{J} = 2\,\tau\,\hat{\mathbf{n}} \times \mathbf{H}_i$ ($\tau = 1$ for a solid surface). It radiates

$$\mathbf{F}_s\,(\hat{\mathbf{r}}) = -\frac{jk\eta_0}{4\pi}\int_S \left[\mathbf{J} - (\mathbf{J}\cdot\hat{\mathbf{r}})\,\hat{\mathbf{r}}\right] e^{jk\hat{\mathbf{r}}\cdot\mathbf{r}'}\,dS, \qquad (25)$$

and the total far field is $\mathbf{F} + \mathbf{F}_s$ (the field of the feed passes the dish on the sides; behind the dish the two cancel in part). The surface is sampled in rings with steps of $\lambda/8$ (about 230 000 points for the 46 m dish); all cores are used. The gain refers to the input power of the feed. The reaction of the dish on the feed (its change of impedance) is neglected.

Wire mesh. A square mesh of cell size a and wire radius r_w ($a \ll \lambda$) is an inductive sheet with the reactance $X = \eta_0\,(a/\lambda)\,\ln\,(a/2\pi r_w)$ [27]; it reflects $\Gamma = -1/\,(1 + 2jX/\eta_0)$ at normal incidence. The PO current is multiplied by $\tau = -\Gamma$, and $|\Gamma|^2$ is reported as the reflected power. A 5 cm mesh of 2 mm wire reflects 91.5 % at 440 MHz (0.38 dB loss); a 2 cm mesh of the same wire 98.9 %.

Efficiencies. With $\theta_0 = 2\arctan(D/4F)$ the half-angle of the rim seen from the focus, the program reports the spillover efficiency (feed power within the cone of the dish), the aperture efficiency $\eta_{\text{ap}} = G/(\pi D/\lambda)^2$, the illumination efficiency $\eta_{\text{ap}}/\,(\eta_{\text{spill}}\,|\Gamma|^2)$ (taper, phase, cross-polarization and blockage), the edge illumination (feed pattern and spreading loss $[(1 + \cos\theta_0)\,/2]^2$), the 3-dB beam widths and the first side lobes in the E- and H-plane.

9.3 Example: the 46 m Dish of the Book Cover at 440 MHz

The example `dish_46m_440MHz.ant` is a sketch of a 46 m UHF dish of the kind on the book cover: prime focus, $F/D = 0.4$ (assumed; the real value can be entered), a 5 cm wire mesh of 2 mm wire and 1 m central blockage. The feed is a half-wave dipole of 12 mm aluminum tube with a screen of five rods 0.15 m behind it. Results (run time about 1 min):

- gain 44.3 dBi, against 46.5 dBi of a uniformly illuminated aperture: aperture efficiency 59.9 % = spillover 76.6 % × illumination 85.5 % × mesh 91.5 %;
- edge illumination -10.2 dB; 3-dB beam width 1.03° (E-plane) and 0.94° (H-plane);
- first side lobes -28 dB (E-plane) and -21 dB (H-plane): the dipole illuminates the H-plane edge more strongly;
- feed impedance $124 + j39\,\Omega$, to be matched with the automatic L network (Section 8).

The spillover of 23 % is the main loss: a feed with a narrower, more symmetric pattern (for example a dipole in a cylindrical cup, or a short backfire) raises the efficiency toward 70–80 %. The same model with $D = 43$ m at 435 MHz (`dish_43m_435MHz.ant`) gives 43.6 dBi, 60.2 % and beam widths of 1.11° and 1.02°.

© 2026 Communications Consulting Corp.

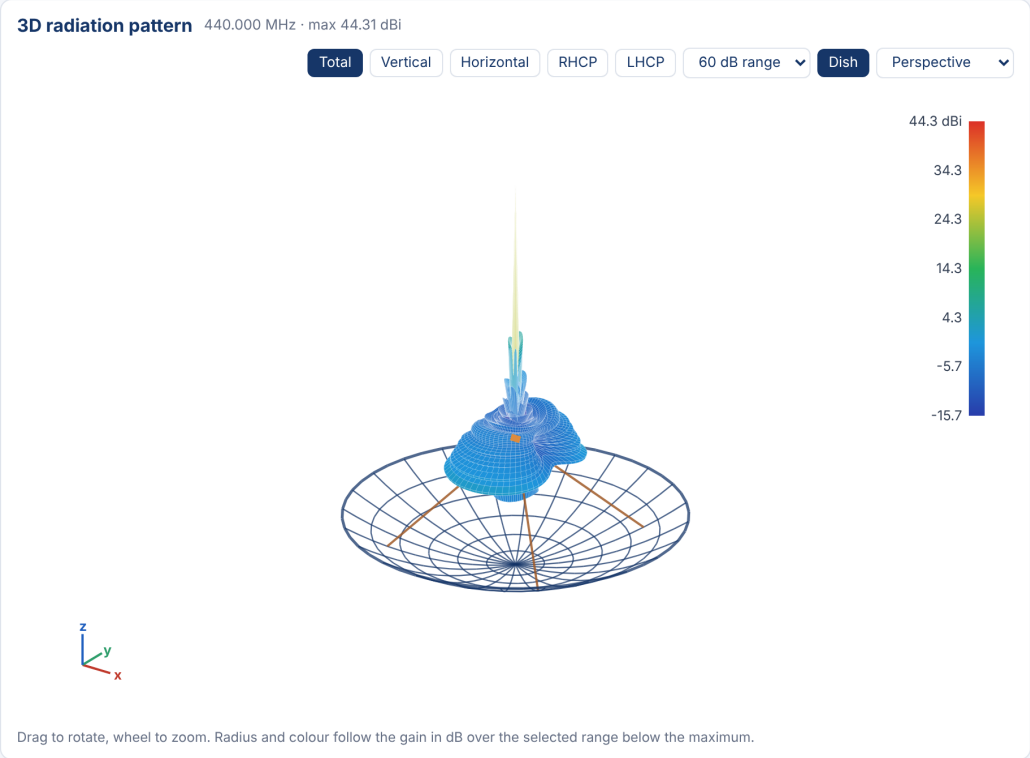


Figure 21. 46 m dish at 440 MHz with a dipole-and-screen feed (`dish_46m_440MHz.ant`): three-dimensional pattern over 60 dB, drawn with the reflector to scale (rim, ribs and feed supports; the feed at the focus is the center of the pattern). The needle-shaped main beam points away from the dish; below are the side lobes, the spillover past the rim and the back radiation.

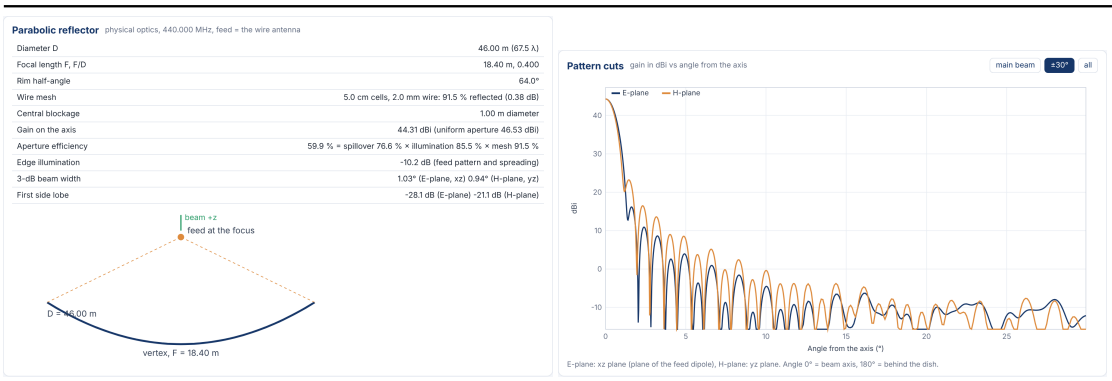


Figure 22. Results view of the dish: card with the efficiencies and the profile (left), E- and H-plane cuts to $\pm 30^\circ$ (right).

9.4 Verification

For the ideal $\cos^q$ feed the aperture efficiency is known in closed form (Silver [26], [4]):

$$\eta_{\text{ap}} = \cot^2\frac{\theta_0}{2}\left|\int_0^{\theta_0}\sqrt{G_f(\psi)}\,\tan\frac{\psi}{2}\,d\psi\right|^2, \quad G_f = 2(2q+1)\cos^{2q}\psi. \qquad (26)$$

Four dishes of 10λ with $q = 1$, 2, 3 and $F/D = 0.3$ to 0.6 agree with this formula within 0.003 dB, the spillover efficiency equals $1 - \cos^{2q+1}\theta_0$, and the radiated power (integral of the gain over the sphere) equals the feed power within 0.4 % (Table 8, cases `dish_*`). The mesh check confirms the gain reduction $10 \log |\Gamma|^2$.

10 Example Antennas

Table 5 lists the native examples with the results at the design frequency, and Figs. 23–38 show their 3D pattern, elevation and azimuth patterns and SWR (or the current distribution). The NEC-2 examples are listed in Table 6.

Table 5: Results of the Example Antennas at the Design Frequency

Example	Ground	f (MHz)	Z_{in} (Ω)	SWR	G_{max} (dBi)	F/B (dB)	Segments	Mesh check (%)
`curved_monopole`	PEC	300	$52.17 + j68.10$	3.49	5.15	–	10	2.6
`dipole_20m`	real	14.175	$71.26 - j12.74$	1.51	7.04	–	18	1.9
`four_square_40m`	PEC	7.15	$19.76 + j6.66$	2.58	10.76	13.8	36	3.3
`gp_vertical_20m`	real	14.15	$60.70 + j8.38$	1.28	0.61	–	45	1.6
`helix_axial_1ghz`	PEC	1000	$167.02 - j76.68$	4.10	9.60	–	224	0.2
`inverted_v_40m`	real	7.1	$47.63 - j23.17$	1.60	4.84	–	18	3.0
`loaded_whip_80m`	PEC	3.75	$18.54 + j0.49$	2.70	-8.73	–	6	2.3
`lpda_14_30`	real	21.2	$101.54 + j25.76$	1.29	10.37	7.0	210	8.1
`magloop_20m`	real	14.1	$0.14 + j0.87$	–	0.51	–	24	0
`meander_dipole`	free	868	$49.56 + j145.69$	10.47	1.95	–	262	0
`moxon_20m`	real	14.15	$41.23 + j8.18$	1.30	11.19	30.7	53	2.4
`quad_2el_20m`	real	14.15	$75.13 + j29.05$	1.85	12.24	20.4	91	2.4
`yagi_3el_20m`	real	14.15	$32.82 + j7.43$	1.58	12.71	23.5	47	3.8
`pcb_ifa_2p45GHz`	free	2450	$62.82 + j3.47$	1.27	2.24	–	366	0
`helix_axial_3p5GHz_cfree`	free	3500	$91.81 - j78.38$	3.43	13.09	19.9	2046	0
`helix_axial_10GHz`	free	10368	$109.35 - j66.78$	3.14	12.40	19.0	1493	0.2

SWR referred to 50 Ω (LPDA 100 Ω); the magnetic loop is series-fed ($R = 0.14\,\Omega$) and needs a coupling loop. Mesh check: change of Z_{in} with twice the segment density.

© 2026 Communications Consulting Corp.

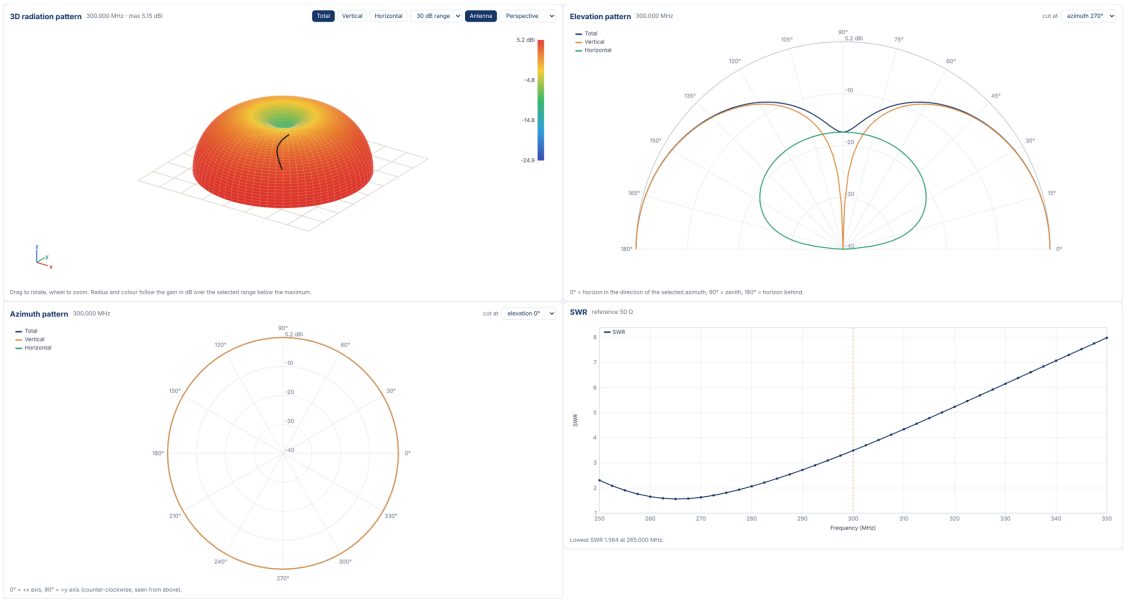


Figure 23. Example `curved_monopole.ant`: Curved monopole over perfect ground, entered as a spline through five points (Figure 6). The curvature tilts the pattern slightly; the horizontal current component adds a horizontally polarized part.

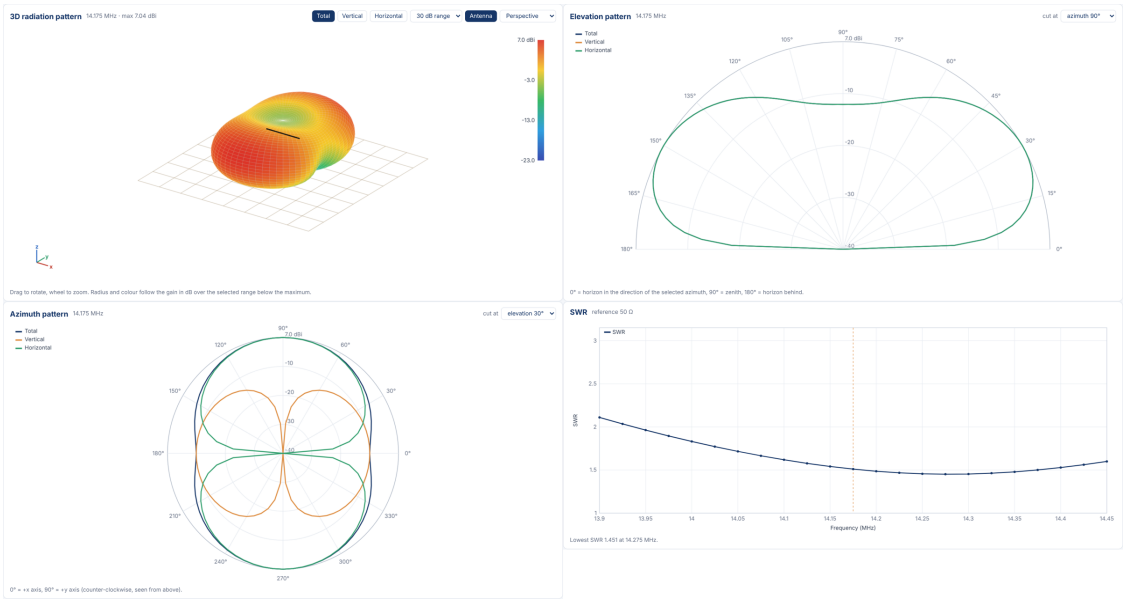


Figure 24. Example `dipole_20m.ant`: Half-wave dipole for 20 m, #12 copper wire, 10 m over average ground. Maximum gain 7.0 dBi at 30° elevation.

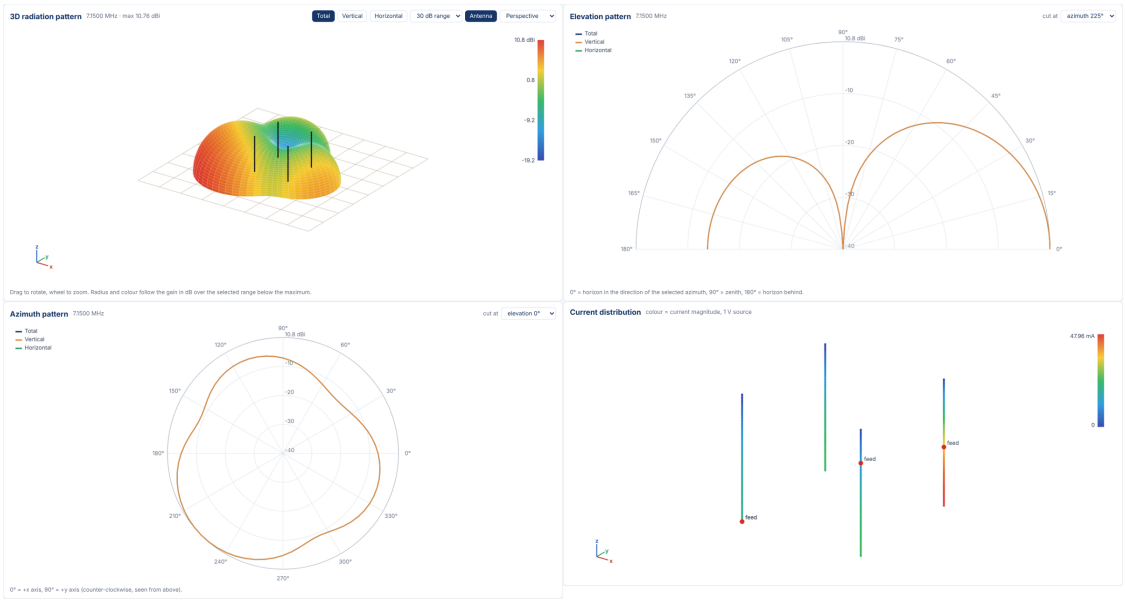


Figure 25. Example `four_square_40m.ant`: Four-square array of quarter-wave verticals over perfect ground with sources at $0^\circ / -90^\circ / -90^\circ / -180^\circ$. With voltage sources the mutual coupling unbalances the element currents; current-forcing feed networks give a deeper rear null.

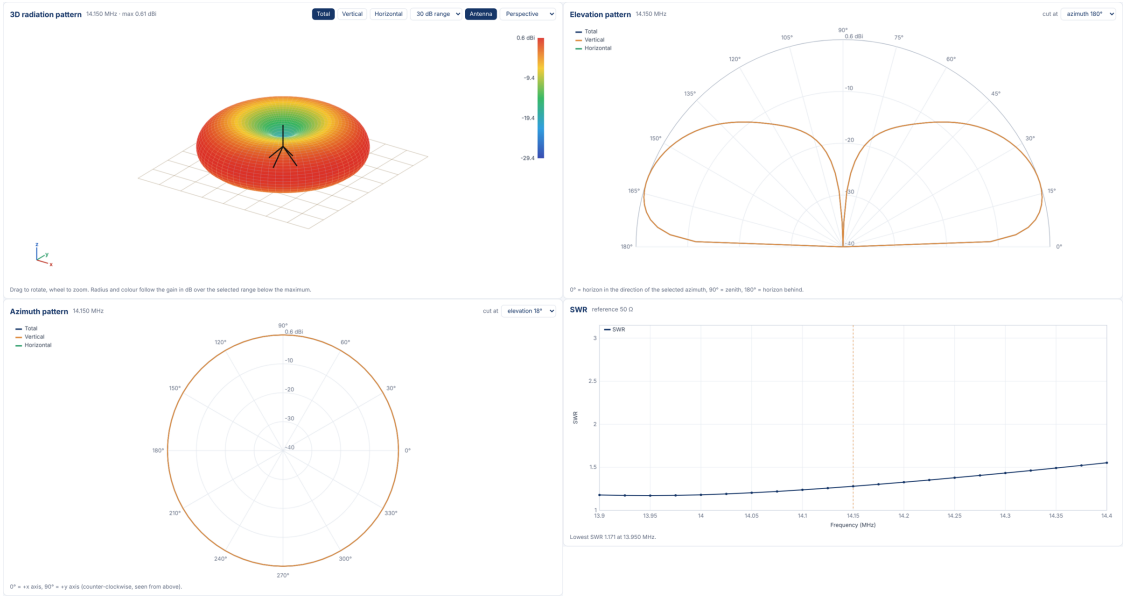


Figure 26. Example `gp_vertical_20m.ant`: Ground-plane vertical with four drooping radials, base 5 m above average ground; feed impedance near 50 Ω.

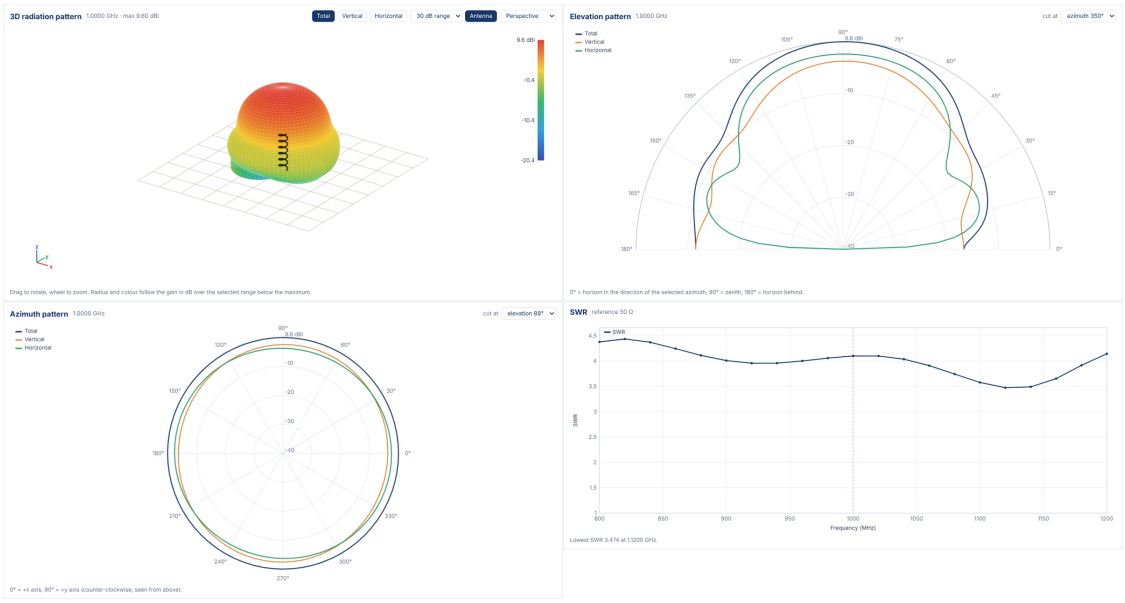


Figure 27. Example `helix_axial_1ghz.ant`: Axial-mode helix (Kraus) over a ground plane: circumference one wavelength, 13° pitch, six turns, 224 segments generated from the `HELIX` command.

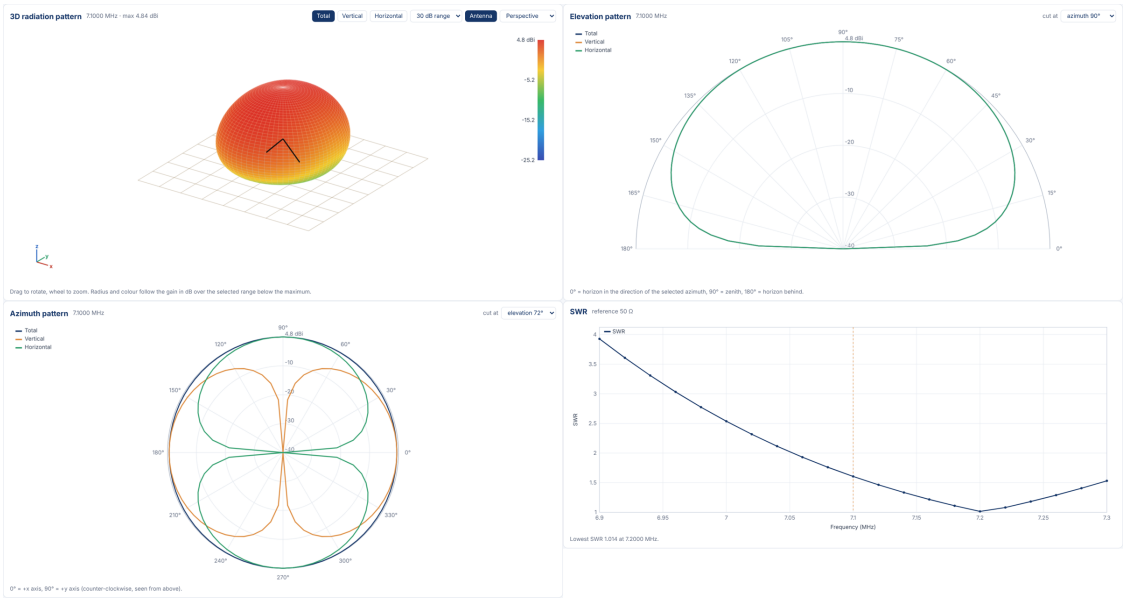


Figure 28. Example `inverted_v_40m.ant`: Inverted-V dipole for 40 m, apex 12 m, over average ground: high-angle radiation.

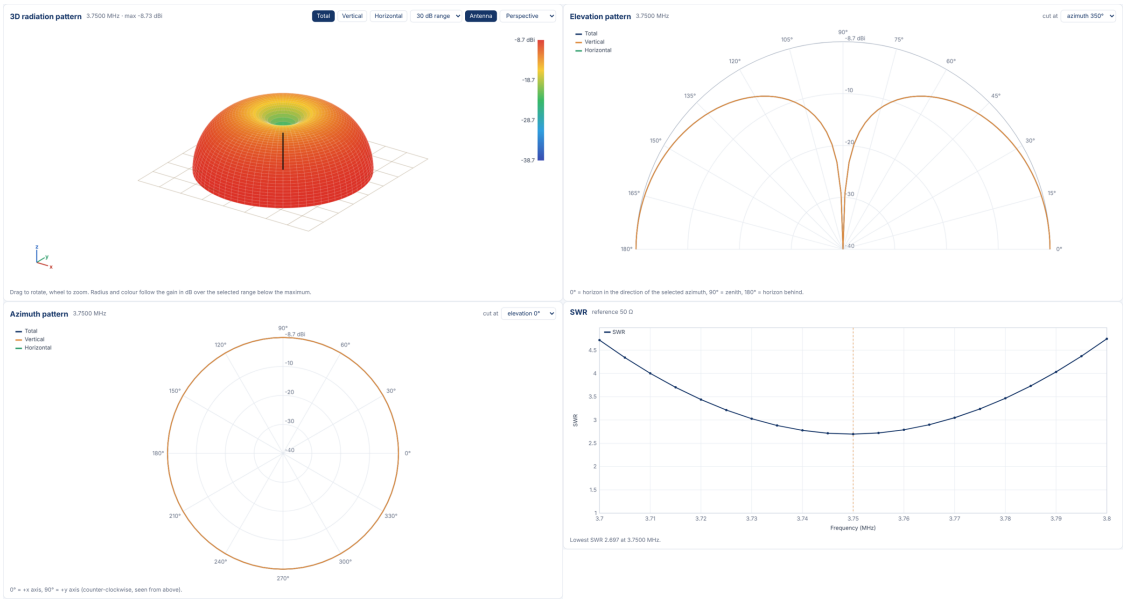


Figure 29. Example `loaded_whip_80m.ant`: 3 m mobile whip for 80 m with base loading coil ($Q \approx 200$) and 10 Ω ground loss; efficiency 4.5 %.

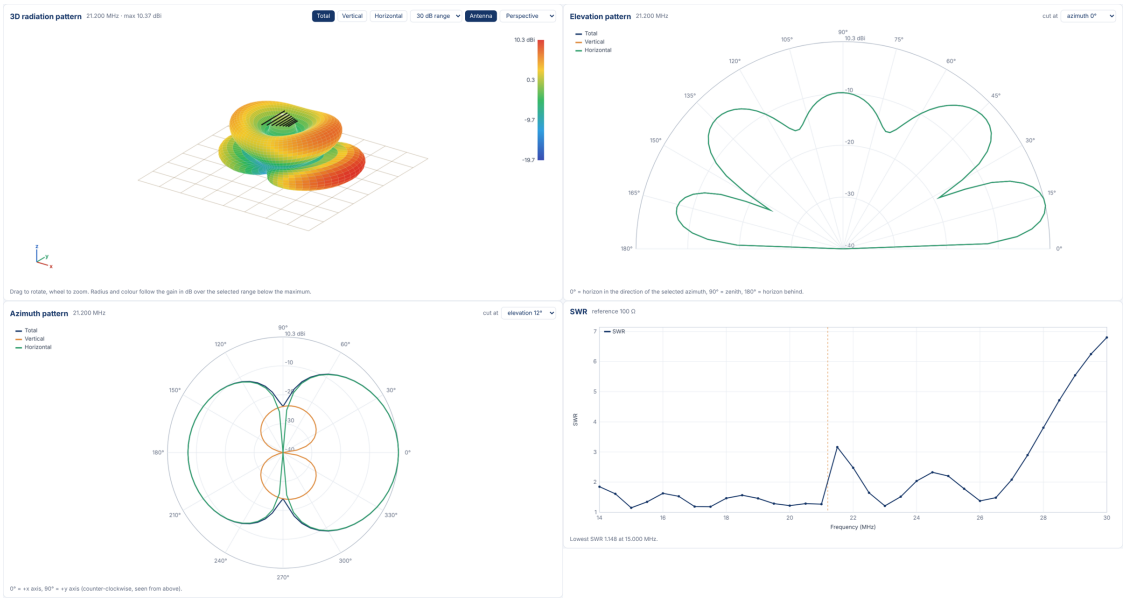


Figure 30. Example `lpda_14_30.ant`: Log-periodic dipole array 14–30 MHz, eight elements, fed by a crossed 100 Ω line (seven `TL` commands).

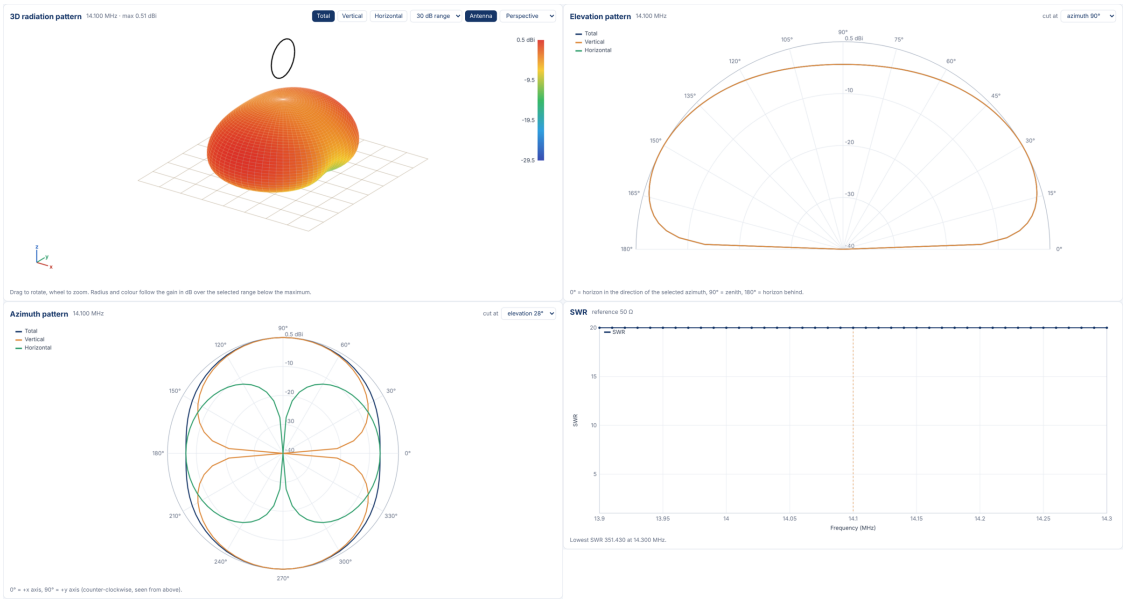


Figure 31. Example `magloop_20m.ant`: Small transmitting loop, 1 m diameter, 22 mm copper tube, tuned to 14.1 MHz by a 47.7 pF capacitor: radiation resistance about 0.1 Ω, copper loss about 0.04 Ω.

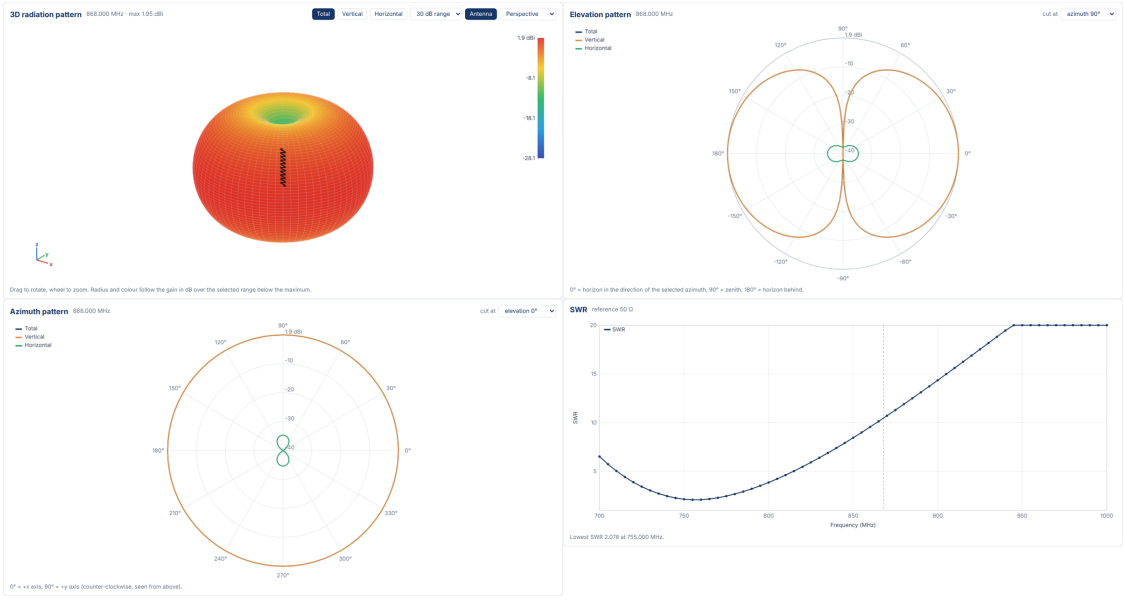


Figure 32. Example `meander_dipole.ant`: Meander-line dipole for 868 MHz defined by the formula $x = 0.008\sin(20\pi t)$; the mesh follows the curvature (262 segments).

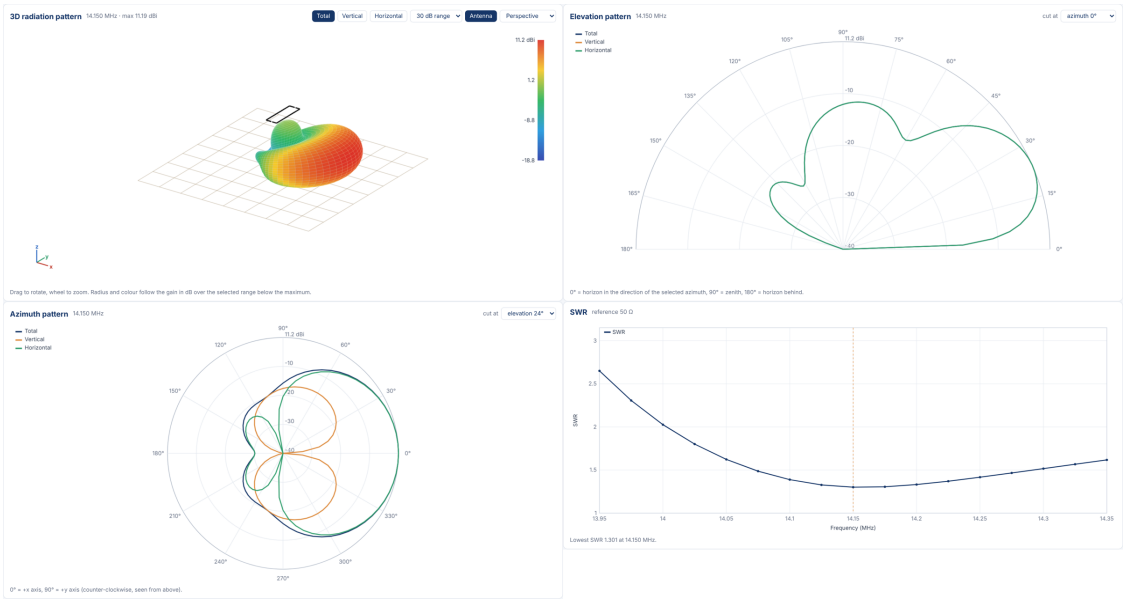


Figure 33. Example `moxon_20m.ant`: Moxon rectangle for 20 m, #12 copper, 12 m over average ground; dimensions optimized with the program for front-to-back ratio and match.

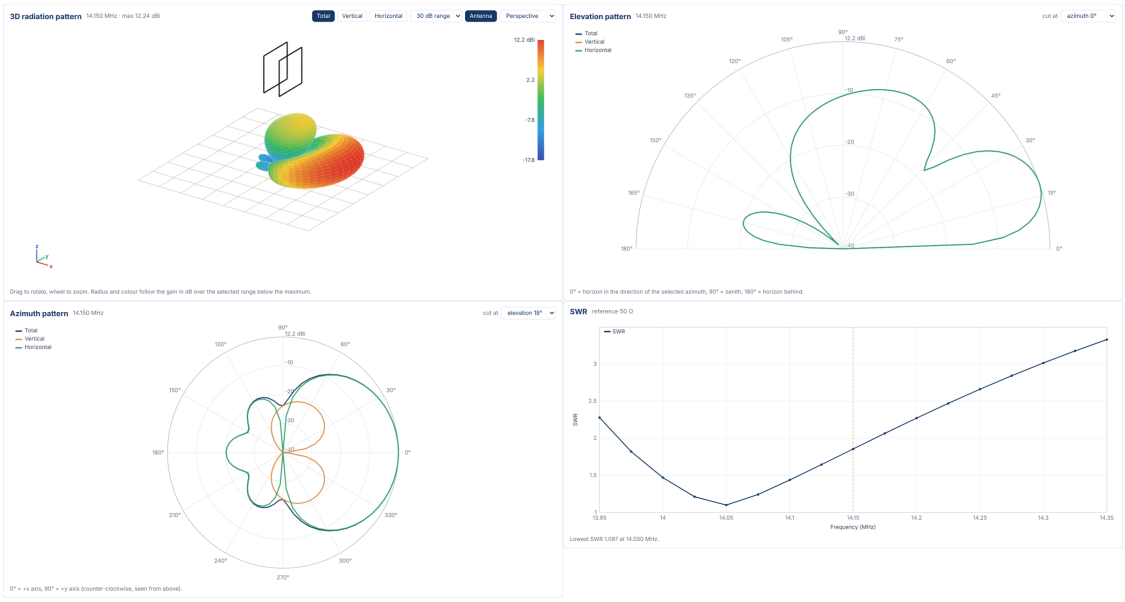


Figure 34. Example `quad_2el_20m.ant`: Two-element cubical quad for 20 m, 15 m over average ground.

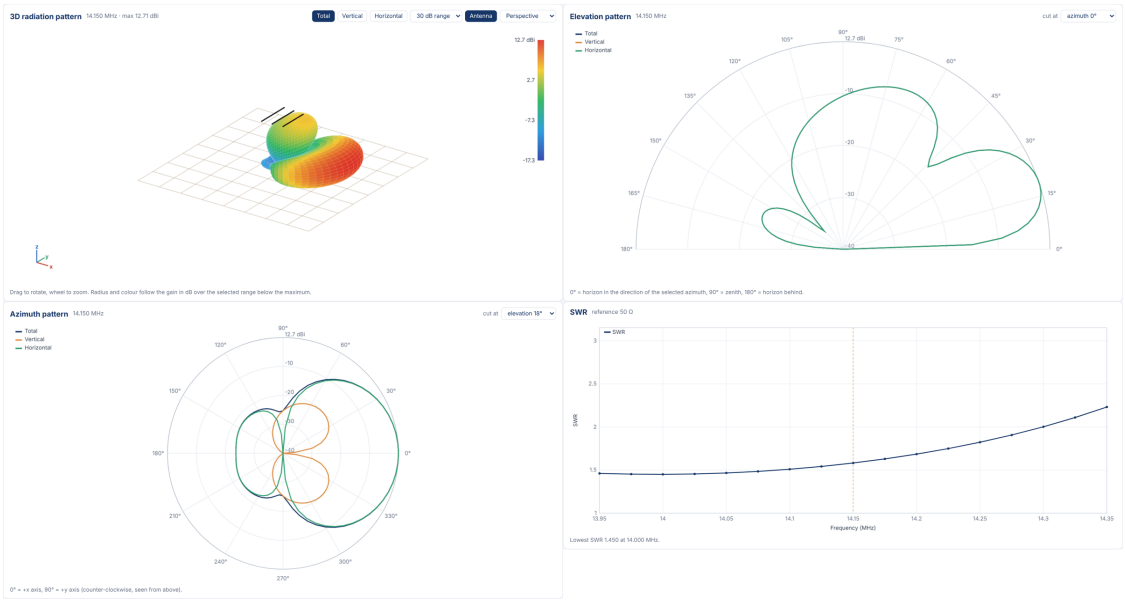


Figure 35. Example `yagi_3el_20m.ant`: 3-element Yagi for 20 m, 25 mm aluminum tubing, 15 m over average ground.

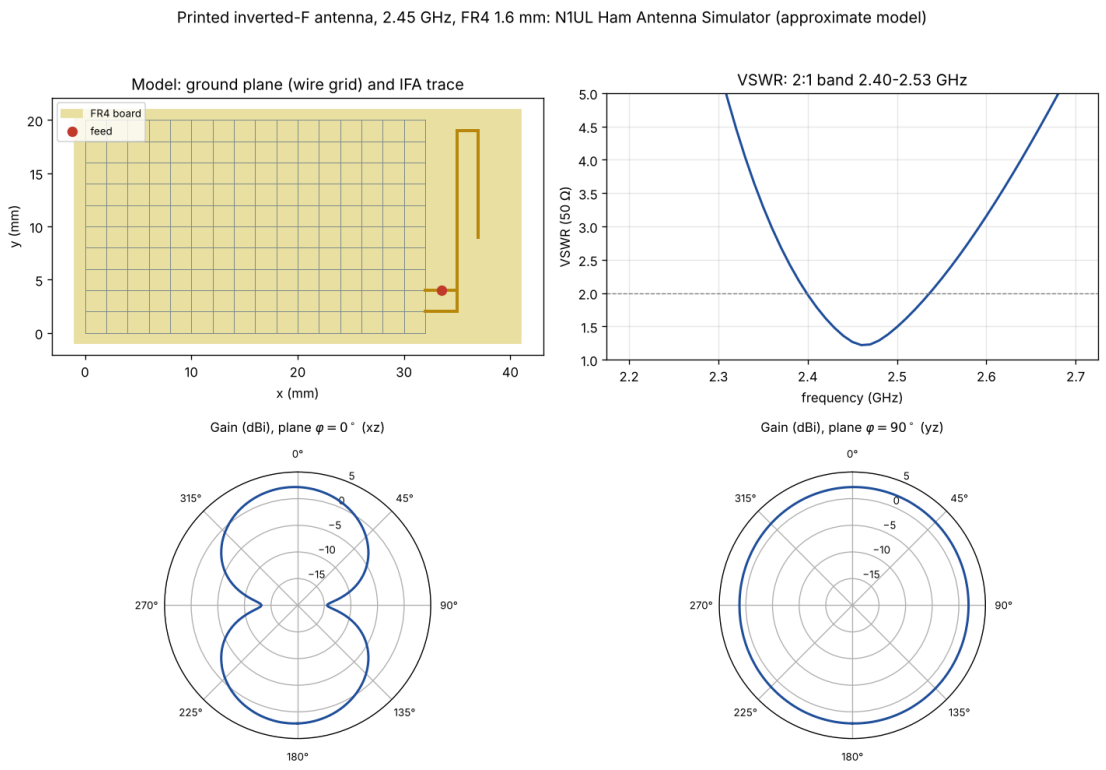


Figure 36. Example `pcb_ifa_2p45GHz.ant`: Printed inverted-F antenna for 2.45 GHz on a 40×20 mm FR4 board (1.6 mm), approximate model: the 0.5 mm trace is an insulated wire ($\varepsilon_r = 4.4$, 0.8 mm coating) and the ground plane a 2 mm wire grid. Match 1.27:1 at 2.45 GHz, 2:1 band 2.40–2.53 GHz, 2.2 dBi. FR4 loss is not included (real efficiency about 70–85 %); the resonance is accurate to about 5–10 %, so the arm is trimmed on the real board.

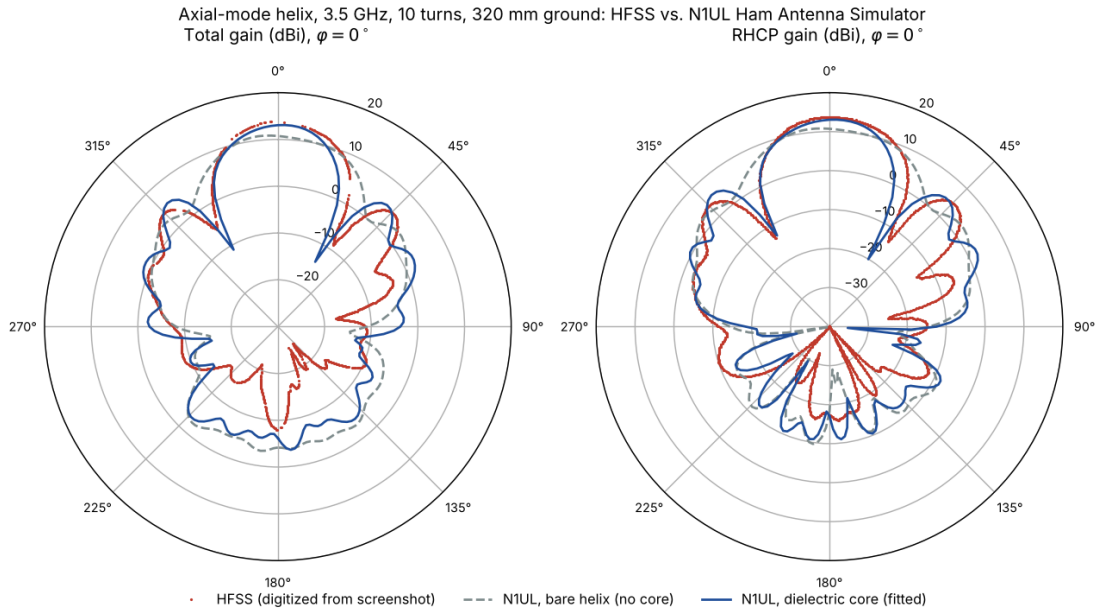


Figure 37. Example `helix_axial_3p5GHz_core.ant`: Axial-mode helix for 3.5 GHz, 10 turns, on a dielectric rod over a 320 mm ground plane, compared with an HFSS simulation (digitized). The bare helix gives 11.0 dBi; the dielectric core, which the thin-wire method cannot represent directly, is modeled by an effective permittivity of 1.6 (helix scaled by 1.265), fitted to the HFSS result: 13.1 dBi against 13.8 dBi, with matching beam width, nulls and RHCP pattern. The new RHCP/LHCP output of the program is used here.

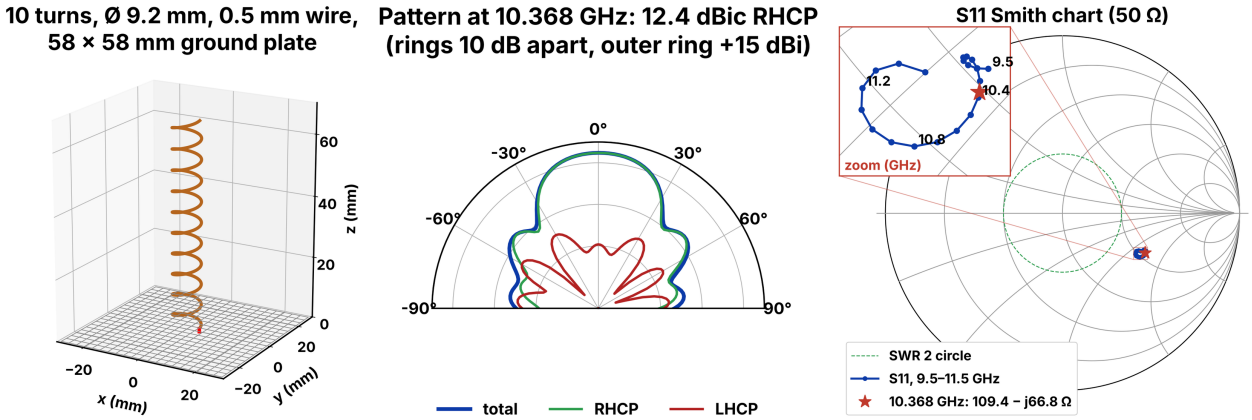


Figure 38. Example `helix_axial_10GHz.ant`: axial-mode helix for the 10 GHz amateur band (10.368 GHz), designed with the Kraus rules: circumference one wavelength (diameter 9.2 mm), pitch angle 13° (6.7 mm per turn), 10 turns, 0.5 mm copper wire, fed by a 1 mm pin over a 58×58 mm ground plate (wire grid). Left: geometry; centre: pattern in the xz plane with the RHCP and LHCP components; right: S_{11} in the Smith chart from 9.5 to 11.5 GHz with an enlarged view of the curve.

10 GHz helix: results. At 10.368 GHz the program gives 12.4 dBic right-hand circular gain along the axis, an axial ratio of 1.4 dB (LHCP 22 dB below RHCP), a half-power beam width of 43.5° and a front-to-back ratio of 19 dB. Across 9.5–11.5 GHz the gain rises smoothly from 12.1 to 13.2 dBi and the impedance stays near $100 - j60\,\Omega$; in the Smith chart the whole band forms one small loop, the typical broadband behavior of the axial-mode helix. The average gain test is 1.0004 and the impedance changes by 0.2 % when the segment density is raised from 20 to 30 segments per wavelength.

For comparison, the Kraus formula $G \approx 10.8 + 10\log_{10}(C_\lambda^2 N S_\lambda)$ gives 14.4 dBi and

$52^\circ/(C_\lambda\sqrt{NS_\lambda}) = 34^\circ$ for the beam width; both are known to be optimistic by about 1–2 dB and several degrees, and measured 10-turn helices typically reach 12–13 dBi. The input resistance of about 110 Ω is close to the textbook value $140\,C_\lambda\ \Omega$ for a low feed point. To match the helix to 50 Ω, builders flatten the first quarter turn into a strip close to the ground plate; the program also prints an L network (at the antenna a shunt capacitance of 0.082 pF, toward the line a series inductance of 1.09 nH).

Because the helix is a pure wire structure in free space, the result scales exactly with frequency: the same model at 3.5 GHz, compared with HFSS in Figure 37, validates the method for this antenna type.

Table 6: Comparison with NEC-2 on the Same Segmentation

	NEC-2					N1UL Ham Antenna Simulator	
Deck	Z_{in} (Ω)	AGT	G (dBi)	R·AGT (Ω)	G corr. (dBi)	Z_{in} (Ω)	G (dBi)
bent_dipole	$52.91 + j6.26$	1.0033	1.86	53.09	1.85	$52.83 + j3.59$	1.85
hdipole_pec	$96.43 + j76.81$	0.9998	7.50	96.41	7.50	$96.96 + j75.07$	7.50
helix	$154.08 - j50.17$	0.8814	8.32	135.81	8.87	$125.61 - j54.21$	8.87
invv_realgnd	$57.61 - j109.66$	–	5.83	–	–	$56.85 - j109.87$	5.84
loaded_dipole	$4.59 - j1237.80$	0.9804	1.71	–	–	$4.31 - j1199.96$	1.71
loop_small	$0.02 + j138.83$	1.0001	1.73	0.02	1.73	$0.02 + j139.93$	1.73
monopole_pec	$42.50 + j24.62$	0.9995	5.19	42.48	5.19	$42.38 + j23.20$	5.19
phased2	$41.98 + j6.47$	0.9989	4.45	41.93	4.45	$41.76 + j4.88$	4.45
slant_monopole	$12.26 - j7.91$	0.9162	4.17	11.23	4.55	$11.09 - j8.26$	4.55
vdipole_bent	$46.87 + j16.86$	0.9636	1.59	45.16	1.75	$44.80 + j12.94$	1.75
vert_radials	$58.22 + j75.17$	–	0.66	–	–	$58.07 + j74.11$	0.69
yagi3	$44.43 + j42.82$	0.9989	8.05	44.38	8.05	$44.98 + j40.66$	8.03

NEC-2: the C++ translation of NEC-2, used only as a reference. AGT normalized to 1 (2 for perfect ground in NEC). R·AGT and G corr.: NEC-2 resistance and gain corrected by its own average gain test. Gains on the same 5° grid. Real-ground decks use the reflection-coefficient ground in both programs.

Table 7: Closed-Form, Image-Theory and Consistency Checks

Check	Result	Reference	
Small loop (C = 0.1 λ): radiation resistance (ohm)	0.022075	0.021952	pass
Small loop (C = 0.1 λ): directivity (dBi)	1.7349	1.73	pass
Short dipole (0.05 λ): directivity (dBi)	1.7645	1.7609	pass
Half-wave dipole (a = 10^{-5} λ): directivity (dBi)	2.1639	2.15	pass
Monopole on perfect ground = half of dipole: R ratio	0.5	0.5	pass
Monopole on perfect ground: gain - dipole gain (dB)	3.0103	3.0103	pass
Horizontal dipole over perfect ground vs antiphase pair: R (ohm)	86.012	86.012	pass
Horizontal dipole over perfect ground vs antiphase pair: X (ohm)	92.591	92.591	pass
Copper half-wave dipole at 14 MHz: loss resistance (ohm)	0.79516	0.79236	pass
Average gain test: curved_monopole.ant	1	1	pass
Average gain test: helix_axial_1ghz.ant	1.0001	1	pass
Average gain test: meander_dipole.ant	1	1	pass
Mesh convergence, 20 m dipole: $\lvert Z_{30} - Z_{120}\rvert / \lvert Z\rvert$	0.028278	0	pass

© 2026 Communications Consulting Corp.

11 Verification

11.1 Traceable Validation Suite

The program contains its own validation: the file `Validation\validation.csv` lists 100 checks, each with the input deck (folder `Validation\decks`), the quantity, the reference value or rule, the tolerance, the kind of reference and its origin. The NEC-2 output files used as references are supplied in `Validation\nec_out`, so every reference value can be traced to its source. Double-click `VALIDATE N1UL Antenna Simulator.bat` in the program folder, or type

```
bin\rsant -check Validation\validation.csv out
```

The program runs all decks (about 2–3 min) and writes `validation_report.txt`. Kinds of reference: *analytic* (closed form or exact property such as image theory and power conservation), *independent* (NEC-2 on the same deck; for three bent-wire decks the NEC-2 values are corrected for NEC-2's own average-gain error, see Section 11.2), *published* (FEKO results of the antenna paper), *convergence* (default against four times finer mesh) and *regression* (stored result). The HFSS helix is marked *fitted*, because its dielectric core is represented by a fitted effective permittivity. Table VIII lists all checks; all 100 pass with the Linux and the Windows program.

11.2 Comparison with NEC-2

Twelve NEC-2 decks were run with NEC-2 and with N1UL Ham Antenna Simulator on the same segmentation (Table 6). For straight wires (dipoles, monopole, Yagi, phased verticals with transmission lines, loaded dipole, small loop, horizontal dipole over ground) the feed resistances agree within 1–5 % and the gains within 0.05 dB; the reactances differ by a few ohms, as expected for the different treatment of the feed gap (NEC-2: segment-centerd point matching; here: Galerkin with triangle functions). The real-ground decks agree within 1.5 %. Seven further decks compare the Sommerfeld ground with NEC-2 (Table III); two analytic checks test its free-space and perfect-ground limits. Fifteen checks validate the printed-board model (Table 4).

For bent and slanted wires (V dipole, slanted monopole, helix) NEC-2 itself does not conserve power: its average gain test is 0.96, 0.92 and 0.88. Corrected by its own AGT, the NEC-2 resistance and gain agree with N1UL Ham Antenna Simulator (V dipole 45.2 vs 44.8 Ω and 1.75 vs 1.75 dBi; slanted monopole 4.55 vs 4.55 dBi; helix 8.87 vs 8.87 dBi), whose AGT is 1.0000 in every case. The remaining difference in the helix resistance (136 vs 126 Ω) is in the region of the feed, where the helix meets the ground plane at a shallow angle.

11.3 Closed Forms, Image Theory and Losses

Table 7 lists checks with independent references: the directivity of a short dipole (1.761 dBi) and of a thin half-wave dipole (2.15 dBi); the monopole over perfect ground, which must have exactly half the resistance and 3.01 dB more gain than the dipole; the horizontal dipole over perfect ground, which must equal a free-space pair driven in antiphase; the skin-effect loss of a copper dipole, $R_{\text{loss}} = R_s\,\ell/(4\pi a)$ for a cosine current; the small loop against NEC-2 (the uniform-current formula $20\pi^2(C/\lambda)^4 = 0.0197\,\Omega$ omits the gap-excited $\cos\phi$ current mode, which raises the resistance to 0.0220 Ω in both programs); the average gain test of the lossless examples; and the mesh convergence of the 20 m dipole. All checks pass.

11.4 Mesh Convergence

For the 20 m dipole over real ground the feed impedance with 15, 30, 60 and 120 segments per wavelength is $69.90 - j16.61$, $71.26 - j12.74$, $71.67 - j11.40$ and $71.83 - j10.77\,\Omega$ (10, 18, 32 and 62 segments). The default of 30 segments per wavelength is within 3 % of the finest mesh; the convergence check in every run shows whether a model needs more.

Table 8: Traceable Validation of the N1UL Ham Antenna Simulator (all checks pass)

No.	Input deck	Qty	Result	Reference	Tol.	Kind	Origin of the reference
1	`v_short.ant`	gmax	1.7645	1.7609	0.02	analytic	Hertzian dipole D = 1.5 (1.761 dBi)
2	`v_short.ant`	agt	1	1	0.003	analytic	power conservation (average gain test)
3	`v_half.ant`	gmax	2.1639	2.15	0.03	analytic	half-wave dipole with sinusoidal current, D = 1.64 (2.15 dBi)
4	`v_dip.ant`	agt	1	1	0.003	analytic	power conservation (reference run for the image-theory checks)
5	`v_pair.ant`	agt	1	1	0.003	analytic	power conservation (reference run for the image-theory checks)
6	`v_mono.ant`	zr	42.949	@v_dip.zr×0.5	0.5%	analytic	image theory: monopole R = half of dipole R
7	`v_mono.ant`	gmax	5.1912	@v_dip.gmax+3.0103	0.02	analytic	image theory: monopole gain = dipole gain + 3.01 dB
8	`v_hpec.ant`	zr	86.012	@v_pair.zr	0.1%	analytic	image theory: dipole over PEC = dipole + antiphase image
9	`v_hpec.ant`	zi	92.591	@v_pair.zi	0.1	analytic	image theory
10	`v_copper.ant`	rloss	0.79516	0.79236	3%	analytic	skin effect: Rs L/(4 pi a), Rs = sqrt(pi f mu0/sigma), cosine current
11	`curved_monopole.ant`	agt	1	1	0.003	analytic	power conservation, curved wire
12	`helix_axial_1ghz.ant`	agt	1.0001	1	0.003	analytic	power conservation, helix

© 2026 Communications Consulting Corp.

No.	Input deck	Qty	Result	Reference	Tol.	Kind	Origin of the reference
13	`meander_dipole.ant`	agt	1	1	0.003	analytic	power conservation, meander
14	`v_conv120.ant`	zr	71.829	71.83	0.5%	regression	stored result of the fine-mesh reference run (release 1.0)
15	`v_conv30.ant`	zr	71.257	@v_conv120.zr	2%	convergence	default mesh vs 4x finer mesh
16	`v_conv30.ant`	zi	-12.743	@v_conv120.zi	3	convergence	default mesh vs 4x finer mesh (ohm)
17	`v_somm_free.ant`	zr	85.898	@v_dip.zr	0.1%	analytic	Sommerfeld ground with eps = 1: no ground, must equal the free-space dipole
18	`v_somm_free.ant`	zi	46.257	@v_dip.zi	0.1	analytic	Sommerfeld ground with eps = 1: no ground (ohm)
19	`v_somm_pec.ant`	zr	86.015	@v_hpec.zr	0.3%	analytic	Sommerfeld ground, eps = sigma = 1e7: perfect-ground limit
20	`v_somm_pec.ant`	zi	92.588	@v_hpec.zi	0.3	analytic	Sommerfeld ground, perfect-ground limit (ohm)
21	`bent_dipole.nec`	zr	52.826	52.91	3%	independen	NEC-2 bent_dipole.out
22	`bent_dipole.nec`	zi	3.5914	6.261	5	independen	NEC-2 bent_dipole.out
23	`bent_dipole.nec`	gmax	1.8491	1.86	0.15	independen	NEC-2 bent_dipole.out
24	`hdipole_pec.nec`	zr	96.963	96.43	3%	independen	NEC-2 hdipole_pec.out
25	`hdipole_pec.nec`	zi	75.069	76.81	5	independen	NEC-2 hdipole_pec.out
26	`hdipole_pec.nec`	gmax	7.501	7.5	0.15	independen	NEC-2 hdipole_pec.out
27	`helix.nec`	zr	125.61	135.8	10%	independen	NEC-2 helix.out (AGT-corrected 0.881)
28	`helix.nec`	zi	-54.21	-50.17	5	independen	NEC-2 helix.out (AGT-corrected 0.881)
29	`helix.nec`	gmax	8.8782	8.87	0.15	independen	NEC-2 helix.out (AGT-corrected 0.881)
30	`invv_realgnd.nec`	zr	56.852	57.61	3%	independen	NEC-2 invv_realgnd.out
31	`invv_realgnd.nec`	zi	-109.87	-109.7	5	independen	NEC-2 invv_realgnd.out

© 2026 Communications Consulting Corp.

No.	Input deck	Qty	Result	Reference	Tol.	Kind	Origin of the reference
32	`invv_realgnd.nec`	gmax	5.8356	5.83	0.15	independent	NEC-2 invv_realgnd.out
33	`loaded_dipole.nec`	zr	4.315	4.593	7%	independent	NEC-2 loaded_dipole.out
34	`loaded_dipole.nec`	zi	-1200	-1238	4%	independent	NEC-2 loaded_dipole.out
35	`loaded_dipole.nec`	gmax	1.7084	1.71	0.15	independent	NEC-2 loaded_dipole.out
36	`loop_small.nec`	zr	0.022378	0.02195	3%	independent	NEC-2 loop_small.out
37	`loop_small.nec`	zi	139.93	138.8	5	independent	NEC-2 loop_small.out
38	`loop_small.nec`	gmax	1.7332	1.73	0.15	independent	NEC-2 loop_small.out
39	`monopole_pec.nec`	zr	42.38	42.5	3%	independent	NEC-2 monopole_pec.out
40	`monopole_pec.nec`	zi	23.202	24.62	5	independent	NEC-2 monopole_pec.out
41	`monopole_pec.nec`	gmax	5.1905	5.19	0.15	independent	NEC-2 monopole_pec.out
42	`phased2.nec`	zr	41.76	41.98	3%	independent	NEC-2 phased2.out
43	`phased2.nec`	zi	4.8781	6.471	5	independent	NEC-2 phased2.out
44	`phased2.nec`	gmax	4.4536	4.45	0.15	independent	NEC-2 phased2.out
45	`slant_monopole.nec`	zr	11.093	11.23	3%	independent	NEC-2 slant_monopole.out (AGT-corrected 0.916)
46	`slant_monopole.nec`	zi	-8.2597	-7.913	5	independent	NEC-2 slant_monopole.out (AGT-corrected 0.916)
47	`slant_monopole.nec`	gmax	4.5498	4.55	0.15	independent	NEC-2 slant_monopole.out (AGT-corrected 0.916)
48	`vdipole_bent.nec`	zr	44.796	45.16	3%	independent	NEC-2 vdipole_bent.out (AGT-corrected 0.964)
49	`vdipole_bent.nec`	zi	12.94	16.86	5	independent	NEC-2 vdipole_bent.out (AGT-corrected 0.964)
50	`vdipole_bent.nec`	gmax	1.7531	1.75	0.15	independent	NEC-2 vdipole_bent.out (AGT-corrected 0.964)
51	`vert_radials.nec`	zr	58.07	58.22	3%	independent	NEC-2 vert_radials.out
52	`vert_radials.nec`	zi	74.11	75.17	5	independent	NEC-2 vert_radials.out
53	`vert_radials.nec`	gmax	0.70701	0.66	0.15	independent	NEC-2 vert_radials.out

© 2026 Communications Consulting Corp.

No.	Input deck	Qty	Result	Reference	Tol.	Kind	Origin of the reference
54	`yagi3.nec`	zr	44.977	44.43	3%	independent	NEC-2 yagi3.out
55	`yagi3.nec`	zi	40.657	42.82	5	independent	NEC-2 yagi3.out
56	`yagi3.nec`	gmax	8.0308	8.05	0.15	independent	NEC-2 yagi3.out
57	`som_hd_low.nec`	zr	101.56	101.4	3%	independent	NEC-2 Sommerfeld (GN 2), nec_out/som_hd_low.out
58	`som_hd_low.nec`	zi	42.158	43.34	3	independent	NEC-2 Sommerfeld (GN 2), nec_out/som_hd_low.out
59	`som_hd_low.nec`	gmax	-6.2543	-6.26	0.15	independent	NEC-2 Sommerfeld (GN 2), nec_out/som_hd_low.out
60	`som_hd_h1p07.nec`	zr	59.332	59.74	3%	independent	NEC-2 Sommerfeld (GN 2), nec_out/som_hd_h1p07.out
61	`som_hd_h1p07.nec`	zi	-18.136	-17	3	independent	NEC-2 Sommerfeld (GN 2), nec_out/som_hd_h1p07.out
62	`som_hd_h1p07.nec`	gmax	-0.42497	-0.43	0.15	independent	NEC-2 Sommerfeld (GN 2), nec_out/som_hd_h1p07.out
63	`som_hd_poor.nec`	zr	72.773	73.24	3%	independent	NEC-2 Sommerfeld (GN 2), nec_out/som_hd_poor.out
64	`som_hd_poor.nec`	zi	-16.443	-15.17	3	independent	NEC-2 Sommerfeld (GN 2), nec_out/som_hd_poor.out
65	`som_hd_poor.nec`	gmax	-0.50008	-0.50	0.15	independent	NEC-2 Sommerfeld (GN 2), nec_out/som_hd_poor.out
66	`som_hd_sea.nec`	zr	8.1766	8.25	3%	independent	NEC-2 Sommerfeld (GN 2), nec_out/som_hd_sea.out
67	`som_hd_sea.nec`	zi	-28.951	-28.1	3	independent	NEC-2 Sommerfeld (GN 2), nec_out/som_hd_sea.out
68	`som_hd_sea.nec`	gmax	7.223	7.22	0.15	independent	NEC-2 Sommerfeld (GN 2), nec_out/som_hd_sea.out
69	`som_vd_low.nec`	zr	85.117	85.92	3%	independent	NEC-2 Sommerfeld (GN 2), nec_out/som_vd_low.out

© 2026 Communications Consulting Corp.

No.	Input deck	Qty	Result	Reference	Tol.	Kind	Origin of the reference
70	`som_vd_low.nec`	zi	-29.306	-27.82	3	independent	NEC-2 Sommerfeld (GN 2), nec_out/som_vd_low.out
71	`som_vd_low.nec`	gmax	0.25643	0.24	0.15	independent	NEC-2 Sommerfeld (GN 2), nec_out/som_vd_low.out
72	`som_gp.nec`	zr	30.214	30.93	3%	independent	NEC-2 Sommerfeld (GN 2), nec_out/som_gp.out
73	`som_gp.nec`	zi	-8.3948	-7.916	3	independent	NEC-2 Sommerfeld (GN 2), nec_out/som_gp.out
74	`som_gp.nec`	gmax	0.1612	0.08	0.15	independent	NEC-2 Sommerfeld (GN 2), nec_out/som_gp.out
75	`som_nvis80.nec`	zr	48.928	49.15	3%	independent	NEC-2 Sommerfeld (GN 2), nec_out/som_nvis80.out
76	`som_nvis80.nec`	zi	-38.383	-37.88	3	independent	NEC-2 Sommerfeld (GN 2), nec_out/som_nvis80.out
77	`som_nvis80.nec`	gmax	-0.935	-0.93	0.15	independent	NEC-2 Sommerfeld (GN 2), nec_out/som_nvis80.out
78	`v_pcb_free.ant`	zr	85.898	@v_dip.zr	0.1%	analytic	board with eps = 1 and no ground plane: must equal the free-space dipole
79	`v_pcb_free.ant`	zi	46.257	@v_dip.zi	0.1	analytic	board with eps = 1: free space (ohm)
80	`v_pcb_image.ant`	zr	86.012	@v_hpec.zr	0.5%	analytic	board with eps = 1 and ground plane at depth h: image theory, dipole at height h over perfect ground
81	`v_pcb_image.ant`	zi	92.592	@v_hpec.zi	0.5	analytic	board with eps = 1 and ground plane: image theory (ohm)

© 2026 Communications Consulting Corp.

No.	Input deck	Qty	Result	Reference	Tol.	Kind	Origin of the reference
82	`ms_fr4.ant`	fres	2440.4	2450	1%	published	microstrip resonator FR-4: Hammerstad-Jensen eps_eff and open-end extension (resonance in MHz)
83	`ms_rt5880.ant`	fres	2446	2450	1%	published	microstrip resonator RT/duroid 5880: Hammerstad-Jensen (MHz)
84	`ms_ro3010.ant`	fres	2443.2	2450	1%	published	microstrip resonator RO3010: Hammerstad-Jensen (MHz)
85	`cps_air_a.ant`	agt	1.0001	1	0.01	analytic	power conservation, coplanar strips in air (reference run)
86	`cps_fr4.ant`	fres	3025.1	@cps_air_a.fres×0.62137	1%	independent	coplanar strips on FR-4 without ground plane: f_air/sqrt(eps_eff), eps_eff = 2.590 from a 2D quasi-static moment method (conformal mapping 2.595)
87	`cps_air_b.ant`	agt	1	1	0.01	analytic	power conservation, coplanar strips in air (reference run)
88	`cps_ro3010.ant`	fres	2366.7	@cps_air_b.fres×0.49739	1%	independent	coplanar strips on RO3010 without ground plane: eps_eff = 4.042 from the 2D quasi-static moment method
89	`patch_air.ant`	agt	1.0116	1	0.02	analytic	power conservation, wire-grid patch on a board with eps = 1 (reference run)

© 2026 Communications Consulting Corp.

No.	Input deck	Qty	Result	Reference	Tol.	Kind	Origin of the reference
90	patch_fr4.ant	fpeak	2244.1	@patch_air.fpeak×0.507781	1.5%	published	patch on FR-4: frequency ratio air/FR-4 = 1.9694 from the transmission-line (cavity) model of the rectangular patch
91	patch_dual_a.ant	fpeak	2327.3	2327.3	0.5%	regression	dual-resonance patch, mode along the 40 mm side: stored result (cavity model 2501 MHz
92	patch_dual_b.ant	fpeak	2994.2	@patch_dual_a.fpeak×1.30797	2.5%	published	dual-resonance patch: ratio of the two resonances 1.3080 from the cavity (transmission-line) model
93	paper_three_segment_fek	gmax	10.103	10.09	0.1	published	FEKO, three-segment monopole (Rohde, A Look at a Novel Antenna Design, Rev. 2, Fig. 14)
94	paper_curvilinear_7MHz.ant	gmax	4.3779	4.3	0.2	published	FEKO, optimized 3/4-wave curvilinear monopole, 7 MHz (Rev. 2, Figs. 20-24
95	helix_axial_3p5GHz_gmax.ant	gmax	13.107	13.8	1.0	independent (fitted)	HFSS axial-mode helix 3.5 GHz (digitized)
96	dish_q1_fd04.ant	gmax	29.119	29.1183	0.05	analytic	Silver aperture efficiency (cos-q feed, q = 1, F/D 0.4): eta = 0.8271, G = eta (pi D / lambda) squared
97	dish_q2_fd05.ant	gmax	29.08	29.0790	0.05	analytic	Silver aperture efficiency (cos-q feed, q = 2, F/D 0.5): eta = 0.8196, G = eta (pi D / lambda) squared

© 2026 Communications Consulting Corp.

No.	Input deck	Qty	Result	Reference	Tol.	Kind	Origin of the reference
98	`dish_q1_fd03.ant`	gmax	28.627	28.6252	0.05	analytic	Silver aperture efficiency (cos-q feed, q = 1, F/D 0.3): eta = 0.7383, G = eta (pi D / lambda) squared
99	`dish_q3_fd06.ant`	gmax	29.065	29.0638	0.05	analytic	Silver aperture efficiency (cos-q feed, q = 3, F/D 0.6): eta = 0.8167, G = eta (pi D / lambda) squared
100	`dish_mesh.ant`	gmax	28.47	@dish_q1_fd04.gmax-0.6492	0.01	analytic	wire mesh 5 cm, 1 mm wire: |Gamma| squared = 0.8612 (Kontorovich sheet reactance) reduces the gain by 0.649 dB

12 Limitations and Good Practice

- *Thin wires.* The method assumes wires thin compared with the wavelength and with the segment length; keep the segment length above $4a$ (the mesh report warns below 4 and below 2). Closely spaced parallel wires should be at least a few radii apart.
- *Real ground.* The reflection-coefficient approximation is accurate for wires higher than about 0.1λ; for lower wires use the Sommerfeld ground (Section 8.5), valid down to about 0.001λ. Wires touching or buried in a lossy earth are not modelled exactly; radials on or in the soil are better modelled over perfect ground with a loss resistance.
- *Printed boards.* The board is laterally infinite: accurate when it extends well beyond the traces (several board thicknesses); for an antenna at the edge of a small board the dielectric loading is overestimated. Flat traces are round wires of radius $w/4$; this is accurate for traces narrower than about half the board thickness and for traces spaced more than their width (wider traces: 2–3 % low effective permittivity). Wires cannot pass through the board (no vias or probe feeds). Solid patches modelled as wire grids resonate 7–10 % low (Section 8.6).
- *Printed patch antennas at millimeter waves.* On electrically thin boards (for example 0.127 mm at 100 GHz) the currents on a wire-grid patch and their image in the ground plane nearly cancel; the program then still predicts the resonance and the match, but not the radiation pattern, gain and efficiency. Use a full-wave planar solver for such antennas; wire antennas (dipoles, Yagis, helices) are modelled correctly at any frequency.
- *Feed gap.* The input reactance of a delta-gap source depends slightly on the size of the segments at the feed, as in every moment-method program; the resistance and the pattern are insensitive.

© 2026 Communications Consulting Corp.

- *Surfaces.* Solid surfaces are modeled as wire grids; large reflectors by physical optics (Section 9).
- *Reflectors.* Physical optics is accurate for the main beam and the first side lobes of dishes larger than about 10λ; far side lobes and the region behind the dish are approximate (no edge diffraction). Struts, the feed–dish interaction and surface errors are not modelled; the mesh formula assumes cells much smaller than the wavelength and normal incidence.
- *Run time.* The matrix grows as the square and the solution as the cube of the number of segments: 200 segments take about 0.1 s per frequency, 1000 segments a few seconds.

13 Command-line Use

The simulator can be run without the window:

```
rsant model.ant -o outdir [-conv] [-mesh] [-q]
      [-dth 2] [-dph 5]
```

It prints the mesh summary, the sweep table and the results at the design frequency, and writes `results.json`. `-conv` adds the convergence check, `-mesh` writes only the mesh (`mesh.json`), `-dth`/`-dph` set the pattern grid. `rsant -check list.csv outdir` runs a validation list (Section 11.1). `N1UL_Ham_Antenna_Simulator.exe /run model.ant` runs a model and writes the results page without opening the window.

Appendix: Model Files of All Examples and Validation Cases

This appendix lists the complete input of every example antenna (folder `Examples`) and of every validation case (folder `Validation\decks`), so that each result in this manual can be traced to the exact model. The native format is described in Section 4; lines beginning with # are comments. NEC-2 decks use the standard card format (`CM` comment, `GW` wire, `GE` geometry end, `GN` ground, `EX` excitation, `LD` load, `TL` line, `FR` frequency). The ground grids of the PCB antenna and of the HFSS helix are generated wire by wire; only their first and last lines are printed. Long lines are wrapped (marked ↪).

Example antennas

cps_air_a.ant

```
TITLE Coplanar strips 0.5 mm, gap 1.0 mm, 30 mm shorted, in air (reference for cps_fr4)
UNITS mm
FREQ 4.8500 GHz
SWEEP 4.6 5.1 11 GHz
WIRE 0 -0.75 0 0 0.75 0 r=0.125 seg=3 name=feed
WIRE 0 0.75 0 30.0 0.75 0 r=0.125 seg=60 name=top
WIRE 0 -0.75 0 30.0 -0.75 0 r=0.125 seg=60 name=bot
WIRE 30.0 -0.75 0 30.0 0.75 0 r=0.125 seg=3 name=short
SOURCE feed 50
MESH taper=off
```

cps_air_b.ant

```
TITLE Coplanar strips 0.2 mm, gap 2.0 mm, 30 mm shorted, in air (reference for cps_ro3010)
```

© 2026 Communications Consulting Corp.

```
UNITS mm
FREQ 4.8500 GHz
SWEEP 4.6 5.1 11 GHz
WIRE 0 -1.1 0 0 1.1 0 r=0.05 seg=3 name=feed
WIRE 0 1.1 0 30.0 1.1 0 r=0.05 seg=60 name=top
WIRE 0 -1.1 0 30.0 -1.1 0 r=0.05 seg=60 name=bot
WIRE 30.0 -1.1 0 30.0 1.1 0 r=0.05 seg=3 name=short
SOURCE feed 50
MESH taper=off
```

cps_fr4.ant

```
TITLE Coplanar strips 0.5 mm, gap 1.0 mm, 30 mm shorted, on FR-4 1.6 mm without ground plane
UNITS mm
FREQ 3.0250 GHz
SWEEP 2.9 3.15 11 GHz
WIRE 0 -0.75 0 0 0.75 0 r=0.125 seg=3 name=feed
WIRE 0 0.75 0 30.0 0.75 0 r=0.125 seg=60 name=top
WIRE 0 -0.75 0 30.0 -0.75 0 r=0.125 seg=60 name=bot
WIRE 30.0 -0.75 0 30.0 0.75 0 r=0.125 seg=3 name=short
SOURCE feed 50
MESH taper=off
GROUND pcb eps=4.4 h=1.6
```

cps_ro3010.ant

```
TITLE Coplanar strips 0.2 mm, gap 2.0 mm, 30 mm shorted, on RO3010 0.635 mm without ground pla
UNITS mm
FREQ 2.4250 GHz
SWEEP 2.3 2.55 11 GHz
WIRE 0 -1.1 0 0 1.1 0 r=0.05 seg=3 name=feed
WIRE 0 1.1 0 30.0 1.1 0 r=0.05 seg=60 name=top
WIRE 0 -1.1 0 30.0 -1.1 0 r=0.05 seg=60 name=bot
WIRE 30.0 -1.1 0 30.0 1.1 0 r=0.05 seg=3 name=short
SOURCE feed 50
MESH taper=off
GROUND pcb eps=10.2 h=0.635
```

curved_monopole.ant

```
TITLE Curved monopole over perfect ground (S-shaped wire, height 0.24 wavelength), smooth spli
UNITS m
FREQ 300 MHz
SWEEP 250 350 41 MHz
SPLINE 0 0 0  -0.03 0 0.07  -0.035 0 0.13  0.0 0 0.19  0.05 0 0.24  r=0.001 name=c
SOURCE c 0
GROUND perfect
```

© 2026 Communications Consulting Corp.

dipole_20m.ant

```
TITLE 20 m half-wave dipole, 10 m above average ground, #12 copper wire
UNITS m
FREQ 14.175 MHz
SWEEP 13.9 14.45 23 MHz
WIRE -5.13 0 10  5.13 0 10  awg=12 name=dipole
SOURCE dipole 50
GROUND real eps=13 sigma=0.005
MATERIAL copper
```

dipole_80m_low_sommerfeld.ant

```
TITLE 80 m NVIS dipole only 3 m above average ground - Sommerfeld ground
# A low antenna couples strongly to the earth. The reflection-coefficient ground
# (GROUND real ...) is not accurate below about 0.1 wavelength; the keyword
# "sommerfeld" computes the exact near field of the ground (as NEC-2 GN 2).
# Remove "sommerfeld" and run again to see the difference.
UNITS m
FREQ 3.6 MHz
SWEEP 3.4 3.8 21 MHz
MATERIAL copper
VAR h=3
WIRE -19.6 0 h  19.6 0 h  awg=12 name=dipole
SOURCE dipole 50
GROUND real eps=13 sigma=0.005 sommerfeld
```

dish_43m_435MHz.ant

```
TITLE 43 m parabolic dish at 435 MHz, prime-focus dipole feed with a reflector screen (sketch)
UNITS m
FREQ 435 MHz
SWEEP 425 445 5 MHz
MATERIAL aluminum
# feed at the focus (origin): half-wave dipole along x, illuminating the dish below it (-z)
WIRE -0.164 0 0      0.164 0 0      dmm=12 name=dipole
SOURCE dipole 50
# reflector screen 0.15 m behind the dipole: five rods, 0.5 m long, 0.15 m apart
WIRE -0.25 -0.30 0.15  0.25 -0.30 0.15  dmm=10
WIRE -0.25 -0.15 0.15  0.25 -0.15 0.15  dmm=10
WIRE -0.25  0.00 0.15  0.25  0.00 0.15  dmm=10
WIRE -0.25  0.15 0.15  0.25  0.15 0.15  dmm=10
WIRE -0.25  0.30 0.15  0.25  0.30 0.15  dmm=10
# reflector: 43 m diameter, F/D = 0.4 (focal length 17.2 m, vertex 17.2 m below the feed),
# wire mesh with 5 cm cells of 2 mm wire, 1 m central blockage by the feed housing.
# The focal length and the mesh are assumptions: put in the values of the real dish.
DISH D=43 FD=0.4 mesh=5cm wire=2mm block=1
PATTERN dth=2 dph=5
```

© 2026 Communications Consulting Corp.

dish_46m_440MHz.ant

```
TITLE 46 m parabolic dish at 440 MHz (size of the steerable UHF dish of the book cover), prime-
UNITS m
FREQ 440 MHz
SWEEP 430 450 5 MHz
MATERIAL aluminum
# feed at the focus (origin): half-wave dipole along x, illuminating the dish below it (-z)
WIRE -0.164 0 0      0.164 0 0      dmm=12 name=dipole
SOURCE dipole 50
# reflector screen 0.15 m behind the dipole: five rods, 0.5 m long, 0.15 m apart
WIRE -0.25 -0.30 0.15  0.25 -0.30 0.15  dmm=10
WIRE -0.25 -0.15 0.15  0.25 -0.15 0.15  dmm=10
WIRE -0.25  0.00 0.15  0.25  0.00 0.15  dmm=10
WIRE -0.25  0.15 0.15  0.25  0.15 0.15  dmm=10
WIRE -0.25  0.30 0.15  0.25  0.30 0.15  dmm=10
# reflector: 46 m diameter, F/D = 0.4 (focal length 18.4 m, vertex 18.4 m below the feed),
# wire mesh with 5 cm cells of 2 mm wire, 1 m central blockage by the feed housing.
# The focal length and the mesh are assumptions: put in the values of the real dish.
DISH D=46 FD=0.4 mesh=5cm wire=2mm block=1
PATTERN dth=2 dph=5
```

four_square_40m.ant

```
TITLE Four-square array of quarter-wave verticals for 40 m over perfect ground (phases 0/-90/-9
UNITS m
FREQ 7.15 MHz
MATERIAL aluminum
WIRE  0     0    0   0     0    10.2  d=0.04 name=v1
WIRE  10.5  0    0   10.5  0    10.2  d=0.04 name=v2
WIRE  0    10.5  0   0    10.5  10.2  d=0.04 name=v3
WIRE  10.5 10.5  0   10.5 10.5  10.2  d=0.04 name=v4
SOURCE v4 0 V=1 phase=0
SOURCE v2 0 V=1 phase=-90
SOURCE v3 0 V=1 phase=-90
SOURCE v1 0 V=1 phase=-180
GROUND perfect
```

gp_vertical_20m.ant

```
TITLE Ground-plane vertical for 20 m with four drooping radials, base 5 m above average ground
UNITS m
FREQ 14.15 MHz
SWEEP 13.9 14.4 21 MHz
MATERIAL aluminum
WIRE 0 0 5   0 0 10.08  d=0.02 name=radiator
WIRE 0 0 5   3.68 0 1.32  awg=12 name=radial1
WIRE 0 0 5   0 3.68 1.32  awg=12 name=radial2
```

© 2026 Communications Consulting Corp.

```
WIRE 0 0 5  -3.68 0 1.32  awg=12 name=radial3
WIRE 0 0 5   0 -3.68 1.32  awg=12 name=radial4
SOURCE radiator 0
GROUND real eps=13 sigma=0.005
```

helical_rod_7MHz_teflon.ant

```
TITLE Helical rod antenna 1.5 m for 7.1 MHz: 206.7 turns of Teflon-insulated 1 mm copper wire
UNITS m
FREQ 7.1 MHz
SWEEP 7.05 7.15 3 MHz
WIRE 0.02 0 0  0.02 0 0.01  d=0.001 name=feed
HELIX 0 0 0.01  0.02 0.007209 206.7000 d=0.001 insmm=0.3 insul=teflon name=helix
SOURCE feed 0
GROUND perfect
MATERIAL copper
MESH angle=22.5
```

helix_axial_1ghz.ant

```
TITLE Axial-mode helix for 1 GHz (Kraus): circumference 1 wavelength, 13 deg pitch, 6 turns, o
UNITS m
FREQ 1.0 GHz
SWEEP 0.8 1.2 21 GHz
WIRE 0.0477 0 0  0.0477 0 0.01  r=0.001 name=feed
HELIX 0 0 0.01  0.0477 0.0697 6  sides=20 r=0.001 name=h
SOURCE feed 0
GROUND perfect
```

helix_axial_1ghz_left.ant

```
TITLE Axial-mode helix for 1 GHz, LEFT-hand winding (mirror of helix_axial_1ghz.ant): LHCP
UNITS m
FREQ 1.0 GHz
SWEEP 0.8 1.2 21 GHz
WIRE 0.0477 0 0  0.0477 0 0.01  r=0.001 name=feed
HELIX 0 0 0.01  0.0477 0.0697 6  sides=20 r=0.001 left name=h
SOURCE feed 0
GROUND perfect
```

helix_axial_3p5GHz_bare.ant

```
TITLE Axial-mode helix 3.5 GHz (HFSS comparison) over 320 mm square ground plane (wire grid 16
UNITS m
FREQ 3.5 GHz
WIRE 0.01265 0 0  0.01265 0 0.004 r=0.001 name=feed
HELIX 0 0 0.004  0.01265 0.0202 10  sides=24 r=0.001 name=h
SOURCE feed 0
```

© 2026 Communications Consulting Corp.

```
WIRE -0.14735 -0.16000 0  -0.14735 -0.14400 0 r=0.0008 seg=2
WIRE -0.14735 -0.16000 0  -0.13135 -0.16000 0 r=0.0008 seg=2
WIRE -0.14735 -0.14400 0  -0.14735 -0.12800 0 r=0.0008 seg=2
# ... 836 further WIRE lines of the ground grid omitted (complete file in the Examples folder)
WIRE 0.15665 0.16000 0  0.17265 0.16000 0 r=0.0008 seg=2
GROUND none
```

helix_axial_3p5GHz_core.ant

```
TITLE Axial-mode helix 3.5 GHz, 10 turns, 320 mm ground (HFSS case); dielectric core modelled h
UNITS m
FREQ 3.5 GHz
WIRE 0.016001124960452 0 0  0.016001124960452 0 0.004 r=0.001 name=feed
HELIX 0 0 0.004  0.016001124960452 0.025551203494160506 10  sides=24 r=0.001 name=h
SOURCE feed 0
WIRE -0.14400 -0.16000 0  -0.14400 -0.14400 0 r=0.0008 seg=2
WIRE -0.14400 -0.16000 0  -0.12800 -0.16000 0 r=0.0008 seg=2
WIRE -0.14400 -0.14400 0  -0.14400 -0.12800 0 r=0.0008 seg=2
# ... 836 further WIRE lines of the ground grid omitted (complete file in the Examples folder)
WIRE 0.16000 0.16000 0  0.17600 0.16000 0 r=0.0008 seg=2
GROUND none
```

helix_axial_10GHz.ant

```
TITLE Axial-mode helix for the 10 GHz ham band (10.368 GHz, Kraus design): C = 1 lambda (28.9 m
# Kraus design rules: circumference = 1 wavelength, pitch angle 13 deg, 10 turns (about 2.3 wav
# Feed pin 1 mm high (SMA centre pin, 0.5 mm diameter) at a node of the ground grid.
# The bare helix shows about 70 - j55 ohm; match to 50 ohm with the L network printed in the re
# or, as builders do, by flattening the first quarter turn into a strip close to the ground pla
UNITS mm
FREQ 10.368 GHz
SWEEP 9.5 11.5 21 GHz
WIRE 4.6020 0 0  4.6020 0 1.0 r=0.25 name=feed
HELIX 0 0 1.0  4.6020 6.6756 10  sides=20 r=0.25 name=h
SOURCE feed 0
WIRE -29.2313 -29.0000 0  -29.2313 -26.5833 0 r=0.3 seg=1
WIRE -29.2313 -26.5833 0  -29.2313 -24.1667 0 r=0.3 seg=1
WIRE -29.2313 -24.1667 0  -29.2313 -21.7500 0 r=0.3 seg=1
# ... 1197 further WIRE lines of the ground grid omitted (complete file in the Examples folder)
MESH segwl=20
GROUND none
```

inverted_v_40m.ant

```
TITLE Inverted-V dipole for 40 m, apex 12 m, legs at 45 degrees, average ground
UNITS m
FREQ 7.1 MHz
SWEEP 6.9 7.3 21 MHz
```

© 2026 Communications Consulting Corp.

```
MATERIAL copper
WIRE -7.25 0 4.75  0 0 12  awg=14 name=left
WIRE  0 0 12  7.25 0 4.75  awg=14 name=right
SOURCE right 0
GROUND real eps=13 sigma=0.005
```

loaded_whip_80m.ant

```
TITLE 3 m mobile whip for 80 m with base loading coil (Q = 200) and 10 ohm ground loss, perfect
UNITS m
FREQ 3.75 MHz
SWEEP 3.7 3.8 21 MHz
MATERIAL steel
WIRE 0 0 0  0 0 0.3  d=0.025 name=mast
WIRE 0 0 0.3  0 0 3.3  d=0.008 name=whip
SOURCE mast 0
LOAD mast 100 L=60.8e-6 R=7.2
LOAD mast 0 R=10
GROUND perfect
```

lpda_14_30.ant

```
TITLE Log-periodic dipole array 14-30 MHz, 8 elements, tau 0.88, sigma 0.06, 100 ohm crossed fe
UNITS m
FREQ 21.2 MHz
SWEEP 14 30 33 MHz
MATERIAL aluminum
WIRE 0.000 -5.700 15  0.000 5.700 15  d=0.02 name=e1
WIRE 1.368 -5.016 15  1.368 5.016 15  d=0.02 name=e2
WIRE 2.572 -4.414 15  2.572 4.414 15  d=0.02 name=e3
WIRE 3.631 -3.884 15  3.631 3.884 15  d=0.02 name=e4
WIRE 4.564 -3.418 15  4.564 3.418 15  d=0.02 name=e5
WIRE 5.384 -3.008 15  5.384 3.008 15  d=0.02 name=e6
WIRE 6.106 -2.647 15  6.106 2.647 15  d=0.02 name=e7
WIRE 6.741 -2.329 15  6.741 2.329 15  d=0.02 name=e8
TL e1 50 e2 50 Z0=100 rev
TL e2 50 e3 50 Z0=100 rev
TL e3 50 e4 50 Z0=100 rev
TL e4 50 e5 50 Z0=100 rev
TL e5 50 e6 50 Z0=100 rev
TL e6 50 e7 50 Z0=100 rev
TL e7 50 e8 50 Z0=100 rev
SOURCE e8 50
Z0 100
GROUND real eps=13 sigma=0.005
```

© 2026 Communications Consulting Corp.

magloop_20m.ant

```
TITLE Small transmitting (magnetic) loop, 1 m diameter, 22 mm copper tube, tuned to 14.1 MHz by
UNITS m
FREQ 14.1 MHz
SWEEP 13.9 14.3 41 MHz
MATERIAL copper
LOOP 0 0 3  0.5 24 axis=x d=0.022 name=lp rot=-90
SOURCE lp1 0
LOAD lp13 0 C=47.7e-12
GROUND real eps=13 sigma=0.005
```

meander_dipole.ant

```
TITLE Meander-line dipole defined by a formula: x = 0.01 sin(20 pi t), length 0.3 wavelength, 8
UNITS m
FREQ 868 MHz
SWEEP 700 1000 61 MHz
CURVE "0.008*sin(20*pi*t)" "0" "-0.052 + 0.104*t" pieces=200 r=0.0004 name=m
SOURCE m 50
```

microstrip_resonator_fr4.ant

```
TITLE Microstrip half-wave resonator on FR-4 (eps 4.4, h 1.6 mm), trace 0.5 mm, centre-fed: ser
UNITS mm
FREQ 2.45 GHz
SWEEP 2.35 2.55 11 GHz
WIRE -17.2615 0 0 17.2615 0 0 r=0.125 seg=61 name=s
SOURCE s 50
GROUND pcb eps=4.4 h=1.6 groundplane
MESH taper=off
```

moxon_20m.ant

```
TITLE Moxon rectangle for 20 m, #12 copper wire, 12 m above average ground (A = 8.05 m, B = 1.0
UNITS m
FREQ 14.15 MHz
SWEEP 13.95 14.35 17 MHz
MATERIAL copper
# driver (front, x = +1.25) with tails bent back
WIRE  1.25 -4.025 12   1.25  4.025 12  awg=12 name=driver
WIRE  1.25  4.025 12   0.20  4.025 12  awg=12 name=dtail_r
WIRE  1.25 -4.025 12   0.20 -4.025 12  awg=12 name=dtail_l
# reflector (back, x = -1.25) with tails bent forward; 0.20 m gap between the tails
WIRE -1.25 -4.025 12  -1.25  4.025 12  awg=12 name=reflector
WIRE -1.25  4.025 12   0.00  4.025 12  awg=12 name=rtail_r
WIRE -1.25 -4.025 12   0.00 -4.025 12  awg=12 name=rtail_l
SOURCE driver 50
GROUND real eps=13 sigma=0.005
```

© 2026 Communications Consulting Corp.

ms_fr4.ant

```
TITLE Microstrip half-wave resonator on FR-4 (eps 4.4, h 1.6 mm), trace 0.5 mm, centre-fed: ser
UNITS mm
FREQ 2.45 GHz
SWEEP 2.35 2.55 11 GHz
WIRE -17.2615 0 0 17.2615 0 0 r=0.125 seg=61 name=s
SOURCE s 50
GROUND pcb eps=4.4 h=1.6 groundplane
MESH taper=off
```

ms_ro3010.ant

```
TITLE Microstrip half-wave resonator on RO3010 (eps 10.2, h 0.635 mm), trace 0.3 mm, centre-fed
UNITS mm
FREQ 2.45 GHz
SWEEP 2.35 2.55 11 GHz
WIRE -11.8377 0 0 11.8377 0 0 r=0.075 seg=61 name=s
SOURCE s 50
GROUND pcb eps=10.2 h=0.635 groundplane
MESH taper=off
```

ms_rt5880.ant

```
TITLE Microstrip half-wave resonator on RT/duroid 5880 (eps 2.2, h 0.787 mm), trace 0.5 mm, cen
UNITS mm
FREQ 2.45 GHz
SWEEP 2.35 2.55 11 GHz
WIRE -22.8949 0 0 22.8949 0 0 r=0.125 seg=61 name=s
SOURCE s 50
GROUND pcb eps=2.2 h=0.787 groundplane
MESH taper=off
```

normal_mode_helix.ant

```
TITLE Normal-mode helical antenna for 2 m: 11 turns, 24.4 mm diameter, 178 mm high, 1.8 mm copp
UNITS mm
FREQ 145 MHz
SWEEP 125 165 41 MHz
WIRE 12.2 0 0   12.2 0 5   d=1.8 name=feed
HELIX 0 0 5   12.2 15.7 11  sides=24 d=1.8 name=helix
SOURCE feed 0
GROUND perfect
MATERIAL copper
```

paper_curvilinear_7MHz.ant

```
TITLE Curvilinear 3/4-wave monopole for 7 MHz over average ground, optimized (16 radials at 2 m
FREQ 7 MHz
```

© 2026 Communications Consulting Corp.

```
SWEEP 6.9 7.3 41 MHz
WIRE 0 0 2 10.7069 0 2 d=0.004 name=r1
WIRE 0 0 2 9.89186 4.09734 2 d=0.004 name=r2
WIRE 0 0 2 7.5709 7.5709 2 d=0.004 name=r3
WIRE 0 0 2 4.09734 9.89186 2 d=0.004 name=r4
WIRE 0 0 2 6.55607e-16 10.7069 2 d=0.004 name=r5
WIRE 0 0 2 -4.09734 9.89186 2 d=0.004 name=r6
WIRE 0 0 2 -7.5709 7.5709 2 d=0.004 name=r7
WIRE 0 0 2 -9.89186 4.09734 2 d=0.004 name=r8
WIRE 0 0 2 -10.7069 1.31121e-15 2 d=0.004 name=r9
WIRE 0 0 2 -9.89186 -4.09734 2 d=0.004 name=r10
WIRE 0 0 2 -7.5709 -7.5709 2 d=0.004 name=r11
WIRE 0 0 2 -4.09734 -9.89186 2 d=0.004 name=r12
WIRE 0 0 2 -1.96682e-15 -10.7069 2 d=0.004 name=r13
WIRE 0 0 2 4.09734 -9.89186 2 d=0.004 name=r14
WIRE 0 0 2 7.5709 -7.5709 2 d=0.004 name=r15
WIRE 0 0 2 9.89186 -4.09734 2 d=0.004 name=r16
SPLINE 0.0000 0.0000 2.0000  13.5650 0.0000 8.4241  -5.7132 0.0000 14.8482  -9.2785 0.0000 21.2
SOURCE m 0
GROUND real eps=13 sigma=0.005
MATERIAL copper
```

paper_three_segment_feko.ant

```
TITLE Three-segment monopole, published FEKO design
FREQ 299.792458 MHz
SWEEP 270 330 31 MHz
WIRE 0 0 0 0 0 0.617 r=0.001 name=v1
WIRE 0 0 0.617 0.236 0 0.617 r=0.001 name=h
WIRE 0.236 0 0.617 0.236 0 1.029 r=0.001 name=v2
SOURCE v1 0
GROUND perfect
```

paper_three_segment_optimized.ant

```
TITLE Three-segment monopole, re-optimized
FREQ 299.792458 MHz
SWEEP 270 330 31 MHz
WIRE 0 0 0 0 0 0.610506 r=0.001 name=v1
WIRE 0 0 0.610506 0.200358 0 0.500507 r=0.001 name=h
WIRE 0.200358 0 0.500507 0.25053 0 0.954992 r=0.001 name=v2
SOURCE v1 0
GROUND perfect
```

patch_2p45GHz_fr4.ant

```
TITLE Rectangular patch antenna 37.3 x 28.8 mm on FR-4 1.6 mm with ground plane (wire grid 18 x
# Patch dimensions from the transmission-line model for 2.45 GHz (Balanis).
```

```
# A solid patch is represented by a grid of wires (radius = cell / 2 pi).
# A solid patch represented by a wire grid resonates 7-10 % lower than the real solid patch
# (here 2.23 GHz instead of 2.45 GHz); scale the dimensions accordingly when designing.
# Feed: 6 mm microstrip line (1 mm wide) at the centre of a radiating edge, source near its end
UNITS mm
FREQ 2.226 GHz
SWEEP 2.15 2.35 21 GHz
WIRE -18.6300 0.0000 0  -18.6300 2.0579 0 r=0.3275 seg=1
WIRE -18.6300 2.0579 0  -18.6300 4.1157 0 r=0.3275 seg=1
WIRE -18.6300 4.1157 0  -18.6300 6.1736 0 r=0.3275 seg=1
# ... 533 further WIRE lines of the ground grid omitted (complete file in the Examples folder)
WIRE 0 -6.0 0  0 0 0 r=0.2500 seg=4 name=feed
SOURCE feed 25
GROUND pcb eps=4.4 tand=0.02 h=1.6mm groundplane
MESH taper=off
```

patch_air.ant

```
TITLE Wire-grid patch 37.26 x 28.81 mm (18 x 14 cells) on a 1.6 mm board with eps=1 and ground
UNITS mm
FREQ 4.4000 GHz
SWEEP 4.25 4.55 11 GHz
WIRE -18.6300 0.0000 0  -18.6300 2.0579 0 r=0.3275 seg=1
WIRE -18.6300 2.0579 0  -18.6300 4.1157 0 r=0.3275 seg=1
WIRE -18.6300 4.1157 0  -18.6300 6.1736 0 r=0.3275 seg=1
# ... 532 further WIRE lines of the ground grid omitted (complete file in the Examples folder)
WIRE 16.5600 28.8100 0  18.6300 28.8100 0 r=0.3275 seg=1
SOURCE feed 50
GROUND pcb eps=1.0 tand=0.0 h=1.6mm groundplane
MESH taper=off
```

patch_dual_a.ant

```
TITLE Dual-resonance patch 40 x 30 mm on RT/duroid 5880, off-centre feed: narrow sweep around r
UNITS mm
FREQ 2.3300 GHz
SWEEP 2.27 2.39 13 GHz
WIRE -20.0000 0.0000 0  -20.0000 2.0000 0 r=0.3183 seg=1
WIRE -20.0000 2.0000 0  -20.0000 4.0000 0 r=0.3183 seg=1
WIRE -20.0000 4.0000 0  -20.0000 6.0000 0 r=0.3183 seg=1
# ... 632 further WIRE lines of the ground grid omitted (complete file in the Examples folder)
WIRE -10.0000 -8.0 0  -10.0000 0 0 r=0.3750 seg=4 name=feed
SOURCE feed 25
GROUND pcb eps=2.2 tand=0.0009 h=1.575mm groundplane
MESH taper=off
```

© 2026 Communications Consulting Corp.

patch_dual_b.ant

```
TITLE Dual-resonance patch 40 x 30 mm on RT/duroid 5880, off-centre feed: narrow sweep around r
UNITS mm
FREQ 3.0000 GHz
SWEEP 2.94 3.06 13 GHz
WIRE -20.0000 0.0000 0  -20.0000 2.0000 0 r=0.3183 seg=1
WIRE -20.0000 2.0000 0  -20.0000 4.0000 0 r=0.3183 seg=1
WIRE -20.0000 4.0000 0  -20.0000 6.0000 0 r=0.3183 seg=1
# ... 632 further WIRE lines of the ground grid omitted (complete file in the Examples folder)
WIRE -10.0000 -8.0 0  -10.0000 0 0 r=0.3750 seg=4 name=feed
SOURCE feed 25
GROUND pcb eps=2.2 tand=0.0009 h=1.575mm groundplane
MESH taper=off
```

patch_dual_resonance_rt5880.ant

```
TITLE Dual-resonance patch 40 x 30 mm on RT/duroid 5880 (eps 2.2, 1.575 mm) with ground plane,
# Test case with two resonances: a rectangular patch with unequal sides has two fundamental
# cavity modes, one along each side. The microstrip feed is 10 mm off the centre line, so both
# Cavity (transmission-line) model [Balanis]: 2.501 GHz (current along the 40 mm side), 3.272 G
# Result: 2.33 and 2.99 GHz. A solid patch represented by a wire grid (radius = cell / 2 pi) re
# 7-10 % lower than the solid patch; the spacing of the resonances (ratio 1.287 vs 1.308) is cl
# A finer grid does not remove this offset. "Feed impedance" on the results page shows the two
UNITS mm
FREQ 3.0 GHz
SWEEP 2.2 3.6 29 GHz
WIRE -20.0000 0.0000 0  -20.0000 2.0000 0 r=0.3183 seg=1
WIRE -20.0000 2.0000 0  -20.0000 4.0000 0 r=0.3183 seg=1
WIRE -20.0000 4.0000 0  -20.0000 6.0000 0 r=0.3183 seg=1
# ... 632 further WIRE lines of the ground grid omitted (complete file in the Examples folder)
WIRE -10.0000 -8.0 0  -10.0000 0 0 r=0.3750 seg=4 name=feed
SOURCE feed 25
GROUND pcb eps=2.2 tand=0.0009 h=1.575mm groundplane
MESH taper=off
```

patch_fr4.ant

```
TITLE The same wire-grid patch on lossless FR-4 (eps 4.4, 1.6 mm) with ground plane: frequency
UNITS mm
FREQ 2.2450 GHz
SWEEP 2.17 2.32 11 GHz
WIRE -18.6300 0.0000 0  -18.6300 2.0579 0 r=0.3275 seg=1
WIRE -18.6300 2.0579 0  -18.6300 4.1157 0 r=0.3275 seg=1
WIRE -18.6300 4.1157 0  -18.6300 6.1736 0 r=0.3275 seg=1
# ... 532 further WIRE lines of the ground grid omitted (complete file in the Examples folder)
WIRE 16.5600 28.8100 0  18.6300 28.8100 0 r=0.3275 seg=1
SOURCE feed 50
```

© 2026 Communications Consulting Corp.

```
GROUND pcb eps=4.4 tand=0.0 h=1.6mm groundplane
MESH taper=off
```

pcb_ifa_2p45GHz.ant

```
TITLE Printed inverted-F antenna 2.45 GHz on FR4 1.6 mm, 40 x 20 mm board (approximate thin-wi
UNITS mm
FREQ 2.45 GHz
SWEEP 2.2 2.7 51 GHz
WIRE 0 0 0  0 2 0 r=0.2 seg=1
WIRE 0 2 0  0 4 0 r=0.2 seg=1
WIRE 0 4 0  0 6 0 r=0.2 seg=1
# ... 342 further WIRE lines of the ground grid omitted (complete file in the Examples folder)
WIRE 30 20 0  32 20 0 r=0.2 seg=1
WIRE 32 2 0  35 2 0 r=0.125 insmm=0.8 inseps=4.4 name=short
WIRE 32 4 0  35 4 0 r=0.125 insmm=0.8 inseps=4.4 name=feed
WIRE 35 2 0  35 19 0 r=0.125 insmm=0.8 inseps=4.4 name=arm1
WIRE 35 19 0  37 19 0 r=0.125 insmm=0.8 inseps=4.4 name=arm2
WIRE 37 19 0  37 9 0 r=0.125 insmm=0.8 inseps=4.4 name=arm3
SOURCE feed 50
GROUND none
```

printed_dipole_2p45GHz.ant

```
TITLE Printed half-wave dipole for 2.45 GHz on FR-4 1.6 mm (no ground plane), 1 mm traces
# The board lies in the plane z = 0 (top surface); the traces are on it.
# GROUND pcb: eps = relative permittivity, tand = loss tangent, h = board thickness.
# w = trace width (a flat trace is modelled by a round wire of radius w/4).
# Far-field power excludes the surface wave guided by the (laterally infinite) board
# and the dielectric loss.
UNITS mm
FREQ 2.45 GHz
SWEEP 2.2 2.7 11 GHz
VAR L=43.4
WIRE -L/2 0 0  L/2 0 0  w=1 name=dipole
SOURCE dipole 50
GROUND pcb eps=4.4 tand=0.02 h=1.6mm
```

quad_2el_20m.ant

```
TITLE 2-element cubical quad for 20 m, 15 m above average ground (square loops, fed at bottom c
UNITS m
FREQ 14.15 MHz
SWEEP 13.95 14.35 17 MHz
MATERIAL copper
# driven element, side 5.38 m, at x = 0
WIRE 0 -2.69 12.31  0  2.69 12.31  awg=12 name=d_bottom
WIRE 0  2.69 12.31  0  2.69 17.69  awg=12 name=d_right
```

```
WIRE 0  2.69 17.69  0 -2.69 17.69  awg=12 name=d_top
WIRE 0 -2.69 17.69  0 -2.69 12.31  awg=12 name=d_left
# reflector, side 5.56 m, at x = -2.5
WIRE -2.5 -2.78 12.22  -2.5  2.78 12.22  awg=12 name=r_bottom
WIRE -2.5  2.78 12.22  -2.5  2.78 17.78  awg=12 name=r_right
WIRE -2.5  2.78 17.78  -2.5 -2.78 17.78  awg=12 name=r_top
WIRE -2.5 -2.78 17.78  -2.5 -2.78 12.22  awg=12 name=r_left
SOURCE d_bottom 50
GROUND real eps=13 sigma=0.005
```

short_vertical_40m.ant

```
TITLE Short vertical for 40 m: 5 m aluminium tube over perfect ground (matching-network example
UNITS m
FREQ 7.1 MHz
SWEEP 6.95 7.25 31 MHz
WIRE 0 0 0  0 0 5  d=0.03 name=whip
SOURCE whip 0
GROUND perfect
MATERIAL aluminum
```

turnstile_2m.ant

```
TITLE Turnstile for 2 m: two crossed dipoles fed 90 degrees apart, free space (circular polariz
UNITS m
VAR L=0.487          # half length of each dipole
FREQ 145.9 MHz
SWEEP 144 148 21 MHz
WIRE -L 0 0  L 0 0  d=0.006 name=dx
WIRE 0 -L 0.02  0 L 0.02  d=0.006 name=dy
SOURCE dx 50 V=1 phase=0
SOURCE dy 50 V=1 phase=-90
MATERIAL copper
```

yagi_3el_20m.ant

```
TITLE 3-element Yagi for 20 m, 25 mm aluminium tubing, 15 m above average ground
UNITS m
FREQ 14.15 MHz
SWEEP 13.95 14.35 17 MHz
MATERIAL aluminum
WIRE -3.2 -5.31 15  -3.2 5.31 15  d=0.025 name=reflector
WIRE  0   -5.13 15   0   5.13 15  d=0.025 name=driver
WIRE  3.2 -4.76 15   3.2 4.76 15  d=0.025 name=director
SOURCE driver 50
GROUND real eps=13 sigma=0.005
```

© 2026 Communications Consulting Corp.

yagi_3el_20m_optimize.ant

```
TITLE 3-element Yagi for 20 m: optimizer demonstration (gain, F/B, SWR)
UNITS m
VAR h=15 d=0.025
VAR Lr=5.31 Ld=5.13 Lx=4.76      # half lengths of reflector, driver, director
VAR Sr=3.2 Sd=3.2                 # spacings
FREQ 14.15 MHz
SWEEP 13.95 14.35 17 MHz
MATERIAL aluminum
WIRE -Sr -Lr h  -Sr Lr h  d=d name=reflector
WIRE 0 -Ld h  0 Ld h  d=d name=driver
WIRE Sd -Lx h  Sd Lx h  d=d name=director
SOURCE driver 50
GROUND real eps=13 sigma=0.005
MESH segwl=30
Z0 50
# optimizer: element lengths and spacings for gain, front-to-back ratio and match
OPTVAR Lr 5.0 5.6
OPTVAR Ld 4.9 5.4
OPTVAR Lx 4.5 5.0
OPTVAR Sr 2.5 4.0
OPTVAR Sd 2.5 4.0
GOAL gmax weight=1
GOAL fb target=25 weight=0.3
GOAL swr target=1.3 weight=1
OPTSET pop=24 gen=25 seed=3
```

yagi_3el_20m_variables.ant

```
TITLE 3-element Yagi for 20 m described with named variables (VAR)
UNITS m
VAR h=15 d=0.025
VAR Lr=5.31 Ld=5.13 Lx=4.76      # half lengths of reflector, driver, director
VAR Sr=3.2 Sd=3.2                 # spacings
FREQ 14.15 MHz
SWEEP 13.95 14.35 17 MHz
MATERIAL aluminum
WIRE -Sr -Lr h  -Sr Lr h  d=d name=reflector
WIRE 0 -Ld h  0 Ld h  d=d name=driver
WIRE Sd -Lx h  Sd Lx h  d=d name=director
SOURCE driver 50
GROUND real eps=13 sigma=0.005
MESH segwl=30
Z0 50
```

© 2026 Communications Consulting Corp.

NEC-2 decks (examples and NEC-2 validation cases)

The same decks are supplied as `Examples\nec_*.nec` and `Validation\decks\.nec`; the NEC-2 output files are in `Validation\nec_out`.

bent_dipole.nec

```
CM dipole with 90deg bends near ends
CE
GW 1 5 0 0.15 0.1 0 0.15 0 0.001
GW 2 15 0 0.15 0 0 -0.15 0 0.001
GW 3 5 0 -0.15 0 0 -0.15 0.1 0.001
GE 0
EX 0 2 8 0 1 0
FR 0 1 0 0 299.792458 0
RP 0 19 73 1000 0 0 5 5
EN
```

hdipole_pec.nec

```
CM horizontal dipole h=0.25 over PEC
CE
GW 1 21 0 -0.25 0.25 0 0.25 0.25 0.0001
GE 0
GN 1
EX 0 1 11 0 1 0
FR 0 1 0 0 299.792458 0
RP 0 19 73 1000 0 0 5 5
EN
```

helix.nec

```
CM axial-mode helix, 5 turns, C = 1 wavelength, over perfect ground plane
CE
GH 1 100 0.0745 0.3725 0.0477 0.0477 0.0477 0.0477 0.001
GE 1
GN 1
EX 0 1 1 0 1 0
FR 0 1 0 0 1000 0
RP 0 19 73 1000 0 0 5 5
EN
```

invv_realgnd.nec

```
CM inverted-V dipole 10 m apex over average ground (RCA)
CE
GW 1 15 -9.0 0 7.0 0 0 10 0.001
GW 2 15 0 0 10 9.0 0 7.0 0.001
GE 1
```

© 2026 Communications Consulting Corp.

```
GN 0 0 0 0 13 0.005
EX 0 2 1 0 1 0
FR 0 1 0 0 7.1 0
RP 0 19 73 1000 0 0 5 5
EN
```

loaded_dipole.nec

```
CM short dipole with series loading coils, copper wire
CE
GW 1 30 0 0 -1.5 0 0 1.5 0.002
GE 0
LD 0 1 8 8 0 4e-6 0
LD 0 1 23 23 0 4e-6 0
LD 5 1 0 0 5.8e7
EX 0 1 15 0 1 0
FR 0 1 0 0 14 0
RP 0 37 1 1000 0 0 5 5
EN
```

loop_small.nec

```
CM small circular loop, circumference 0.1 wavelength (GA arc, 36 wires)
CE
GA 1 36 0.015915 0 360 0.0005
GE 0
EX 0 1 1 0 1 0
FR 0 1 0 0 299.792458 0
RP 0 37 73 1000 0 0 5 5
EN
```

monopole_pec.nec

```
CM quarter-wave monopole on perfect ground
CE
GW 1 20 0 0 0 0 0 0.25 0.001
GE 1
GN 1
EX 0 1 1 0 1 0
FR 0 1 0 0 299.792458 0
RP 0 91 1 1000 0 0 1 1
EN
```

phased2.nec

```
CM two verticals, quarter-wave spacing, fed through transmission lines (TL cards)
CE
GW 1 21 0 0 -2.5 0 0 2.5 0.005
```

```
GW 2 21 5.3 0 -2.5 5.3 0 2.5 0.005
GW 3 1 10 0 0 10 0 0.1 0.005
GE 0
TL 3 1 1 11 50 5.3 0 0 0 0
TL 3 1 2 11 50 10.6 0 0 0 0
EX 0 3 1 0 1 0
FR 0 1 0 0 28.3 0
RP 0 37 73 1000 0 0 5 5
EN
```

slant_monopole.nec

```
CM slanted monopole 30 deg
CE
GW 1 20 0 0 0 0.2165 0 0.125 0.001
GE 1
GN 1
EX 0 1 1 0 1 0
FR 0 1 0 0 299.792458 0
RP 0 19 73 1000 0 0 5 5
EN
```

som_gp.nec

```
CM elevated ground plane, 4 radials 0.047 wavelength above average ground (Sommerfeld, GN 2)
CE
GW 1 10 0 0 1.0 0 0 6.3 0.001
GW 2 10 0 0 1.0 5.3 0.0 1.0 0.001
GW 3 10 0 0 1.0 3.245314017740486e-16 5.3 1.0 0.001
GW 4 10 0 0 1.0 -5.3 6.490628035480972e-16 1.0 0.001
GW 5 10 0 0 1.0 -9.735942053221457e-16 -5.3 1.0 0.001
GE 1
GN 2 0 0 0 13 0.005
EX 0 1 1 0 1 0
FR 0 1 0 0 14 0
RP 0 46 73 1000 0 0 2 5
EN
```

som_hd_h1p07.nec

```
CM half-wave dipole 0.05 wavelength above average ground (Sommerfeld, GN 2)
CE
GW 1 21 -5.1 0 1.07 5.1 0 1.07 0.001
GE 1
GN 2 0 0 0 13 0.005
EX 0 1 11 0 1 0
FR 0 1 0 0 14 0
RP 0 46 73 1000 0 0 2 5
```

© 2026 Communications Consulting Corp.

```
EN
```

som_hd_low.nec

```
CM half-wave dipole 0.012 wavelength above average ground (Sommerfeld, GN 2)
CE
GW 1 21 -5.1 0 0.25 5.1 0 0.25 0.001
GE 1
GN 2 0 0 0 13 0.005
EX 0 1 11 0 1 0
FR 0 1 0 0 14 0
RP 0 46 73 1000 0 0 2 5
EN
```

som_hd_poor.nec

```
CM half-wave dipole 0.05 wavelength above poor ground (Sommerfeld, GN 2)
CE
GW 1 21 -5.1 0 1.07 5.1 0 1.07 0.001
GE 1
GN 2 0 0 0 5 0.001
EX 0 1 11 0 1 0
FR 0 1 0 0 14 0
RP 0 46 73 1000 0 0 2 5
EN
```

som_hd_sea.nec

```
CM half-wave dipole 0.05 wavelength above sea water (Sommerfeld, GN 2)
CE
GW 1 21 -5.1 0 1.07 5.1 0 1.07 0.001
GE 1
GN 2 0 0 0 81 5
EX 0 1 11 0 1 0
FR 0 1 0 0 14 0
RP 0 46 73 1000 0 0 2 5
EN
```

som_nvis80.nec

```
CM 80 m NVIS dipole 3 m (0.036 wavelength) above average ground (Sommerfeld, GN 2)
CE
GW 1 31 -19.6 0 3 19.6 0 3 0.001026
GE 1
GN 2 0 0 0 13 0.005
EX 0 1 16 0 1 0
FR 0 1 0 0 3.6 0
RP 0 46 73 1000 0 0 2 5
EN
```

© 2026 Communications Consulting Corp.

som_vd_low.nec

```
CM vertical dipole, lower end 0.023 wavelength above average ground (Sommerfeld, GN 2)
CE
GW 1 21 0 0 0.5 0 0 10.7 0.001
GE 1
GN 2 0 0 0 13 0.005
EX 0 1 11 0 1 0
FR 0 1 0 0 14 0
RP 0 46 73 1000 0 0 2 5
EN
```

vdipole_bent.nec

```
CM V dipole, 90 deg apex angle, free space
CE
GW 1 10 -0.1768 0 0.1768 0 0 0 0.001
GW 1 10 0 0 0 0.1768 0 0.1768 0.001
GE 0
EX 0 1 10 0 1 0
FR 0 1 0 0 299.792458 0
RP 0 19 73 1000 0 0 5 5
EN
```

vert_radials.nec

```
CM ground-plane vertical with 4 sloping radials, 3 m above average ground (RCA)
CE
GW 1 10 0 0 3 0 0 8.3 0.005
GW 2 10 0 0 3 6.6 0 0.5 0.002
GW 3 10 0 0 3 0 6.6 0.5 0.002
GW 4 10 0 0 3 -6.6 0 0.5 0.002
GW 5 10 0 0 3 0 -6.6 0.5 0.002
GE 1
GN 0 0 0 0 13 0.005
EX 0 1 1 0 1 0
FR 0 1 0 0 14.1 0
RP 0 19 73 1000 0 0 5 5
EN
```

yagi3.nec

```
CM 3-element Yagi, 14.2 MHz, free space
CE
GW 1 21 -5.36 -5.5 0 -5.36 5.5 0 0.006
GW 2 21 0 -5.18 0 0 5.18 0 0.006
GW 3 21 4.5 -4.8 0 4.5 4.8 0 0.006
GE 0
EX 0 2 11 0 1 0
```

© 2026 Communications Consulting Corp.

```
FR 0 1 0 0 14.2 0
RP 0 37 73 1000 0 0 5 5
EN
```

Validation cases (analytic checks)

v_conv120.ant

```
TITLE 20 m dipole 10 m over average ground, fine mesh (120 segments per wavelength)
FREQ 14.175 MHz
WIRE -5.13 0 10 5.13 0 10 awg=12 name=d
SOURCE d 50
GROUND real eps=13 sigma=0.005
MATERIAL copper
MESH segwl=120
```

v_conv30.ant

```
TITLE 20 m dipole 10 m over average ground, default mesh (30 segments per wavelength)
FREQ 14.175 MHz
WIRE -5.13 0 10 5.13 0 10 awg=12 name=d
SOURCE d 50
GROUND real eps=13 sigma=0.005
MATERIAL copper
MESH segwl=30
```

v_copper.ant

```
TITLE Copper half-wave dipole, 14 MHz, radius 1 mm
FREQ 14 MHz
WIRE 0 0 -5.1 0 0 5.1 r=0.001 name=d
MESH segwl=60
SOURCE d 50
MATERIAL copper
```

v_dip.ant

```
TITLE Half-wave dipole, radius 0.001 wavelength, free space
FREQ 300 MHz
WIRE 0 0 -0.25 0 0 0.25 r=0.001 seg=40 name=d
SOURCE d 50
```

v_half.ant

```
TITLE Thin half-wave dipole, radius 1e-5 wavelength
FREQ 300 MHz
WIRE 0 0 -0.25 0 0 0.25 r=0.00001 name=d
MESH segwl=80
SOURCE d 50
```

© 2026 Communications Consulting Corp.

v_hpec.ant

```
TITLE Horizontal dipole 0.2 wavelength over perfect ground
FREQ 300 MHz
WIRE 0 -0.25 0.2 0 0.25 0.2 r=0.001 seg=40 name=d
SOURCE d 50
GROUND perfect
```

v_loop.ant

```
TITLE Small loop, circumference 0.1 wavelength, 300 MHz
FREQ 300 MHz
LOOP 0 0 0 0.0159155 48 axis=z r=0.00005 name=lp
SOURCE lp1 0
```

v_mono.ant

```
TITLE Quarter-wave monopole, radius 0.001 wavelength, perfect ground
FREQ 300 MHz
WIRE 0 0 0 0 0 0.25 r=0.001 seg=20 name=m
SOURCE m 0
GROUND perfect
```

v_pair.ant

```
TITLE Horizontal dipole and its antiphase image, free space
FREQ 300 MHz
WIRE 0 -0.25 0.2 0 0.25 0.2 r=0.001 seg=40 name=a
WIRE 0 -0.25 -0.2 0 0.25 -0.2 r=0.001 seg=40 name=b
SOURCE a 50 V=1
SOURCE b 50 V=-1
```

v_pcb_free.ant

```
TITLE Half-wave dipole on a printed board with eps=1 (no ground plane): must equal the free-spa
FREQ 300 MHz
WIRE -0.25 0 0 0.25 0 0 r=0.001 seg=40 name=d
SOURCE d 50
GROUND pcb eps=1 h=0.1
```

v_pcb_image.ant

```
TITLE Dipole on a board with eps=1, thickness 0.2 wavelength, ground plane: must equal the dipo
FREQ 300 MHz
WIRE 0 -0.25 0 0 0.25 0 r=0.001 seg=40 name=d
SOURCE d 50
GROUND pcb eps=1 h=0.2 groundplane
```

© 2026 Communications Consulting Corp.

v_short.ant

```
TITLE Short dipole, 0.05 wavelength
FREQ 300 MHz
WIRE 0 0 -0.025 0 0 0.025 r=0.00001 seg=21 name=d
SOURCE d 50
```

v_somm_free.ant

```
TITLE Horizontal dipole 0.2 wavelength over Sommerfeld ground with eps=1, sigma=0 (must equal
FREQ 300 MHz
WIRE 0 -0.25 0.2 0 0.25 0.2 r=0.001 seg=40 name=d
SOURCE d 50
GROUND real eps=1 sigma=0 sommerfeld
```

v_somm_pec.ant

```
TITLE Horizontal dipole 0.2 wavelength over Sommerfeld ground with eps=1e7, sigma=1e7 S/m (mus
FREQ 300 MHz
WIRE 0 -0.25 0.2 0 0.25 0.2 r=0.001 seg=40 name=d
SOURCE d 50
GROUND real eps=1e7 sigma=1e7 sommerfeld
```

References

[1] R. F. Harrington, *Field Computation by Moment Methods*. New York: Macmillan, 1968.

[2] G. J. Burke and A. J. Poggio, “Numerical Electromagnetics Code (NEC)—Method of Moments,” Lawrence Livermore National Laboratory, Tech. Rep. UCID-18834, 1981.

[3] D. R. Wilton and C. M. Butler, “Efficient numerical techniques for solving Pocklington’s equation and their relationships to other methods,” *IEEE Trans. Antennas Propag.*, vol. 24, no. 1, pp. 83–86, Jan. 1976.

[4] C. A. Balanis, *Antenna Theory: Analysis and Design*, 4th ed. Hoboken, NJ: Wiley, 2016.

[5] J. D. Kraus and R. J. Marhefka, *Antennas for All Applications*, 3rd ed. New York: McGraw-Hill, 2002.

[6] R. W. P. King, *The Theory of Linear Antennas*. Cambridge, MA: Harvard Univ. Press, 1956.

[7] S. A. Schelkunoff and H. T. Friis, *Antennas: Theory and Practice*. New York: Wiley, 1952.

[8] D. M. Pozar, *Microwave Engineering*, 4th ed. Hoboken, NJ: Wiley, 2012.

[9] R. Storn and K. Price, “Differential evolution—A simple and efficient heuristic for global optimization over continuous spaces,” *J. Global Optim.*, vol. 11, no. 4, pp. 341–359, 1997.

[10] J. A. Nelder and R. Mead, “A simplex method for function minimization,” *Comput. J.*, vol. 7, no. 4, pp. 308–313, 1965.

[11] *IEEE Standard for Definitions of Terms for Antennas*, IEEE Std 145-2013.

[12] L. J. Chu, “Physical limitations of omni-directional antennas,” *J. Appl. Phys.*, vol. 19, no. 12, pp. 1163–1175, Dec. 1948.

© 2026 Communications Consulting Corp.

[13] A. D. Yaghjian and S. R. Best, “Impedance, bandwidth, and Q of antennas,” *IEEE Trans. Antennas Propag.*, vol. 53, no. 4, pp. 1298–1324, Apr. 2005.

[14] F. M. Landstorfer and R. R. Sacher, *Optimisation of Wire Antennas*. Letchworth, U.K.: Research Studies Press, 1985.

[15] A. Sommerfeld, “Über die Ausbreitung der Wellen in der drahtlosen Telegraphie,” *Ann. Phys.*, vol. 333, no. 4, pp. 665–736, 1909.

[16] A. Baños, *Dipole Radiation in the Presence of a Conducting Half-Space*. Oxford: Pergamon, 1966.

[17] G. J. Burke and E. K. Miller, “Modeling antennas near to and penetrating a lossy interface,” *IEEE Trans. Antennas Propag.*, vol. 32, no. 10, pp. 1040–1049, Oct. 1984.

[18] K. A. Michalski, “Extrapolation methods for Sommerfeld integral tails,” *IEEE Trans. Antennas Propag.*, vol. 46, no. 10, pp. 1405–1418, Oct. 1998.

[19] K. A. Michalski and J. R. Mosig, “Multilayered media Green’s functions in integral equation formulations,” *IEEE Trans. Antennas Propag.*, vol. 45, no. 3, pp. 508–519, Mar. 1997.

[20] W. C. Chew, *Waves and Fields in Inhomogeneous Media*. New York: Van Nostrand Reinhold, 1990.

[21] J. R. Mosig and F. E. Gardiol, “General integral equation formulation for microstrip antennas and scatterers,” *IEE Proc. H*, vol. 132, no. 7, pp. 424–432, Dec. 1985.

[22] D. M. Pozar, “Input impedance and mutual coupling of rectangular microstrip antennas,” *IEEE Trans. Antennas Propag.*, vol. 30, no. 6, pp. 1191–1196, Nov. 1982.

[23] E. Hammerstad and Ø. Jensen, “Accurate models for microstrip computer-aided design,” in *IEEE MTT-S Int. Microwave Symp. Dig.*, 1980, pp. 407–409.

[24] K. C. Gupta, R. Garg, I. Bahl and P. Bhartia, *Microstrip Lines and Slotlines*, 2nd ed. Boston: Artech House, 1996.

[25] R. K. Shevgaonkar and U. L. Rohde, *Electromagnetic Waves: Theory and Applications, with a Special Focus on Circuit and Antenna Design*. Springer.

[26] S. Silver, Ed., *Microwave Antenna Theory and Design*, MIT Radiation Laboratory Series, vol. 12. New York: McGraw-Hill, 1949.

[27] M. I. Kontorovich, M. I. Astrakhan, V. P. Akimov and G. A. Fersman, *Electrodynamics of Grid Structures*. Moscow: Radio i Svyaz, 1987.

© 2026 Communications Consulting Corp.